

NATURE OF FORCES RESPONSIBLE FOR STACKING INTERACTIONS

Aditya Chhikara

B.Sc. (hons.), Chemical Biology, Thompson Rivers University, 2007

A thesis

Submitted to the School of Graduate Studies

of the University of Lethbridge

in Partial Fulfilment of the

Requirements for the Degree

[M.Sc. CHEMISTRY]

Department of Chemistry and Biochemistry

University of Lethbridge

LETHBRIDGE, ALBERTA, CANADA

© Aditya Chhikara, 2010

Abstract

Stacking interactions, also known as π - π or face-to-face interactions, occur between molecules whose π bonds are in parallel planes. They are used to design self-assembling structures in nanotechnology, influence organic reactions and are ubiquitous in nature.

The stacking interactions of substituted benzene heterodimers and substituted benzene-natural nucleobase heterodimers are examined. Both electron-donating and withdrawing groups are studied by varying their type, number and location around the benzene ring. The studies are done by carrying out systematic scans of the potential energy surface at the MP2/6-31G*(0.25) level of theory. Charge transfer interactions and extent of charge separation in the monomer are found to be dominant when the difference in ESP between the monomers is large and small, respectively. Dipole-dipole interactions are also found to affect stacking interactions. The results from MP2/6-31G*(0.25) are checked against those at the CCSD(T)/CBS limit for select cases and are found to be within 81-110%.

Acknowledgements

I'd like to thank my supervisor Dr Stacey Wetmore for giving me the opportunity to pursue a Masters under her supervision. Coming in without a computational background, this thesis would not have been possible without her patience, guidance and support. I especially appreciate her openness to my ideas and for encouraging me to incorporate those ideas in my research. My other committee members, Dr Rene Boere and Dr Theresa Burg, played an indispensable part in my Masters by helping and encouraging me every time I seemed to hit a road block and I am thankful for their substantial feedback, guidance and patience.

I'd like to thank my parents for their invaluable support and encouragement. Last but not least, I'd like to thank my lab mates for their feedback on my work.

Table of Contents

Chapter		Page
1	Introduction to stacking interactions	1
1.1	General Introduction	1
1.2	What are stacking interactions?	1
1.3	Applications of stacking interactions	3
1.3.1	Stacked structures in biology	4
1.3.2	Stacked structures in nanotechnology	4
1.3.3	Stacked structures in organic chemistry	5
1.4	Forces involved in stacking interactions	5
1.5	Overview of theoretical and experimental benzene, biological and stacking application literature	9
1.5.1	Overview of experimental data from studies on stacking interactions..	9
1.5.2	Overview of theoretical data from studies on stacking interactions	13
1.5.3	Why are there differences between experimental and theoretical studies?	16
1.5.4	Overview of data from biological stacking studies and studies on self-assembled stacked structures	16
1.6	Thesis Overview.....	17
2	Methods	24
2.1	Methods used to calculate the energies of molecules	24
2.1.1	Schrodinger Equation	24
2.1.2	Hartree-Fock theory	25
2.1.3	Perturbation theory	26
2.1.4	CCSD(T) theory	27
2.1.5	Basis Sets.....	28
2.2	Supermolecular method of calculating stacking interactions	29
2.3	Calculating the CCSD(T)/CBS energy	30
3	Stacking of benzene dimers	32
3.1	Introduction	32
3.2	Computational Methodology	33
3.2.1	Potential Energy Surface Scans	33
3.2.2	Level of Theory	34
3.3	Results and Discussion	35
3.3.1	Monosubstituted benzene-benzene dimers	35
3.3.2	Polysubstituted benzene-benzene dimers	39
3.3.3	Polysubstituted benzene-monosubstituted benzene dimers	43
3.3.4	Hexasubstituted benzene-polysubstituted benzene dimers	52
3.3.5	Affect of HF, MP2, and CCSD(T) levels of theory on stacking interactions	55
3.4	Conclusions	60
4.	Stacking of nucleobase-benzene dimers	63
4.1	Introduction	63
4.2	Computational Methodology	64
4.3	Results and Discussion	65
4.3.1	Nucleobase-monosubstituted benzene dimers	65
4.3.2	Nucleobase-polysubstituted benzene dimers	70
4.4	Conclusions	82

5	Global Conclusions and Future Work	85
	5.1 Global Conclusions	85
	5.2 Future Work	86
	Appendix	89

List of Tables	Page
Table 1 Experimentally determined stacking interactions for some lightly substituted phenyl dimers where the identities of the electron-donating and electron-withdrawing groups are given in brackets.....	11
Table 2 Experimentally determined stacking interactions for pentafluorophenyl dimers where the identities of the electron-donating and electron-withdrawing groups are given in brackets.....	12
Table 3 Theoretically determined stacking interactions for dimers of benzene-monosubstituted benzene and hexafluorobenzene-monosubstituted benzene where the identities of the electron-donating and electron-withdrawing groups are given in brackets.....	15
Table 4 HF and MP2 binding energy for the 6-31G*(0.25) basis set. All energies are in kJ mol ⁻¹	56
Table 5 HF and MP2 binding energy for the aug-cc-pVDZ basis set. All energies are in kJ mol ⁻¹	57
Table 6 HF and MP2 binding energy for the aug-cc-pVTZ basis set. All energies are in kJ mol ⁻¹	57
Table 7 Results from the CCSD(I)/CBS extrapolation. All energies are in kJ mol ⁻¹ . The aug-cc-pVTZ calculations for the hexaaminobenzene-aminobenzene and hexaaminobenzene-cyanobenzene dimers were calculated using the RI approximation with Turbomole V5-9-1 18	59
Table 8 The dipole moments of the different monomers, dipole alignments and their coefficients of correlation and slopes (with and without benzenecarboxamide) when the stabilization energy of their dimers with monosubstituted benzenes are plotted as a function of the dipole moment of the monosubstituted benzenes (Figure 23)	68
Table 9 Stacking stabilization energies of zero-dipole uracil-polyfluorobenzenes and uracil-polyaminobenzenes at the HF/6-31G*(0.25) and MP2/6-31G*(0.25) level and the stacking stabilization due to electron correlation at the MP2/6-31G*(0.25) level	78
Table 10 Sample results from the R1 and α potential energy surface scans (for 1,2,4-triaminobenzene and benzonitrile dimer)	89
Table 11 Sample results from the R2 potential energy surface scans (for 1,2,4-triaminobenzene and benzonitrile dimer)	89
Table 12 Summary of information from potential energy surface scans of the benzene-monosubstituted benzene dimers at the counterpoise corrected MP2/6-31G*(0.25) level of theory. All energies are in kJ mol ⁻¹ , dipoles in Debye and distances are in Å	90
Table 13 Summary of information from potential energy surface scans of the benzene-polysubstituted benzene dimers at the counterpoise corrected MP2/6-31G*(0.25) level of theory. All energies are in kJ mol ⁻¹ and all distances are in Å	92
Table 14 Summary of information from potential energy surface scans of the cyanobenzene-polycyanobenzene dimers and cyanobenzene-polyaminobenzene dimers at the counterpoise corrected MP2/6-31G*(0.25) level of theory. All energies are in kJ mol ⁻¹ and all distances are in Å	94
Table 15 Summary of information from potential energy surface scans of the aminobenzene-polycyanobenzene dimers and aminobenzene-polyaminobenzene dimers at the counterpoise corrected MP2/6-31G*(0.25) level of theory. All energies are in kJ mol ⁻¹ and all distances are in Å	95

Table 16	Summary of information from potential energy surface scans of the hexacyanobenzene-polycyanobenzene dimers and hexacyanobenzene-polyaminobenzene dimers at the counterpoise corrected MP2/6-31G*(0.25) level of theory. All energies are in kJ mol ⁻¹ and all distances are in Å	98
Table 17	Summary of information from potential energy surface scans of the hexacyanobenzene-polycyanobenzene dimers and hexacyanobenzene-polyaminobenzene dimers at the counterpoise corrected MP2/6-31G*(0.25) level of theory. All energies are in kJ mol ⁻¹ and all distances are in Å	99
Table 18	Summary of information from potential energy surface scans of the adenine-monosubstituted benzene dimers at the counterpoise corrected MP2/6-31G*(0.25) level of theory. All energies are in kJ mol ⁻¹ , dipoles in Debye and distances are in Å. The “-fl” suffix represents the flipped monomer	101
Table 19	Summary of information from potential energy surface scans of the cytosine-monosubstituted benzene dimers at the counterpoise corrected MP2/6-31G*(0.25) level of theory. All energies are in kJ mol ⁻¹ , dipoles in Debye and distances are in Å. The “-fl” suffix represents the flipped monomer	101
Table 20	Summary of information from potential energy surface scans of the guanine-monosubstituted benzene dimers at the counterpoise corrected MP2/6-31G*(0.25) level of theory. All energies are in kJ mol ⁻¹ , dipoles in Debye and distances are in Å. The “-fl” suffix represents the flipped monomer	102
Table 21	Summary of information from potential energy surface scans of the thymine-monosubstituted benzene dimers at the counterpoise corrected MP2/6-31G*(0.25) level of theory. All energies are in kJ mol ⁻¹ , dipoles in Debye and distances are in Å. The “-fl” suffix represents the flipped monomer	102
Table 22	Summary of information from potential energy surface scans of the uracil-monosubstituted benzene dimers at the counterpoise corrected MP2/6-31G*(0.25) level of theory. All energies are in kJ mol ⁻¹ , dipoles in Debye and distances are in Å. The “-fl” suffix represents the flipped monomer	103
Table 23	Summary of information from potential energy surface scans of the adenine-polyfluorobenzene and adenine-polyaminobenzene dimers at the counterpoise corrected MP2/6-31G*(0.25) level of theory. All energies are in kJ mol ⁻¹ and distances are in Å. The “-fl” suffix represents the flipped monomer	106
Table 24	Summary of information from potential energy surface scans of the cytosine-polyfluorobenzene and cytosine-polyaminobenzene dimers at the counterpoise corrected MP2/6-31G*(0.25) level of theory. All energies are in kJ mol ⁻¹ and distances are in Å. The “-fl” suffix represents the flipped monomer	107
Table 25	Summary of information from potential energy surface scans of the guanine-polyfluorobenzene and guanine-polyaminobenzene dimers at the counterpoise corrected MP2/6-31G*(0.25) level of theory. All energies are in kJ mol ⁻¹ and distances are in Å. The “-fl” suffix represents the flipped monomer	108
Table 26	Summary of information from potential energy surface scans of the thymine-polyfluorobenzene and thymine-polyaminobenzene dimers at the counterpoise corrected MP2/6-31G*(0.25) level of theory. All energies are in kJ mol ⁻¹ and distances are in Å. The “-fl” suffix represents the flipped monomer	109
Table 27	Summary of information from potential energy surface scans of the uracil-polyfluorobenzene and uracil-polyaminobenzene dimers at the counterpoise corrected MP2/6-31G*(0.25) level of theory. All energies are in kJ mol ⁻¹ and distances are in Å. The “-fl” suffix represents the flipped monomer	110

List of Figures

Figure 1	a) π - π stacking and b) π - π T-shaped interactions of the benzene dimer.....	2
Figure 2	a) The sandwich benzene dimer with the two monomers eclipsed. b) Parallel-displaced benzene dimer with the two monomers off-set. Both a side (top) and top (bottom) view are provided.....	3
Figure 3	Figure showing the different electrostatic potential (ESP) maps calculated at MP2/6-31G* level of theory. Top row is the ESP map of hexafluorobenzene. Bottom row, left to right represents the ESP maps of aminobenzene, benzene and nitrobenzene. The numbers below represent the ESP over the center of the ring. The colours (not standardized) correspond to the sign of ESP, with red representing negative ESP and colours far away from red in electromagnetic spectrum representing increasingly positive ESP with blue being the area of the most positive ESP.....	13
Figure 4	The substituents are indicated by the letter X. For the benzene dimmers, electron withdrawing cyano and fluoro substituents and electron donating amino substituents are considered. For the nucleobase benzene dimmers, the same substituents with the exception of cyano groups are examined. For the hexasubstituted benzene-polysubstituted benzene dimmers, cyano or amino substitutions are considered for certain benzenes (marked with an asterisk(*)).....	19
Figure 5	The variables considered in the potential energy surface scans. First, the relative orientation (α) and the distance between the monomers (R1) are changed. The most stable structure is then used for a horizontal displacement (R2) scan.....	33
Figure 6	The different polysubstituted benzenes considered, where X denotes electron-donating amino or electro-withdrawing cyano or fluoro substituents. The circles indicate the hydrogen atoms that were aligned before the α rotations...	34
Figure 7	Plot of the stacking interaction energies of the monosubstituted benzene-benzene dimers as a function of the dipole magnitude of the monosubstituted benzene.....	37
Figure 8	Plot of the stacking interaction energies of the monosubstituted benzene-benzene dimers as a function of the dipole magnitude of the monosubstituted benzene. The stacking interaction energies are for the most stable structures after the R1, α and R2 scans and the dipole moments are calculated at the MP2/6-31G(d) level of theory	40
Figure 9	The stacking interaction of the polysubstituted benzene-benzene dimers plotted as a function of the number of substituents.....	41
Figure 10	The stacking interaction energies of the polycyanobenzene-monosubstituted benzene dimers as a function of the number of cyano substituents.....	45
Figure 11	Increase in stacking stabilization energy of zero-dipole tri-, tetra- and hexacyanobenzene in comparison to the zero-dipole polycyanobenzene with the next fewest number of cyano substituents.....	46
Figure 12	The increase in stacking stabilization energies on going from a zero-dipole polycyanobenzene to the maximum dipole polycyanobenzene with the same number of substituents.....	47
Figure 13	Stacking stabilization energies of polyaminobenzene-monosubstituted benzene dimers plotted as a function of number of amino substituents.....	48

Figure 14	Increase in stacking stabilization with increasing number of substituents for zero-dipole polyaminobenzene containing dimers with benzene, aminobenzene and cyanobenzene. For example, for 3 substituents, the difference in stacking energy with 1,4-diaminobenzene minus the stacking energy with 1,3,5-triaminobenzene is shown for benzene, aminobenzene and cyanobenzene.....	49
Figure 15	The increase in stacking stabilization energy on going from a zero-dipole polyaminobenzene to the maximum dipole polyaminobenzene with the same number of substituents	50
Figure 16	Stacking stabilization energies after R1/ α scans of the hexasubstituted benzene-polysubstituted benzene dimers plotted as a function of the number of substituents	53
Figure 17	Stacking stabilization energies of hexasubstituted benzene-polysubstituted benzene dimers after the R2 scans plotted as a function of number of substituents	54
Figure 18	The 5 natural nucleobases adenine, guanine, cytosine, thymine and uracil and the numbering of their ring atoms	64
Figure 19	(a) Stacking stabilization energies of the pyrimidine-monosubstituted dimers and benzene-monosubstituted dimers plotted as a function of the dipole moments of the monosubstituted benzenes. (b) Stacking stabilization energies of the purine-monosubstituted benzene dimers plotted as a function of the dipole moments of the monosubstituted benzenes	66
Figure 20	Electrostatic potential maps of the different nucleobases. (Top row, left to right: thymine, uracil and guanine. Bottom row, left to right: adenine, benzene and cytosine)	67
Figure 21	Increase in stacking stabilization energy on going from a zero-dipole polyaminobenzene to the maximum dipole polyaminobenzene with the same number of amino substituents plotted as a function of the number of amino substituents for (a) pyrimidines-polyaminobenzene and benzene polyaminobenzene dimers, and (b) purine-polyaminobenzene dimers	71
Figure 22	Increase in stacking stabilization energy on going from a zero-dipole polyfluorobenzene to the maximum dipole polyfluorobenzene with the same number of substituents for (a) pyrimidines and benzene dimers, and (b) purine dimers	73
Figure 23	(a) The stacking stabilization energies of the pyrimidine-polyaminobenzene and benzene-polyaminobenzene dimers after the R1/ α scans plotted as a function of the number of amino substituents. (b) The stacking stabilization energies of the pyrimidine-polyaminobenzene and benzene-polyaminobenzene dimers after the R2 scans plotted as a function of the number of amino substituents	75
Figure 24	(a) The stacking stabilization energies of the pyrimidine-polyfluorobenzene and benzene-polyfluorobenzene dimers after the R1/ α scans plotted as a function of the number of fluoro substituents. (b) The stacking stabilization energies of the pyrimidine-polyfluorobenzene and benzene-polyfluorobenzene dimers after the R2 scans plotted as a function of the number of fluoro substituents	76
Figure 25	(a) The stacking stabilization energies of the purine-polyaminobenzene dimers after the R1/ α scans plotted as a function of the number of amino substituents. (b) The stacking stabilization energies of the purine-polyaminobenzene dimers after the R2 scans plotted as a function of the number of amino substituents	79

Figure 26	(a) The stacking stabilization energies of the purine-polyfluorobenzene dimers after the R1/ α scans plotted as a function of the number of fluoro substituents. (b) The stacking stabilization energies of the purine-polyfluorobenzene dimers after the R2 scans plotted as a function of the number of fluoro substituents	81
Figure 27	The dimer conformation corresponding to the most stable structure after the R2 scans for the benzene-monosubstituted benzenes. The carbon attached to the substituent is over the benzene ring in all cases except for fluorobenzene (5) where the carbon atom is close to the ring. The different dimers are C ₆ H ₆ -C ₆ H ₅ X where X=-NH ₂ , -CONH ₂ , -H, -CN, -OH, -CH ₃ , -F, -NO ₂ for structures 1-8 respectively	91
Figure 28	Figure showing the effect of increasing number of substitutions on horizontal displacements for all the zero dipole polysubstituted benzenes in the benzene-polysubstituted benzene dimers. The horizontal displacements represent the distance between the centers of the ring. The overlap between the rings increases with increasing number of amino, fluoro and cyano substituents	93
Figure 29	Final structures of the hexaminobenzene-benzene dimer, hexafluorobenzene-benzene dimer and the hexacyanobenzene-benzene dimer. The rings show a considerable degree of overlap in the dimers	93
Figure 30	Figure showing the effect of increasing number of substitutions on horizontal displacements for all the zero dipole polysubstituted benzenes in the monosubstituted benzene-polysubstituted benzene dimers. The horizontal displacements represent the distance between the centers of the ring. The overlap between the rings generally increases with increasing number of amino, fluoro and cyano substituents	96
Figure 31	Representative pictures of the structures found in monosubstituted benzene-polysubstituted benzene dimers. Structures a) and b) are 1,2,4,5-tetraaminobenzene-aminobenzene and 1,2,4,5-tetracyanobenzene-cyanobenzene respectively. They represent the typical structure with the rings overlapping and the most polarized carbon atom of the monosubstituted benzene over the benzene ring. In addition, the polycyanobenzenes-cyanobenzenes typically have the carbon atom of the cyano substituent overlapping with ring of the other benzene monomer. Structures c) and d) are hexaminobenzene-aminobenzene and 1,3,5-triaminobenzene-aminobenzene respectively, the two exceptions which are exceptions to the above mentioned trend because substituent-ring interactions dominate over charge-transfer interactions	97
Figure 32	Figure showing the effect of increasing number of substitutions on horizontal displacements for all the zero dipole polysubstituted benzenes in the hexasubstituted benzene-polysubstituted benzene dimers. The horizontal displacements represent the distance between the centers of the ring. The overlap between the rings generally increases with increasing charge-transfer interactions	99

- Figure 33 Figures representative of the final horizontal displacement structures for the zero-dipole hexasubstituted benzene-polysubstituted benzene systems. There are five representative figures of the final conformations. a) The hexacyanobenzene-hexaaminobenzene structure shows the overlapping benzene dimers with the most polarized carbon atom over the benzene ring. This structure is representative of hexacyanobenzene-polyaminobenzene and hexaaminobenzene-polycyanobenzene dimers where there are strong charge-transfer interactions. b) The hexacyanobenzene-1,2,4,5-tetracyanobenzene dimer with the most polarized carbon atom and the substituents over the benzene ring. This structure is representative of all of the hexacyanobenzene-polycyanobenzene dimers except for the hexacyanobenzene dimer. c) The hexaaminobenzene-hexaaminobenzene dimer with only the substituents interacting with each other. d) The hexacyanobenzene dimer showing no ring overlap and substituent-ring interactions. e) The hexaaminobenzene-1,2,4,5-tetraaminobenzene dimer with no ring overlap and the amino substituent interacting with the ring. This structure is representative of the polyaminobenzene-hexaaminobenzene dimers 100
- Figure 34 Figure showing the final structures for all the aminobenzene and fluorobenzene dimers. The final structures of all of the monosubstituted benzene-nucleobase dimers were examined and the most polarized carbon atom on the monosubstituted benzene ring was always over the nucleobase ring. Since there was not a large difference between the structures for the monosubstituted benzene-nucleobase dimers, the aminobenzene and fluorobenzene dimers were chosen to represent the stacking interactions of an electron rich and electron deficient monosubstituted benzene. a) Cytosine-aminobenzene, b) cytosine-fluorobenzene, c) thymine-aminobenzene, d) thymine-fluorobenzene, e) uracil-aminobenzene, f) uracil-fluorobenzene, g) adenine-aminobenzene, h) adenine-fluorobenzene, i) guanine-aminobenzene, j) guanine-fluorobenzene 105
- Figure 35 The pictures of the final structures for zero dipole diaminobenzene and hexaaminobenzene dimers are shown since they were found to be representative of the rest of the dimer structures. The electron deficient fluorobenzene rings stack over the part of the nucleobases with the most negative ESP. The electron rich aminobenzene rings stack over the part of the nucleobases with the most positive ESP. 1,5,9,13,17,21 are 1,4-difluorobenzene dimers with benzene, cytosine, thymine, uracil, adenine and guanine respectively. 2,6,10,14,18,22 are hexafluorobenzene dimers with benzene, cytosine, thymine, uracil, adenine and guanine respectively. 3,7,11,15,19,23 are 1,4-diaminobenzene dimers with benzene, cytosine, thymine, uracil, adenine and guanine respectively. 4,8,12,16,20,24 are hexaaminobenzene dimers with benzene, cytosine, thymine, uracil, adenine and guanine respectively 116

1 Introduction to stacking interactions

1.1 General Introduction

Stacking interactions are a specific class of non-covalent interactions found in biological systems,¹⁻⁵ used in nanotechnology⁶⁻¹² and are thought to influence reactions in organic chemistry.¹³⁻¹⁶ Given their widespread prevalence, extensive experimental and theoretical studies on stacking interactions have been done. These studies have primarily been carried out in two main contexts: biology¹⁷⁻⁶⁶ and to understand the fundamentals of stacking interactions.⁶⁷⁻⁹⁶ In the context of biology, stacking interactions between various biological molecules (such as nucleobases and amino acid side-chains) have been studied in order to better understand their role in natural processes such as stabilizing DNA and RNA helices and in protein-DNA interactions.¹⁷⁻⁶⁶ In the context of understanding the fundamentals of stacking interactions, benzene and substituted benzene dimers have been studied in order to determine the effect of electrostatics, dispersion and charge transfer on stacking stabilization.⁶⁷⁻⁹⁶ In addition, papers in the field of nanotechnology attempt to manipulate stacking interactions with the aim of building new materials for photovoltaics and non-linear opticals.⁶⁻¹²

1.2 What are stacking interactions?

Stacking interactions are a sub-group of π - π interactions. These are defined as interactions between systems containing π -bonds and are considered weak since they are weaker than covalent and ionic bonds. The importance of π -bonds is demonstrated by Grimme⁸⁷ who shows that the stabilization for systems with π -bonds is greater than for systems without π -bonds (for the same number of atoms). Studies of π - π interactions can be divided into two broad categories: stacking interactions and T-shaped interactions.⁷⁸ The interactions between neutral closed-shell molecules whose π bonds are in parallel planes are called stacking interactions (Figure 1a), whereas the interactions between molecules whose π -bonds are in perpendicular planes are called T-shaped

interactions (Figure 1b).⁷⁸ The properties of stacking interactions are different from T-shaped interactions with the former being dominated by dispersion interactions while the latter are dominated by electrostatic interaction.⁷⁸ Therefore this thesis specifically examines stacking interactions in order to sharpen the focus and thereby increase the depth of the study.

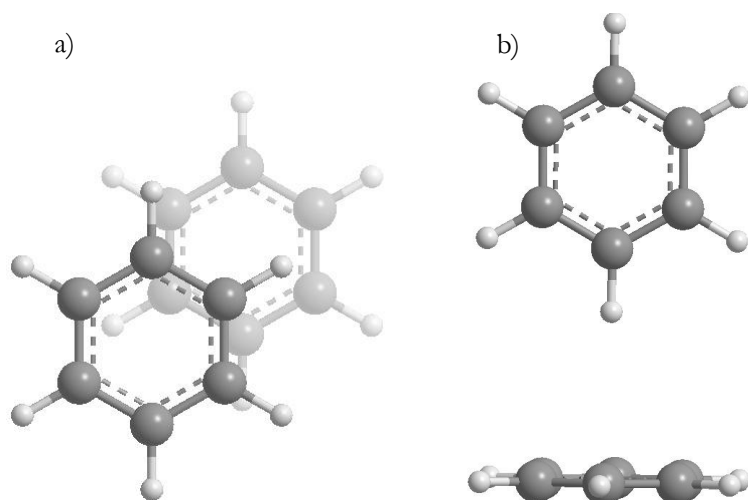


Figure 1 a) π - π stacking and b) π - π T-shaped interactions of the benzene dimer.

Computational and experimental studies of stacking interactions have most often been carried out on dimers, where in this thesis dimers is used to refer to both heterodimers as well as homodimers.^{67-96,17-66} In dimers, stacked structures have been divided into two main categories: sandwich (Figure 2a) and parallel-displaced (Figure 2b). In the sandwich configuration of dimers, the atoms in the rings perfectly eclipse each other when viewed from the top. In the parallel-displaced configuration, one monomer is shifted in the horizontal molecular plane so that the atoms are no longer eclipsed.

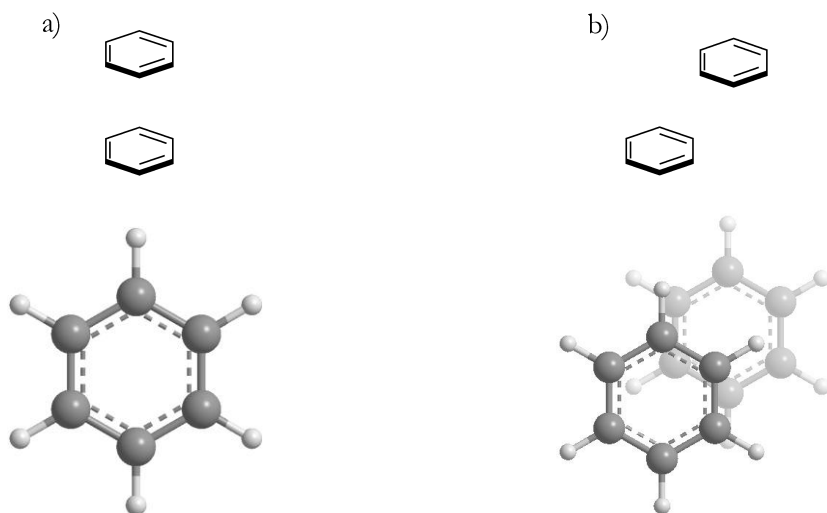


Figure 2 a) The sandwich benzene dimer with the two monomers eclipsed. b) The parallel-displaced benzene dimer with the two monomers off-set. Both a side (top) and top (bottom) view are provided.

Discrepancy exists in the literature regarding the nature of the forces responsible for stacking interactions as will be shown in section 1.4. The benzene studies, studies on biological systems and the papers in the area of nanotechnology do not agree on the nature of the dominant (strongest) forces in stacking interactions. The goal of this thesis is to examine some of the discrepancies and thereby bring the literature closer together on the nature of the forces responsible for stacking interactions.

1.3 Applications of stacking interactions

As mentioned in the previous sections, stacked structures are found in a variety of different fields ranging from biology,¹⁻⁵ to nanotechnology,⁶⁻⁹ and traditional chemistry.¹³⁻¹⁶ This section elaborates on the importance of the role of stacked structures in each of these areas.

1.3.1 Stacked structures in biology

Stacked structures play a crucial role in stabilizing DNA and RNA molecules.¹ The interaction energy associated with stacking is as essential to stabilizing the conformations of DNA and RNA as that associated with hydrogen bonding.¹ Stacked structures are also present in the interactions between protein side-chains and nucleic acids.³⁻⁴ Furthermore, stacking interactions are found to occur between DNA and certain cancer-causing molecules, such as acridine, which intercalate into DNA.⁵ Therefore, understanding stacking is an important factor in better understanding these important phenomena.

Another specific example of a biological application of stacking interactions is their potential role in the design of universal nucleobases. A universal nucleobase, in theory, should be able to replace any other nucleobase in a DNA or RNA strand.⁹⁷ For this to happen, any potential universal nucleobase should have equal affinity toward all natural nucleobases without destabilizing the helix and should also be able to act as a substrate for DNA enzymes. Universal nucleobases have potential applications in gene therapy, as hybridization probes and in the design of primers for PCR.⁹⁷ While some universal nucleobases are currently in use, they have shortcomings such as their ability to act as substrates for DNA enzymes.⁹⁷ Indeed, it has been challenging to find molecules that satisfy all of these criteria. Since the specificity of natural nucleobases results from their hydrogen bonding and stacking interactions, understanding stacking interactions is one key aspect to designing universal nucleobases.

1.3.2 Stacked structures in nanotechnology

Stacking interactions are useful in creating self-assembling systems used in nanotechnology. Self-assembled stacked structures are attractive because of their simplicity and low cost to manufacture,⁶ and this has resulted in extensive research in this particular field of study. One

application of self-assembled stacked structures is in the field of photovoltaics.⁶⁻⁷ Self-assembled photovoltaics are attractive because they combine the electronic properties of semiconductors with the processivity of polymers.⁶ These structures have also been shown to have unique photophysical characteristics,⁹ such as non-linear optical properties.⁸ The market for non-linear optical materials in industries such as telecommunications was estimated to be \$856.1 million in 2005⁹⁸.

1.3.3 Stacked structures in organic chemistry

Stacked structures have also been shown to play a role in synthetic chemistry. Stacked structures enable stereospecificity of a number of common organic reactions such as Diels-Alder, Friedel Crafts, alkylation reactions, as well as less common reactions, such as the addition of 2-trimethylsilyloxyfuran to N-benzyl nitron.¹⁶

An example of the ability of π -stacking to control the stereoselectivity of product formation can be seen in the addition of cyclopentadiene to a derivative of levoglucosenone (the major product of the pyrolysis of cellulose).¹³ In this Diels-Alder reaction, one of the two faces able to take part in the reaction is blocked due to stacking with a phenoxy group. As a result, the reaction gives a product with S-stereochemistry (up to 87%). Interestingly, if more than 1.5 equivalents of the Lewis acid EtAlCl₃ are present, a change in stereoselectivity leads to the formation of the R-stereoisomer (by up to 97%).¹³ This change in stereoselectivity has been attributed to a change in the preferred stacking configuration caused by coordination of the molecules with Al in the Lewis acid.¹³

1.4 Forces involved in stacking interactions

Different forces have been deemed responsible for stacking interactions, the main ones being electrostatics, dispersion and charge transfer.⁸³

Electrostatic interactions are the interactions between the permanent charge separations in the monomers.⁹⁵ The most basic definition of electrostatic interactions accepted in the literature is

that these are governed by Coulomb's Law,⁹³⁻⁹⁶ where the interactions between any two charges in the system are directly proportional to the product of the magnitude of the charge and inversely proportional to the square of the distance between the two charges. Specifically, the force can be calculated as:

$$F = \frac{k.q_1.q_2}{r^2} \quad \dots(1)$$

where q_1 and q_2 are the magnitude of the charges, r is the distance between the two charges and k is the constant of proportionality.

In cases where multiple point charges exist in a monomer, the electrostatic interactions between the monomers can be calculated as the sum of the interactions between the point charges. However, calculating the interaction between each point charge can be time consuming. Therefore, the interaction is simplified to the interaction between the monomer multipole moments. The multipole moment chosen to represent the charge distributions can range from the simplest monopole, to dipole, quadrupole or even higher multipole moments, such as hexadecapole. This is done by representing the charge interaction as a power series in the inverse distance between the charges.

The literature on stacking interactions also discusses the electrostatic contribution in terms of the electron density over the (benzene) ring.⁶⁸⁻⁶⁹ For interactions with electron rich molecules, increased electron density over the (benzene) ring causes increased electron repulsion and results in weaker stacking interactions, whereas decreased electron density caused by electron-withdrawing groups results in smaller electron repulsion and therefore increases stacking interactions.⁶⁹ For interactions with electron deficient molecules, the opposite trend is said to hold where electron-donating groups increase the stacking interactions with the electron deficient ring, while electron-withdrawing groups decrease the stacking interactions with the electron deficient ring.⁶⁸

A third method of estimating electrostatic interactions used in the literature is to examine the interactions at the Hartree-Fock (HF) level of theory (Chapter 2, section 2.1.2).¹¹⁰ The HF interaction energy allows an estimate of the effect of electrostatics and exchange repulsion to the net stacking interaction.^{95,99}

Dispersion interactions, also known as van-der Waals interactions, are the interactions between the instantaneous and induced dipoles in the monomers. Dispersion interactions occur most strongly at the distance equal to the sum of the van der Waals radii of the atoms. Incorporating dispersion interaction models of stacked structures is essential since the largest stabilizing contributor to stacking has been found to be dispersion.^{78,87} Dispersion is modeled either empirically ($E_{\text{disp}} = -C_6/R^6$, where C_6 is the calculated molecular coefficients of dispersion and R is the distance between the molecules) or by including electron correlation using ab initio methods (refer to Methods sections 2.1.3 and 2.1.4 for more detail). It has been shown that the dispersion interactions in π - π stacking need to be modeled using ab initio electron correlation methods since empirical methods do not correctly account for π - π stacking.⁸⁷ Therefore, the studies in this thesis use ab initio methods.

Dispersion interactions are thought to be related to the polarizability of the monomers since a larger polarizability is associated with stronger stacking interactions.¹⁰⁰ The electronic polarizability discussed in this thesis is the dipole polarizability, which is defined as the ratio of the induced dipole moment, p , of an atom to the electric field, E , that produces this dipole moment. Specifically,

$$\alpha = p / E \quad \dots(2)$$

where α is the dipole polarizability whose units are Bohr³.

The literature has also suggested that substituent-ring interactions are a source of the dispersion contribution to stacking (this does not rule out the possibility of stabilization due to electrostatics). This is because the stacking stabilization always increases with an increase in the

number of substituents, irrespective of whether the substituents are electron-donating or electron-withdrawing.¹⁰⁴ Since electron-withdrawing and electron-donating groups have the same net effect, electrostatics has been ruled out as a source of stabilization. Instead, increased substituent-ring interactions may result from dispersion interactions.

Finally, charge transfer interactions are caused by the partial transfer of charge from one monomer to another. These interactions occur at distances shorter than the sum of the van-der Waals radii and are a result of differing electrostatic potentials. Charge transfer can occur either in the ground state (as seen for ions) or as a result of electron excitation from the ground state. The latter complexes are called exciplexes and are associated with coloured compounds.¹⁰⁵ During charge transfer, electrons move from the electron donor to the electron acceptor because the electron acceptor provides lower energy orbitals. As a result, the energy of the whole system decreases, which causes stacking stabilization. In exciplexes, the electrons move from the electron donor to the electron acceptor only in the excited state of the dimer.

There is discrepancy in the literature on the nature of the dominant interactions in stacked structures. Most of the literature studying stacked benzene structures only discusses electrostatics and dispersion as being responsible for stacking interactions.^{68-70,73-74,78-80,86,89-92} In contrast, a handful of studies on stacked benzene structures attribute trends in stacking interaction to charge transfer.⁸³⁻⁸⁵ The literature on stacked self-assembling structures^{6-7,10-12,106} attributes stacking interactions to dipole-dipole interactions (electrostatics) and charge transfer. Both intramolecular and intermolecular charge transfer have been found to be important in these studies (based on observed charge transfer bands). Lastly, papers studying stacking between neutral molecules in a biological context have noted the importance of dipole-dipole interactions (electrostatics) and polarizabilities (dispersion) in determining stacking interactions^{2,102-103} The rings are the same within the benzene studies but are different between the benzene, nucleobase and stacking self-assembling systems and it shall be

examined whether the incongruities on the nature of forces dominating stacking interactions within different parts of the literature are a result of ring types or can similarities be found across systems with different ring types.

1.5 Overview of theoretical and experimental benzene, biological and stacking application literature

In this section, the theoretical and experimental literature on benzene dimers, biological dimers and applications of stacking is reviewed from the viewpoint of the nature of forces said to be responsible for stacking interactions. Furthermore, the differences between the theoretical and experimental benzene studies are examined in more detail, as well as possible reasons for differences in the data sets.

1.5.1 Overview of experimental data from studies on stacking interactions

Various experimental models have been used to study stacking interactions. These include the 1,8-diarylnaphthalene model,⁶⁹ the triptycene based model,⁸⁶ and the chemical double mutant cycle.⁹² The 1,8-diarylnaphthalene model and the triptycene model are molecular torsion balance experiments which use NMR to study different conformations of the molecules. In the 1,8-diarylnaphthalene model, the stacking interactions were measured using the barrier to rotation between the two stacked conformations, with a higher barrier corresponding to stronger stacking interactions.⁶⁹ In the triptycene based model, the ratio of stacked to unstacked conformation were measured using NMR, which was in turn used to calculate the ΔG for conversion from the unstacked to the stacked conformation.⁸⁶ In the chemical double mutant cycle, the ΔG of dimerization between two molecules (consisting of phenyl rings attached to a backbone) were calculated using ¹H NMR titrations. Each of the phenyl rings were then removed and replaced by non-interacting substituents

in a step-wise manner and the differences in ΔG ($\Delta\Delta G$) were used to determine the strength of the stacking interactions between the phenyl rings.

Most of these studies examined either the phenyl-monosubstituted phenyl dimers (analogous to the benzene-monosubstituted benzene dimers studied in theoretical studies)⁷⁸, or the pentafluorophenyl-monosubstituted phenyl dimers (analogous to the hexafluorobenzene-monosubstituted benzene dimers studied in theoretical studies)^{84,88}. For the monosubstituted phenyl-lightly substituted phenyl dimers (where lightly substituted phenyl refers to rings with up to 3 substituents), it is found that electron-donating substituents weaken the stacking interactions relative to unsubstituted phenyl (Table 1). This is attributed to the fact that electron-donating groups increase the electron density between the rings and thereby increase the electron-electron repulsion. Electron-withdrawing groups have the opposite effect and increase the stacking interactions relative to phenyl. This is attributed to the fact that electron-withdrawing groups decrease the electron density between the rings and thereby decrease the electron-electron repulsion. As a result, electrostatics (lack of electron-electron repulsion) was concluded to be responsible for stacking interactions in these dimers.^{68-69,85-86,89-90}

In the pentafluorophenyl-phenyl dimers, the trend is reversed (Table 2). In this case, the electron-withdrawing substituents cause the weakest stacking interactions, while the electron-donating substituents cause the strongest stacking interactions. In some experimental studies,^{68,91} this trend has been attributed to electrostatics because of quadrupole interactions. Another study has also provided an electrostatics based explanation, but used electrostatic potential maps to explain the stacking interactions.⁸⁹ The authors used the fact that pentafluorophenyl has a large positive potential on the ring and will therefore stack the strongest with molecules with the most negative potential over the ring (Figure 3). However, the exact nature of these electrostatic interactions (ie, dipole vs quadrupole vs higher multipole) has not been deduced.

Table 1: Experimentally determined stacking interactions for some lightly substituted phenyl dimers where the identities of the electron-donating and electron-withdrawing groups are given in brackets.

	1,8-diarylnaphthalene derived model when stacked with nitrotoluene phenyl (barrier to rotation in kJ mol ⁻¹)*	Triptycene derived model when stacked with phenyl (ΔG in kJ mol ⁻¹)	Chemical double mutant cycle when stacked with 1,5-dimethyl phenyl ($\Delta\Delta G$ in kJ mol ⁻¹)
Electron-donating	103 (-OMe)	0.3 ± 0.2 (-OMe)	6.3 ± 3 (-NMe ₂)
Unsubstituted	104 (-H)	0.08 ± 0.2 (-H)	2 ± 2 (-H)
Electron-withdrawing	106 (-COOMe)	-2.3 ± 0.2 (-CN)	-3 ± 4 (-NO ₂)

* Note: For the 1,8-diarylnaphthalene derived model, a higher barrier to rotation corresponds to stronger stacking interactions.

Table 2: Experimentally determined stacking interactions for pentafluorophenyl dimers where the identities of the electron-donating and electron-withdrawing groups are given in brackets.

	1,8-diarylnaphthalene derived model (barrier to rotation in kJ mol ⁻¹)	Triptycene derived model (ΔG in kJ mol ⁻¹)	Chemical double mutant cycle ($\Delta\Delta G$ in kJ mol ⁻¹)
Electron-donating	84.6 (-Me)	-90.8 ± 0.2 (-NMe ₂)	-9.2 ± 4 (-NMe ₂)
Unsubstituted	-	-57.4 ± 0.2 (-H)	-12 ± 4 (-H)
Electron-withdrawing	81.6 (-NO ₂)	-56.5 ± 0.2 (-F)	-0.8 ± 0.4 (-NO ₂)

In addition to the electrostatics based explanation, one study suggested charge transfer can explain the trends in the stacking interactions of pentafluorophenyl.⁸³ The argument used was that the more electron rich the monosubstituted phenyl ring, the more electron density it can donate to the electron deficient pentafluorophenyl ring. This results in greater charge transfer and therefore stronger stacking interactions. As a result, electron-donating groups cause the strongest stacking interactions, while electron-withdrawing groups cause the weakest stacking interactions.

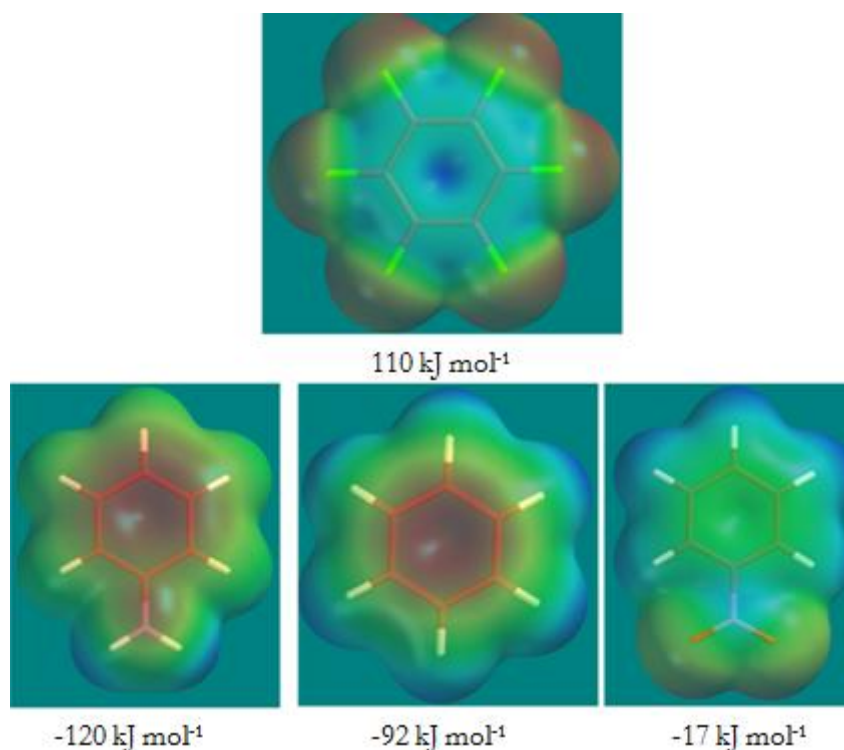


Figure 3: The electrostatic potential (ESP) maps calculated at the MP2/6-31G* level of theory for (a) hexafluorobenzene (b) aminobenzene, (c) benzene and (d) nitrobenzene. The numbers below represent the ESP over the center of the ring. The colours (not standardized) correspond to the sign of ESP, with red representing negative ESP and colours far away from red in electromagnetic spectrum representing increasingly positive ESP with blue being the area of the most positive ESP.

A question then arises: why do different studies give different explanations (electrostatics vs. charge transfer) for the same trends in stacking interactions? The first part of the answer to this question has to do with the fact that the same trends are expected based on both electrostatics and charge transfer, and charge transfer in fact results from a difference in the monomer electrostatic potentials. Secondly, in their foundational study, Cozzi et al. proved that charge transfer interactions are not dominant in dimers of lightly substituted phenyls.⁶⁹ This was done by comparing the stacking interactions of the phenyl-cyanophenyl dimer and the cyanophenyl-cyanophenyl dimer and finding that the cyanophenyl-cyanophenyl dimer has the stronger stacking interactions. This showed that charge transfer interactions are not dominant in the monosubstituted phenyl dimers. However, this result was then extrapolated to heavily substituted pentafluorophenyl dimers.⁶⁸ Therefore, one of the central goals of this thesis is to determine whether the stacking interactions are the same for lightly substituted phenyl dimers and heavily substituted phenyl dimers. This thesis will try and accomplish this goal by examining changes in stacking interactions for a wider range of substituents around the benzene ring. This will also allow the evaluation of the effects of other forces such as dipole-dipole interactions, which have been found to contribute to stacking stabilization in biological dimers.^{50,56,61,101,103}

1.5.2 Overview of theoretical data from studies on stacking interactions

The trends reported in theoretical studies^{78,84,88} (Table 3) differ slightly from the trends from experimental studies. For the benzene-monosubstituted benzene systems, it was found that the benzene dimer stacks the weakest (-7.5 kJ mol^{-1}), while electron-withdrawing groups cause the strongest stacking interactions ($-12.8 \text{ kJ mol}^{-1}$ for cyano substituent).⁷⁸ While experiment agrees with calculations on the effect of electron-withdrawing groups, the two approaches disagree on the effect of electron-donating groups. Experimental studies find that electron-donating substituents weaken stacking interactions. For example, the experimental study by Cozzi et al.⁶⁹ found that stacking

stabilization was decreased by 0.8 kJ mol⁻¹ when a hydrogen on a phenyl group is replaced by the electron-donating methoxyl group (error margins were not reported in the paper). However, the theoretical studies find that the electron-donating hydroxyl group actually stabilizes the stacked dimer by 1.5 kJ mol⁻¹.⁷⁸ Electrostatics was used to explain the stronger interaction energy caused by electron-withdrawing groups in the theoretical studies.⁷⁸ However, the interaction energy of electron-donating groups cannot be explained on the basis of electrostatics alone and has been attributed to dispersion.⁷⁸

Table 3: Theoretically determined stacking interactions for dimers of benzene-monosubstituted benzene and hexafluorobenzene-monosubstituted benzene dimers where the identities of the electron-donating and electron-withdrawing groups are given in brackets.

	Benzene-monosubstituted benzene (CCSD(T)/aug-cc-pVTZ) ⁷⁸	Hexafluorobenzene-monosubstituted benzene (MP2/aug-cc-pVDZ) ⁸⁴	Hexafluorobenzene-monosubstituted benzene (M05-2X/6-31+G(d)) ⁸⁸
Electron-donating	-9.0 (-OH)	-38.5 (-NH ₂)	-23.8 (-NH ₂)
Unsubstituted	-7.5 (-H)	-31.1 (-H)	-20.5 (-H)
Electron-withdrawing	-12.8 (-CN)	-32.0 (-CN)	-15.2 (-CN)

There have been two studies on the interaction energies in hexafluorobenzene-monosubstituted benzene dimers, which are analogous to the pentafluorophenyl-monosubstituted phenyl dimers studied experimentally in terms of the electron densities over the rings.^{84,88} The results of both studies differ slightly as they were carried out at different levels of theory (ab-initio MP2/aug-cc-pVDZ vs. the DFT functional M05-2X/6-31+G(d) respectively). While DFT functionals usually fail to model dispersion interactions, this particular DFT functional was created to

correctly model the stacking interactions of benzene-monosubstituted benzenes. In both studies, electron-donating groups like amino substituents stack the strongest ($-38.5 \text{ kJ mol}^{-1}$ and $-23.8 \text{ kJ mol}^{-1}$, respectively, for the different levels of theory).^{84,88} However, the studies differ in the effect of electron-withdrawing groups. Some electron-withdrawing groups cause stronger stacking interactions relative to unsubstituted benzene (by 0.9 kJ mol^{-1} for the cyanobenzene-benzene dimer) in the study carried out at MP2/aug-cc-pVDZ level of theory⁸⁴, while all electron-withdrawing groups cause weaker stacking interactions relative to unsubstituted benzene in the other study carried out at M05-2X/6-31+G(d) (by 5.3 kJ mol^{-1} for the cyanobenzene-benzene dimer).⁸⁸ However, the second study only considered sandwich, not parallel-displaced, configurations. For the sandwich configuration, cyanobenzene was also found to stack weaker than benzene in the first study at MP2/aug-cc-pVDZ level of theory, but by a smaller amount (2.97 kJ mol^{-1}). It is interesting to note that while the trends in the studies differ for the hexafluorobenzene-benzene dimers, they are the same between MP2/aug-cc-pVDZ⁷⁸ and M05-2X/6-31+G(d) level of theory for the monosubstituted benzene-benzene dimers.⁸⁸ This could be because the M05-2X level of theory was optimized using the interaction energies of monosubstituted benzene-benzene dimers.¹¹¹ The stronger stacking interaction in the parallel displaced configuration at MP2/aug-cc-pVDZ⁸⁴ has been attributed to dispersion, while the weaker stacking interaction in the sandwich configuration at M05-2X/6-31+G(d) has been attributed to electrostatics.⁸⁸ Lastly, the relative trends from the study at MP2/aug-cc-pVDZ level of theory do not match experiment, while the results from the study at M05-2X/6-31+G(d) match experiment.

In addition to electrostatics and dispersion interactions, charge transfer interactions and substituent-ring interactions have also been implicated in stacking interactions in theoretical studies.^{74,84,88,104} Charge transfer interactions have been proposed for the hexafluorobenzene-dimethylaniline dimer.⁸⁴ Substituent-ring interactions have been proposed based on the fact that increasing number of substituents always cause increasing stacking interactions.⁷⁴ Electrostatics were

said to be responsible for stacking interactions based on the trends of hexafluorobenzene with various monosubstituted benzenes.⁸⁸ However, a later paper¹⁰⁴ shows that increasing the number of both electron-withdrawing and electron-donating groups increases the stacking stabilization with benzene and therefore electrostatics cannot be responsible for the stacking interactions. It was suggested that dispersion interactions are likely responsible for the substituent-ring interactions.

1.5.3 Why are there differences between experimental and theoretical studies?

Both experimental and theoretical studies have limitations and differences that must be kept in mind while comparing data. Experimental studies are affected by environmental variables such as solvent effects and secondary interactions. Theoretical studies, on the other hand, have shortcomings in the way electron correlation is treated and basis sets are defined. The shortcomings in theoretical studies are a result of the fact that our computational resources are finite and are not powerful enough to treat electron correlation and basis sets completely. Furthermore, experimentalists measure ΔG at a certain temperature, whereas theoreticians typically measure the electronic energy at 0K. The electronic energy is closer to experimental ΔH values than ΔG , since the electronic energies do not take into account entropic considerations.

1.5.4 Overview of data from biological stacking studies and studies on self-assembled stacked structures

For biological systems, theoretical studies have found stacking interactions to be dependent on dipole-dipole interactions because the conformations with the dipoles aligned favourably had greater stacking stabilization than the conformations where the dipoles were not aligned.^{50,56,61,101,103} In addition, both theoretical and experimental studies have shown that stacking interactions increase with increased polarizability of the monomers, particularly between systems of different sizes.^{2,100-103}

This has been attributed to stabilization caused by dispersion interactions. A possible role of charge transfer has been suggested, but only for cationic nucleobases.¹⁰¹ Lastly, hydrophobic effects have been found to be important when evaluating the stacking interactions between nucleobases in experimental studies in solvent.¹⁰⁷⁻¹⁰⁸

Both dipole moments and charge transfer have been implicated in the formation of self-assembling stacked structures. The importance of dipoles is shown by a study on merocyanine dyes, which found that the Gibbs free energy of dimerization has a high degree of correlation with the square of the dipole moment of the dyes.^{79,109} The role of charge transfer is inferred from the charge transfer bands which appear in the self-assembled complexes.^{6-8,10-12} Both intramolecular and intermolecular charge transfer bands are seen in the self-assembled stacked structures.

One reason why papers studying stacking interactions have not been able to attribute stacking stabilization solely to electrostatics or charge transfer is because both forces explain the trends seen with changing substituents. In this thesis, I examine the stacking interaction of a wider range of systems (as elaborated on in section 1.6) so that the trends expected based on electrostatics and charge transfer are different. Furthermore, I examine the effects of dipoles in benzene systems, since, although dipole effects have been noted in biological systems, these arguments have not been used in the benzene dimers literature to the best of my knowledge. Lastly, nucleobases are stacked with substituted benzenes in order to determine whether the trends seen in substituted benzene systems can be reproduced with nucleobases.

1.6 Thesis overview

Chapter 2 of the thesis presents the methods used to calculate the energy of the molecules. The Schrödinger Equation is presented, followed by an introduction to the HF method, perturbation theory, CCSD(T) method and basis sets. Next, the supermolecular approach used to calculate

stacking interactions is explained. Lastly, the CCSD(T)/complete basis set (CBS) extrapolation scheme used in this thesis is introduced.

In the present chapter, a number of unanswered questions regarding the nature of the dominant interaction responsible for stacking were outlined. This thesis will attempt to shed more light on these questions in Chapter 3 by first examining the stacking interactions of substituted benzene dimers. First, the stacking interactions between benzene and a series of monosubstituted benzenes is studied, where a number of electron-donating and electron-withdrawing substituents are considered. Next, the effects of changing the number and position of electron-withdrawing or electron-donating substituents on the benzene ring are examined in a systematic manner for stacking with the benzene, aminobenzene and cyanobenzene monomers. Figure 4 shows the number and combination of substituents examined around the benzene ring. This will allow the study of the effect of substituents on stacking interactions in more depth than has been done in the past with the goal of determining whether electrostatics, dispersion or charge transfer interactions are dominant in stacking. In addition, the effect of dipole-dipole interactions in benzene systems will be examined. Subsequently, the stacking interactions of hexasubstituted benzenes are studied as a function of the number of cyano or amino substituents. This will provide further information on the nature of interactions responsible for stacking. Lastly, the effect of increasing the basis set size and using different levels of theory are considered, which will also provide a better understanding of the nature of forces responsible for stacking interactions.

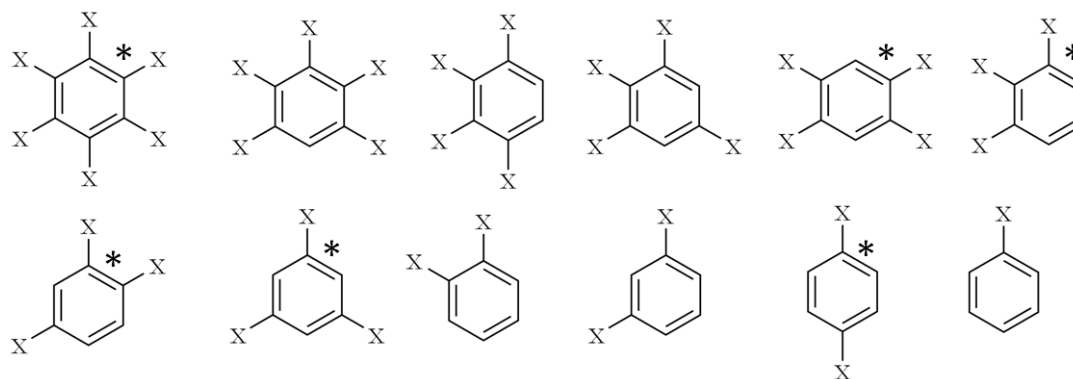


Figure 4: The substituents are indicated by the letter X. For the benzene dimers, electron withdrawing cyano and fluoro substituents and electron donating amino substituents are considered. For the nucleobase benzene dimers, the same substituents with the exception of cyano groups are examined. For the hexasubstituted benzene-polysubstituted benzene dimers, cyano or amino substitutions are considered for certain benzenes (marked with an asterisk (*)).

In Chapter 4, the stacking interactions between substituted benzenes and the natural nucleobases are examined. First, the stacking interactions between monosubstituted benzenes and the natural nucleobases are examined where a variety of electron-donating and electron-withdrawing substituents are considered. Next, the number of electron-withdrawing fluoro or electron-donating amino substituents is systematically varied to examine the trends in stacking interactions with respect to changing monomer dipole moments and number of substituents (Figure 4). This will be done to compare the results with the findings of Chapter 3 to conclude whether the nature of stacking interactions involving benzene and the natural nucleobases are the same. An explicit comparison has never been made between the stacking characteristics of benzene and nucleobase dimers as seen in the discordant views in the benzene and biological literature. If the nature of the forces responsible for stacking interactions are the same between benzene and natural nucleobases, then this will give strong support for the conclusions of Chapter 3 and give more confidence when applying the

findings reported in this thesis to other systems. Lastly, these results will also lend credibility to the use of benzene systems for understanding the fundamentals of stacking interactions.

Chapter 5 of the thesis reviews the Global Conclusions from this study and the impact of this work on the current understanding of stacking interactions. In addition, this Chapter will discuss possible directions for future work.

References

- (1) Kool, E. T. *Chem. Rev.* **1997**, *97*, 1473.
- (2) Wheaton, C. A.; Dobrowolski, S. L.; Millen, A. L.; Wetmore, S. D. *Chem. Phys. Lett.* **2006**, *428*, 157.
- (3) Xia, T.; Becker, H. C.; Wan, C.; Frankel, A.; Roberts, R. W.; Zewail, A. H. *PNAS* **2003**, *100*, 8119.
- (4) Kim, J. L.; Nikolov, D. B.; Burley, S. K. *Nature* **1993**, *365*, 520.
- (5) Lerman, L. S. *J. Mol. Biol.* **1961**, *13*.
- (6) Schmidt-Mende, L.; Fechtenkotter, A.; Mullen, K.; Moons, E.; Friend, R. H.; MacKenzie, J. D. *Science* **2001**, *293*, 1119.
- (7) Yamamoto, Y.; Fukushima, T.; Suna, Y.; Ishii, N.; Saeki, A.; Seki, S.; Tagawa, S.; Taniguchi, M.; Kawai, T.; Aida, T. *Science* **2006**, *314*, 1761.
- (8) Yufit, D. S.; Chetina, O. V.; Howard, J. A. K. *J. Mol. Struc.* **2006**, *784*, 214.
- (9) Watson, M. D.; Fechtenkotter, A.; Mullen, K. *Chem. Rev.* **2001**, *101*, 1267.
- (10) Zhang, C.; Zhang, X.; Zhang, X.; Fan, X.; Jie, J.; Chang, J. C.; Lee, C.-S.; Zhang, W.; Lee, S.-T. *Adv. Mater.* **2008**, *20*, 1716.
- (11) Xu, J.; Wen, L.; Zhou, W.; Lv, J.; Guo, Y.; Zhu, M.; Liu, H.; Li, Y.; Jiang, L. *J. Phys. Chem. C* **2009**, *113*, 5924.
- (12) Zhang, X.; Zhang, X.; Shi, W.; Meng, X.; Lee, C.; Lee, S. *Angew. Chem. Int. Ed.* **2007**, *46*, 1525.
- (13) Sarotti, A. M.; Fernandez, I.; Spanevello, R. A.; Sierra, M. A.; Suarez, A. G. *Org. Lett.* **2008**, *10*, 3389.
- (14) Ishihara, K.; Gao, Q.; Yamamoto, H. *J. Am. Chem. Soc.* **1993**, *115*, 10412.
- (15) Corey, E. J.; Loh, T. P.; Roper, T. D.; Azimioara, M. D.; Noe, M. C. *J. Am. Chem. Soc.* **1992**, *114*, 8290.
- (16) Jones, G. B. *Tetrahedron* **2001**, *57*, 7999.
- (17) Kabelac, M.; Hobza, P. *PCCP* **2007**, *9*, 903.
- (18) Kabelac, M.; Sherer, E. C.; Cramer, C. J.; Hobza, P. *Chem.-Eur.J.* **2007**, *13*, 2067.
- (19) Rezac, J.; Hobza, P. *Chem.-Eur.J.* **2007**, *13*, 2983.
- (20) de Vries, M. S.; Hobza, P. *Annu. Rev. Phys. Chem.* **2007**, *58*, 585.
- (21) Abo-Riziq, A.; Crews, B. O.; Compagnon, I.; Oomens, J.; Meijer, G.; Von Helden, G.; Kabelac, M.; Hobza, P.; de Vries, M. S. *J. Phys. Chem. A* **2007**, *111*, 7529.
- (22) Riley, K. E.; Hobza, P. *J. Phys. Chem. A* **2007**, *111*, 8257.

- (23) Kabelac, M.; Valdes, H.; Sherer, E. C.; Cramer, C. J.; Hobza, P. *PCCP* **2007**, *9*, 5000.
- (24) Cerny, J.; Hobza, P. *PCCP* **2007**, *9*, 5291.
- (25) Jurecka, P.; Cerny, J.; Hobza, P.; Salahub, D. R. *J. Comput. Chem.* **2007**, *28*, 555.
- (26) Reha, D.; Hocek, M.; Hobza, P. *Chem.-Eur.J.* **2006**, *12*, 3587.
- (27) Zendlova, L.; Hobza, P.; Kabelac, M. *ChemPhysChem* **2006**, *7*, 439.
- (28) Sponer, J.; Jurecka, P.; Marchan, I.; Luque, F. J.; Orozco, M.; Hobza, P. *Chem.-Eur.J.* **2006**, *12*, 2854.
- (29) Jurecka, P.; Sponer, J.; Cerny, J.; Hobza, P. *PCCP* **2006**, *8*, 1985.
- (30) Valdes, H.; Reha, D.; Hobza, P. *J. Phys. Chem. B* **2006**, *110*, 6385.
- (31) Dabkowska, I.; Gonzalez, H. V.; Jurecka, P.; Hobza, P. *J. Phys. Chem. A* **2005**, *109*, 1131.
- (32) Dabkowska, I.; Jurecka, P.; Hobza, P. *J. Chem. Phys.* **2005**, *122*, 204322/1.
- (33) Perez, A.; Sponer, J.; Jurecka, P.; Hobza, P.; Luque, F. J.; Orozco, M. *Chem.-Eur.J.* **2005**, *11*, 5062.
- (34) Rejnek, J.; Hanus, M.; Kabelac, M.; Ryjacek, F.; Hobza, P. *PCCP* **2005**, *7*, 2006.
- (35) Hanus, M.; Kabelac, M.; Nachtigallova, D.; Hobza, P. *Biochemistry* **2005**, *44*, 1701.
- (36) Reha, D.; Valdes, H.; Vondrasek, J.; Hobza, P.; Abu-Riziq, A.; Crews, B.; de Vries, M. S. *Chem.-Eur.J.* **2005**, *11*, 6803.
- (37) Vondrasek, J.; Bendova, L.; Klusak, V.; Hobza, P. *J. Am. Chem. Soc.* **2005**, *127*, 8232.
- (38) Kabelac, M.; Zendlova, L.; Reha, D.; Hobza, P. *J. Phys. Chem. B* **2005**, *109*, 12206.
- (39) Jurecka, P.; Sponer, J.; Hobza, P. *J. Phys. Chem. B* **2004**, *108*, 5466.
- (40) Pittner, J.; Hobza, P. *Chem. Phys. Lett.* **2004**, *390*, 496.
- (41) Hanus, M.; Kabelac, M.; Rejnek, J.; Ryjacek, F.; Hobza, P. *J. Phys. Chem. B* **2004**, *108*, 2087.
- (42) Sychrovsky, V.; Sponer, J.; Hobza, P. *J. Am. Chem. Soc.* **2004**, *126*, 663.
- (43) Chocholousova, J.; Vacek, J.; Hobza, P. *J. Phys. Chem. A* **2003**, *107*, 3086.
- (44) Jurecka, P.; Hobza, P. *J. Am. Chem. Soc.* **2003**, *125*, 15608.
- (45) Sponer, J.; Hobza, P. *Collect. Czech. Chem. Comm.* **2003**, *68*, 2231.
- (46) Hanus, M.; Ryjacek, F.; Kabelac, M.; Kubar, T.; Bogdan, T. V.; Trygubenko, S. A.; Hobza, P. *J. Am. Chem. Soc.* **2003**, *125*, 7678.
- (47) Jurecka, P.; Hobza, P. *Chem. Phys. Lett.* **2002**, *365*, 89.
- (48) Reha, D.; Kabelac, M.; Ryjacek, F.; Sponer, J.; Sponer, J. E.; Elstner, M.; Suhai, S.; Hobza, P. *J. Am. Chem. Soc.* **2002**, *124*, 3366.
- (49) Hobza, P.; Sponer, J. *J. Am. Chem. Soc.* **2002**, *124*, 11802.
- (50) Sponer, J.; Leszczynski, J.; Hobza, P. *Biopolymers* **2002**, *61*, 3.
- (51) Trygubenko, S. A.; Bogdan, T. V.; Rueda, M.; Orozco, M.; Luque, F. J.; Sponer, J.; Slavicek, P.; Hobza, P. *PCCP* **2002**, *4*, 4192.
- (52) Elstner, M.; Hobza, P.; Frauenheim, T.; Suhai, S.; Kaxiras, E. *J. Chem. Phys.* **2001**, *114*, 5149.
- (53) Jurecka, P.; Nachtigall, P.; Hobza, P. *PCCP* **2001**, *3*, 4578.
- (54) Kabelac, M.; Hobza, P. *J. Phys. Chem. B* **2001**, *105*, 5804.
- (55) Ryjacek, F.; Engkvist, O.; Vacek, J.; Kratochvil, M.; Hobza, P. *J. Phys. Chem. A* **2001**, *105*, 1197.
- (56) Sponer, J.; Leszczynski, J.; Hobza, P. *J. Mol. Struct.* **2001**, *573*, 43.
- (57) Sponer, J. V.; Leszczynski, J.; Hobza, P. *Theochem* **2001**, *573*, 43.
- (58) Sponer, J.; Hobza, P.; Leszczynski, J. *J. Comp. Chem.* **2000**, *5*, 171.
- (59) Sponer, J.; Hobza, P. *J. Phys. Chem. A* **2000**, *104*, 4592.

- (60) Hobza, P.; Sponer, J.; Cubero, E.; Orozco, M.; Luque, F. J. *J. Phys. Chem. B* **2000**, *104*, 6286.
- (61) Hobza, P.; Sponer, J. *Chem. Rev.* **1999**, *99*, 3247.
- (62) Hobza, P.; Havlas, Z. *Coll. Czech. Chem. Commun.* **1998**, *63*, 1343.
- (63) Hobza, P.; Sponer, J. *Chem. Phys. Lett.* **1998**, *288*, 7.
- (64) Kratochvil, M.; Engkvist, O.; Sponer, J.; Jungwirth, P.; Hobza, P. *J. Phys. Chem. A* **1998**, *102*, 6921.
- (65) Hobza, P.; Kabelac, M.; Sponer, J.; Mejzlik, P.; Vondrasek, J. *J. Comp. Chem.* **1997**, *18*, 1136.
- (66) Sponer, J.; Gabb, H. A.; Leszczynski, J.; Hobza, P. *Biophys. J.* **1997**, *73*, 76.
- (67) Cozzi, F.; Annunziata, R.; Benaglia, M.; Cinquini, M.; Raimondi, L.; Baldridge, K. K.; Siegel, J. S. *Org. Biomol. Chem.* **2003**, *1*, 157.
- (68) Cozzi, F.; Siegel, J. S. *Pure Appl. Chem.* **1995**, *67*, 683.
- (69) Cozzi, F.; Cinquini, M.; Annunziata, R.; Siegel, J. S. *J. Am. Chem. Soc.* **1993**, *115*, 5330.
- (70) Arnstein, S. A.; Sherrill, C. D. *PCCP* **2008**, *10*, 2646.
- (71) Smith, T.; Slipchenko, L. V.; Gordon, M. S. *J. Phys. Chem. A* **2008**, *112*, 5286.
- (72) Takatani, T.; Sherrill, C. D. *PCCP* **2007**, *9*, 6106.
- (73) Sinnokrot, M. O.; Sherrill, C. D. *J. Phys. Chem. A* **2006**, *110*, 10656.
- (74) Ringer, A. L.; Sinnokrot, M. O.; Lively, R. P.; Sherrill, C. D. *Chem. Eur. J.* **2006**, *12*, 3821.
- (75) Ringer, A. L.; Figgs, M. S.; Sinnokrot, M. O.; Sherrill, C. D. *J. Phys. Chem. A* **2006**, *110*, 10822.
- (76) Tauer, T. P.; Derrick, M. E.; Sherrill, C. D. *J. Phys. Chem. A* **2005**, *109*, 191.
- (77) Tauer, T. P.; Sherrill, C. D. *J. Phys. Chem. A* **2005**, *109*, 10475.
- (78) Sinnokrot, M. O.; Sherrill, C. D. *J. Am. Chem. Soc.* **2004**, *126*, 7690.
- (79) Sinnokrot, M. O.; Sherrill, C. D. *J. Phys. Chem. A* **2004**, *108*, 10200.
- (80) Sinnokrot, M. O.; Sherrill, C. D. *J. Phys. Chem. A* **2003**, *107*, 8377.
- (81) Sinnokrot, M. O.; Valeev, E. F.; Sherrill, C. D. *J. Am. Chem. Soc.* **2002**, *124*, 10887.
- (82) Gung, B. W.; Wekesa, F.; Barnes, C. L. *J. Org. Chem.* **2008**, *73*, 1803.
- (83) Gung, B. W.; Xue, X. W.; Zou, Y. *J. Org. Chem.* **2007**, *72*, 2469.
- (84) Gung, B. W.; Amicangelo, J. C. *J. Org. Chem.* **2006**, *71*, 9261.
- (85) Gung, B. W.; Patel, M.; Xue, X. W. *J. Org. Chem.* **2005**, *70*, 10532.
- (86) Gung, B. W.; Xue, X.; Reich, H. J. *J. Org. Chem.* **2005**, *70*, 3641.
- (87) Grimme, S. *Angew. Chem. Int. Ed.* **2008**, *47*, 3430.
- (88) Wheeler, S. E.; Houk, K. N. *J. Am. Chem. Soc.* **2008**, *33*, 10854-10855.
- (89) Cockroft, S. L.; Perkins, J.; Zonta, C.; Adams, H.; Spey, S. E.; Low, C. M. R.; Vinter, J. G.; Lawson, K. R.; Urch, C. J.; Hunter, C. A. *Org. Biomol. Chem.* **2007**, *5*, 1062.
- (90) Cockroft, S. L.; Hunter, C. A.; Lawson, K. R.; Perkins, J.; Urch, C. J. *J. Am. Chem. Soc.* **2005**, *127*, 8594.
- (91) Adams, H.; Blanco, J. L. J.; Chessari, G.; Hunter, C. A.; Low, C. M. R.; Sanderson, J. M.; Vinter, J. G. *Chem. Eur. J.* **2001**, *7*, 3494.
- (92) Adams, H.; Hunter, C. A.; Lawson, K. R.; Perkins, J.; Spey, S. E.; Urch, C. J.; Sanderson, J. M. *Chem. Eur. J.* **2001**, *7*, 4863.
- (93) Tsuzuki, S.; Mikami, M.; Yamada, S. *J. Am. Chem. Soc.* **2007**, *129*, 8656.
- (94) Tsuzuki, S.; Honda, K.; Uchimaru, T.; Mikami, M. *J. Chem. Phys.* **2005**, *122*, 8.
- (95) Tsuzuki, S.; Honda, K.; Uchimaru, T.; Mikami, M.; Tanabe, K. *J. Am. Chem. Soc.* **2002**, *124*, 104.

- (96) Tsuzuki, S.; Uchimaru, T.; Sugawara, K.; Mikami, M. *J. Chem. Phys.* **2002**, *117*, 11216.
- (97) Loakes, D. *Nucleic Acids Res.* **2001**, *29*, 2437.
- (98) Kalisky, O. *BCC Research* **2005**, *Research Report # GB117N*.
- (99) Jeziorski, B.; Moszynski, R.; Szalewicz, K. *Chem. Rev.* **1994**, *94*, 1887.
- (100) Rosemeyer, H.; Seela, F. *J. Chem. Soc. Perkin Trans. 2* **2002**, 746.
- (101) Rutledge, L. R.; Campbell-Verduyn, L. S.; Hunter, K. C.; Wetmore, S. D. *J. Phys. Chem. B* **2006**, *110*, 19652.
- (102) Rutledge, L. R.; Wheaton, C. A.; Wetmore, S. D. *PCCP* **2007**, *9*, 497.
- (103) Rutledge, L. R.; Campbell-Verduyn, L. S.; Wetmore, S. D. *Chem. Phys. Lett.* **2007**, *444*, 167.
- (104) Ringer, A. L.; Sherrill, C. D. *J. Am. Chem. Soc.* **2009**, *131*, 4574.
- (105) Sukumaran S. Babu; Vakayil K. Praveen; Seelam Prasanthkumar; Ayyappanpillai Ajayaghosh *Chem. Eur. J.* **2008**, *14*, 9577.
- (106) Yamauchi, Y.; Yoshizawa, M.; Fujita, M. *J. Am. Chem. Soc.* **2008**, *130*, 5832.
- (107) Guckian, K. M.; Schweitzer, B. A.; Ren, R. X. F.; Sheils, C. J.; Tahmassebi, D. C.; Kool, E. T. *J. Am. Chem. Soc.* **2000**, *122*, 2213.
- (108) Kool, E. T.; Morales, J. C.; Guckian, K. M. *Angew. Chem. Int. Ed.* **2000**, *39*, 990.
- (109) Chen, Z.; Lohr, A.; Saha-Moller, C. R.; Wurthner, F. *Chem. Soc. Rev.* **2009**, *38*, 564.
- (110) Jensen, Frank *Introduction to Computational Chemistry*, 2nd ed.; Wiley & Sons: New Jersey, **2007**.
- (111) Zhao, Y.; Schultz, N. E.; Truhlar, D. G. *J. Chem. Theory Comp.* **2006**, *2*, 364–382.

2 Methods

This Chapter introduces the reader to the different computational chemistry tools used to study stacking interactions in this thesis. These include the methods used to calculate the energies of molecules (HF, MP2 and CCSD(T)) and the supermolecular approach for calculating the strength of stacking interactions. For a more detailed explanation of the different methods, the reader is referred to any undergraduate computational chemistry textbook.¹ Lastly, the methodology used to estimate the stacking interaction energy at the CCSD(T)/CBS limit will be explained.

2.1 Methods used to calculate the energies of molecules

Three types of ab initio methods are used in this thesis to calculate the stacking interactions of molecules: Hartree-Fock (HF), Moller-Plesset perturbation theory up to the second order of correction (MP2), and coupled cluster theory including single, double and perturbative triple excitations (CCSD(T)). The underlying theories of these approaches shall be outlined below.

2.1.1 Schrödinger Equation

The Schrödinger Equation describes a molecular system using a wavefunction (ψ) and the energy (E) of the system can be calculated by applying the Hamiltonian operator (\hat{H}) onto the wavefunction as follows:

$$\hat{H}\psi = E\psi \quad \dots(3)$$

The different contributions to \hat{H} are as follows:

$$\hat{H} = \hat{T}_p + \hat{T}_e + \hat{V}_{pp} + \hat{V}_{ee} + \hat{V}_{pe} \quad \dots(4)$$

where \hat{T}_p represents the kinetic energy of protons, \hat{T}_e represents the kinetic energy of electrons, \hat{V}_{pp} represents the potential energy due to internuclear interactions, \hat{V}_{ee} represents the potential energy due to interelectronic interactions and \hat{V}_{pe} represents the potential energy due to the interactions between protons and electrons.

A limitation of the Schrödinger equation is that an exact solution cannot be determined for any but the simplest systems. Therefore, ab initio (first principles) quantum chemistry uses different approximations to solve the Schrödinger Equation and calculate the energies of chemical systems. I shall discuss these assumptions in the appropriate sections below. The simplest level of approximation, Hartree-Fock (HF) theory, will first be discussed in the following section.

2.1.2 Hartree-Fock Theory

Hartree-Fock theory estimates the energy of a given system by calculating an approximate wavefunction. The approximations included in the Hartree Fock wavefunction include the Born-Oppenheimer approximation, the allowed atomic orbitals are not always complete, energy eigenfunction is assumed to be describable by a single Slater determinant, and the electron-electron interactions are modeled by calculating the interaction between one electron and the average electronic field of all the other electrons. The wavefunction is written as a single Slater determinant and the orbitals are optimized iteratively until the change in energy falls below a set threshold, at which point the wavefunction is said to be self-consistent with itself.

The Born-Oppenheimer approximation is common to all ab initio methods used in this thesis and is justified based on the fact that nuclei are much heavier than electrons and therefore move much more slowly than electrons. The Born-Oppenheimer equation reduces the proton-proton potential energy in the Hamiltonian to a constant and the kinetic energy of the protons to zero. As a result, the Hamiltonian operator is simplified to the equation:

$$\hat{H} = \hat{T}_e + \hat{V}_{ee} + \hat{V}_{pe} \quad \dots(5)$$

The second major challenge for ab initio methods is to calculate the electron-electron interactions. In Hartree-Fock, this is done by calculating the interactions between each electron and the average electronic field of all other electrons. The shortcoming to this approach is that electron correlation is not taken completely into account, which is important for accurately describing

dispersion interactions. Therefore, in the present thesis, HF energies are used to approximate the contribution to stacking due to electrostatics and exchange. In order to take into account dispersion interactions, electron correlation is modeled using more sophisticated methods such as perturbation theory and CCSD(T), which are discussed in the following sections.

2.1.3 Møller-Plesset Perturbation Theory

Møller-Plesset perturbation theory divides the exact Hamiltonian (\hat{H}) into a known, “unperturbed”, Hamiltonian ($\hat{H}^{(0)}$) and a perturbation (\hat{H}') that does not have an exact solution.

$$\hat{H} = \hat{H}^{(0)} + \hat{H}' \quad \dots(6)$$

The unperturbed Hamiltonian is the HF Hamiltonian, while the perturbed Hamiltonian is defined as the difference between the correct electronic-electron interactions and the HF Hamiltonian.

Perturbation theory obtains the energy of the system by first solving the Schrödinger Equation for the unperturbed Hamiltonian and thereby obtaining the energy of the known unperturbed system.

$$\hat{H}^{(0)} \psi_n^{(0)} = E_n^{(0)} \psi_n^{(0)} \quad \dots(7)$$

Second, the energy and wavefunction are expressed as an infinite power series.

$$E_n = E_n^{(0)} + E_n^{(1)} + E_n^{(2)} + \dots \quad \dots(8)$$

$$\psi_n = \psi_n^{(0)} + \psi_n^{(1)} + \psi_n^{(2)} + \dots \quad \dots(9)$$

As the order of the corrections becomes larger, the magnitude of the corrections becomes smaller for well-behaved systems. The first-order correction is equal to the HF energy. The second order correction is calculated as:

$$E_n^{(2)} = \int_{-\infty}^{\infty} \psi_n^{(0)*} \hat{H}^{(1)} \psi_n^{(1)} \quad \dots(10)$$

or,

$$E_n^{(2)} = \sum_{i < j}^{occ} \sum_{a < b}^{vir} \frac{\langle \psi^{(0)} | \hat{H}^{(1)} | \psi_{ij}^{ab} \rangle \langle \psi_{ij}^{ab} | \hat{H}^{(1)} | \psi^{(0)} \rangle}{E_n^{(0)} - E_{ij}^{ab}} \quad \dots(11)$$

where ψ_{ij}^{ab} represents the excited wavefunction in which two electrons have been promoted from occupied orbitals i and j in the HF wavefunction to unoccupied orbitals a and b.

This thesis uses the Møller-Plesset implementation of perturbation theory (which is described above) up to second order corrections since higher-order corrections are not computationally feasible given the size of the systems being studied.

2.1.4 Coupled Cluster Theory

Coupled Cluster theory accounts for electron correlation by incorporating different excited state wave functions, in addition to the HF wavefunction, into the total wavefunction. In coupled cluster, the wavefunction is represented by the expression:

$$\Psi = e^{\hat{T}} \psi_0 \quad \dots(12)$$

where Ψ is the “exact” coupled cluster electronic wavefunction, \hat{T} is the excitation operator and ψ_0 is the HF wavefunction. The excitation operator is defined as follows:

$$e^{\hat{T}} = 1 + (\hat{T}_1 + \hat{T}_2 + \hat{T}_3 + \dots) + (\hat{T}_1 + \hat{T}_2 + \hat{T}_3 + \dots)^2 + (\hat{T}_1 + \hat{T}_2 + \hat{T}_3 + \dots)^3 + \dots \quad \dots(13)$$

or,

$$e^{\hat{T}} = 1 + \left(\hat{T}_2 + \frac{1}{2} \hat{T}_1^2 \right) + (\hat{T}_3 + \hat{T}_1 \hat{T}_2 + \frac{1}{6} \hat{T}_1^3) \dots \quad \dots(14)$$

where \hat{T}_1 operator yields all of all single excitations

$$\hat{T}_1 \psi_0 = \sum_i^{occ} \sum_a^{virt} t_i^a \psi_i^a \quad \dots(15)$$

\hat{T}_2 operator yields all of the doublet excitations

$$\hat{T}_2\psi_0 = \sum_{i>j}^{occ} \sum_{a>b}^{virt} t_{ij}^{ab} \psi_{ij}^{ab} \quad \dots(16)$$

\hat{T}_3 operator yields all of the triplet excitations, and so on.

$$\hat{T}_3\psi_0 = \sum_{i>j>k}^{occ} \sum_{a>b>c}^{virt} t_{ijk}^{abc} \psi_{ijk}^{abc} \quad \dots(17)$$

Because of computational limits, only single and double excitations are calculated in the present thesis using coupled cluster theory while the effects of the triple excitations are calculated perturbatively. This method is called CCSD(T) and has been referred to as the “gold standard” in computational chemistry due to the highly accurate results it yields.²

2.1.5 Basis sets

Pople basis sets use a set of functions to mimic atomic orbitals, which are regions of space which the electrons are allowed to occupy. Basis sets are usually specified after the level of theory. For example, MP2/6-31G*(0.25) states that the MP2 level of theory was used with the 6-31G*(0.25) basis set.

When determining the wavefunction of a particular system, the molecular orbitals are built using a linear combination of atomic orbitals. The basis functions most often used to describe the atomic orbitals are Gaussian type orbitals (GTOs). A general form of a Gaussian type atomic orbital is:

$$\Phi_{abc}^{GTO}(x, y, z) = Nx^a y^b z^c e^{-\zeta r^2} \quad \dots(18)$$

where N is a normalization constant, a,b,c control the total angular momentum (L=a+b+c) and ζ controls the width of the orbital (small ζ gives diffuse functions and vice-versa).

The most widely used basis set in this thesis is the modified 6-31G*(0.25) Pople basis set. 6-31G*(0.25) is a split-valence double zeta basis set, where “split” indicates that core orbitals and

valence orbitals are treated differently. Specifically, each core electron has only one atomic orbital, while the “double zeta” indicates that each valence electron has two basis functions. The 6 signifies that 6 primitive GTOs make up the core atomic orbitals. Primitive GTOs are used to mimic Slater Type Orbitals, the latter being physically more accurate but also more computationally expensive. The 31 indicates that each valence electron has two basis functions, the first one made up of 3 primitive GTOs and the second one made up of 1 primitive GTO. The * indicates that six d-type polarization functions have been added to the 6-31G basis functions. The (0.25) indicates that the ζ for the d-type polarization functions has been modified from 0.8 to 0.25, which making the basis function more diffuse. The rationale for changing the ζ is discussed in Chapter 3, section 3.2.2.

Other basis sets used in this thesis are the correlation consistent aug-cc-pVDZ and aug-cc-pVTZ Dunning’s basis sets. These basis sets are designed to converge smoothly to the complete basis set (CBS) limit for correlation methods and are therefore used to calculate the MP2/CBS limit. The CBS limit gives the energy of the system at an infinite basis sets and can only be determined by extrapolation. The “aug” in these basis sets stands for augmented (diffuse) orbitals, the “cc” stands for correlation consistent, “p” stands for polarized orbitals, “VDZ” stands for valence double zeta and “VTZ” stands for valence triple zeta.

2.2 Supermolecular method of calculating stacking interactions

Stacking interactions are calculated in this thesis by subtracting the energy of the monomer from the energy of the dimer, where all energies are calculated using the same level of theory and basis sets.

$$\Delta E = E_{dimer} - E_{monomer1} - E_{monomer2} \quad \dots(19)$$

A more negative ΔE corresponds to a stronger stacking energy. Basis Set Superposition Error (BSSE) occurs when the monomers in the dimer borrow the basis set of the other monomer and is a result of incomplete basis sets. BSSE errors are corrected for in this thesis using the method

described by Boys and Bernardi.³ In this method, the energy of each of the monomers is calculated using its own basis set and the basis set of the adjacent molecule. Once this is done, this difference for each of the monomer is then subtracted from the intermolecular interaction energy of the dimer.

2.3 Calculating the CCSD(T)/CBS energy

The most accurate energies calculated in this thesis are those extrapolated to the CCSD(T)/complete basis set (CBS) limit. These calculations are done to test the validity of the computationally efficient MP2/6-31G*(0.25) level of theory. Calculating the CCSD(T)/CBS limit is time consuming and computationally expensive. Specifically, three calculations are done using MP2 and three different basis sets (6-31G*(0.25), aug-cc-pVDZ and aug-cc-pVTZ). The latter two calculations are computationally expensive because the basis sets are large. A third calculation is done using the computationally expensive CCSD(T) method at the 6-31G*(0.25) basis set. First, the HF and MP2 energies obtained using the correlation consistent aug-cc-pVDZ and the aug-cc-pVTZ basis sets are extrapolated to calculate the MP2/CBS limit energies as described by Helgaker et al. in their two-point extrapolation method.^{4,5} Following this extrapolation, the $\Delta E_{\text{CCSD(T)-MP2}}$ energies are calculated with the 6-31G*(0.25) basis set and added to the MP2/CBS energy to yield the CCSD(T)/CBS extrapolated energy.^{4,5}

References

- (1) Jensen, Frank Introduction to Computational Chemistry, 2nd ed.; Wiley & Sons: New Jersey, **2007**.
- (2) Sinnokrot, M. O.; Sherrill, C. D. *Journal of the American Chemical Society* **2004**, *126*, 7690.
- (3) Boys, S. F.; Bernardi, F. *Molecular Physics* **1970**, *19*, 553.
- (4) Halkier, A.; Helgaker, T.; Jorgensen, P.; Klopper, W.; Koch, H.; Olsen, J.; Wilson, A. K. *Chemical Physics Letters* **1998**, *286*, 243.
- (5) Halkier, A.; Helgaker, T.; Jorgensen, P.; Klopper, W.; Olsen, J. *Chemical Physics Letters* **1999**, *302*, 437.

3 Stacking of benzene dimers

3.1 Introduction

This chapter examines the effects of different electron-withdrawing and electron-donating substituents on the stacking interaction energy of the benzene dimer. Previous studies on substituted benzene dimers have identified a number of different interactions as being responsible for stacking energy trends, such as electrostatics,¹⁻¹⁰ charge transfer,^{3,6} dispersion,¹¹⁻¹⁶ and substituent-ring interactions.^{10,12-13} However, there is no consensus on the nature of forces responsible for these stacking interactions. Furthermore, studies on stacking in non-benzene systems have noted the importance of dipole-dipole interactions,¹⁷⁻²³ intramolecular charge transfer and intermolecular charge transfer.²¹⁻²³ While a small section of the literature on benzene dimers has noted the presence of intermolecular charge transfer,^{3,6} the role of dipoles and intramolecular charge transfer has not yet been recognized in benzene dimers.

The goal of this chapter is to bring these disparate views on the source of stabilization of benzene dimers closer together. This will be done by examining a wider range of dimers than considered in the past. First, the role of dipoles in stacking shall be examined in the absence of dipole-dipole interactions by studying the stacking interactions of benzene-monosubstituted benzene dimers. In order to further understand the role of dipoles in the absence of dipole-dipole interactions, polysubstituted benzene-benzene dimers are studied where electron-withdrawing (cyano, fluoro) or electron-donating (amino) substituents are added to the polysubstituted benzene. In order to understand the role of charge transfer and dipole-dipole interactions in stacking, polysubstituted benzene-monosubstituted benzene dimers are studied next, where the effects of the cyano and amino substituents are examined. In order to test conclusions drawn for these dimers, the stacking interactions of hexasubstituted benzene-polysubstituted benzene dimers are investigated where the substituents are either the electron-withdrawing cyano group or the electron-donating amino group. Lastly, the stacking interactions of a select group of dimers is studied at the HF, MP2 and CCSD(T)

level in order to further elucidate the nature of stacking stabilizations, as well as verify the main computational approach.

3.2 Computational Methodology

3.2.1 Potential Energy Surface Scans

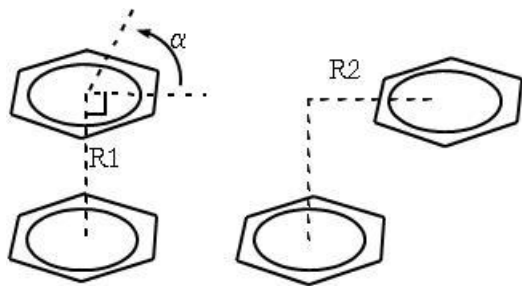


Figure 5: The variables considered in the potential energy surface scans. First, the relative orientation (α) and the distance between the monomers (R1) are simultaneously changed. The most stable structure is then used for a horizontal displacement (R2) scan where monomer was moved in 2 directions.

Potential energy surface scans are carried out in this study instead of optimizations because previous studies have found that the dimers adopt a tilted conformation upon optimization.²⁴⁻²⁵ Since T-shaped conformations are governed by substituent effects different from stacking interactions,¹¹⁻¹² potential energy scans were chosen to examine the structure-energy relationships on definitive stacking interactions.

Each monomer was fixed in C_s symmetry and optimized at the MP2/6-31G(d) level of theory. The monomers were fixed in C_s symmetry in order to minimize the number of conformations needed to be studied and to avoid stabilizing/destabilizing secondary interactions caused by, for example, puckering of the substituents. The optimized monomers were stacked so that their centers of mass were on top of each other along a cartesian axes. First, the effect of the relative orientation between the monomers was studied by simultaneously rotating the less substituted monomer counter-clockwise in 30° increments (defined as α) and changing the vertical distance

(defined as R1) between the monomers by 0.1 Å increments, usually between 3.2 Å and 3.6 Å (Figure 5). The starting structure for each set of rotations was set to the point where the torsional angle was 0° between the centers of mass of the two monomers and the substituent shown in Figure 6 with the less substituted monomer on top. Next, the molecule on top was rotated counter-clockwise in 30° increments.

Once the relative monomer orientation with the strongest stacking was determined with respect to α and R1, the molecule with the smaller number of substituents was moved on a horizontal grid 3 Å by 3 Å wide in 0.5 Å increments (R2 shifts, Figure 5). If the structure with the strongest stacking energy was on the edge of the 3 X 3 Å grid, then the grid was expanded to ensure that the minimum was identified. All dimer energies in this thesis report the strongest (most negative) stacking energy after the R2 shifts unless otherwise specified. To see an illustration of the PES resulting from R1, α and R2 scans, please refer to Tables 10 and 11 in the Appendix.

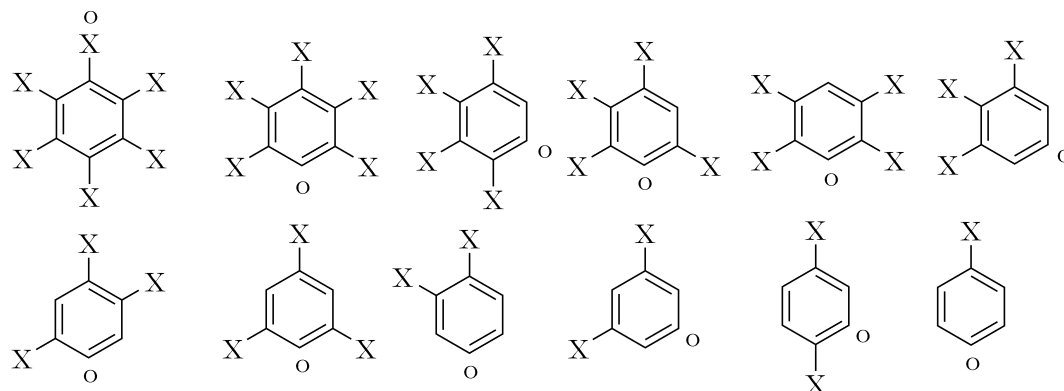


Figure 6: The different polysubstituted benzenes considered, where X denotes electron-donating amino or electro-withdrawing cyano or fluoro substituents. The circles indicate the hydrogen atoms aligned before the α rotations.

3.2.2 Level of Theory

All energies were calculated at the counterpoise corrected MP2/6-31G*(0.25) level of theory.²⁶ The level of theory and the associated basis set are based on the study by Hobza et al., who determined that MP2/6-31G*(0.25) is a good compromise between speed and accuracy for stacking

interactions of natural nucleobase dimers.²⁷ While MP2 is not as accurate as other methods, such as CCSD(T), and overestimates the binding energy with large basis sets, the medium-sized 6-31G*(0.25) basis set has been shown to give accurate results through a cancellation of errors. Specifically, this method yields binding energies within 75-90% of more expensive computational methods such as CCSD(T)/CBS for the natural nucleobase dimers.²⁸

A major difference between the benzene dimers and nucleobase dimers is that the benzene monomers in some cases do not have a dipole moment. Furthermore, MP2/6-31G*(0.25) has not been tested for dimers where the monomers do not have a dipole. However, the MP2/6-31G*(0.25) binding strength of the sandwiched benzene dimer (-7.4 kJ mol^{-1}) is very close to previously published CCSD(T) values at the complete basis set (CBS) limit (-7.6 kJ mol^{-1} and -6.2 kJ mol^{-1}).^{11,14} Similarly, the MP2/6-31G*(0.25) binding strength for the sandwich minima of the hexafluorobenzene-benzene dimer ($-25.4 \text{ kJ mol}^{-1}$) is close to the interaction energy at the CCSD(T)/CBS level ($-21.2 \text{ kJ mol}^{-1}$) although for a parallel displaced conformation.¹ As a result, the MP2/6-31G*(0.25) method seems appropriate for the present study, especially given the large number of calculations inherent in the potential energy scans employed (108 calculations per dimer). All calculations were carried out in the gas phase using the Gaussian 03 program.²⁹

3.3 Results and Discussion

3.3.1 Monosubstituted benzene-benzene dimers

The first set of dimers to be studied have unsubstituted benzene stacked with various monosubstituted benzenes. Both electron-withdrawing ($-\text{CN}$, $-\text{CONH}_2$, $-\text{F}$ and $-\text{NO}_2$) and electron-donating ($-\text{NH}_2$, $-\text{OH}$, and $-\text{CH}_3$) substituents are considered on the monosubstituted benzene ring. In addition, the unsubstituted benzene dimer is examined as a reference. The benzene-monosubstituted benzene dimers have been extensively studied in the past.^{2,10-11,14-16,24-25,30-31} However, the relationship between monomer dipole moments and stacking, which has been documented in studies on biological dimers¹⁷⁻²⁰ and self-assembled stacked structures,^{21-23,32} has never

been examined for benzene dimers. Furthermore, while biological studies have examined the effect of dipole-dipole interactions, the role of a monomer dipole moment in the absence of dipole-dipole interactions has not been studied. Therefore, the benzene-monosubstituted benzene dimers are studied in order to see if a single monomer dipole moment affects the stacking interactions of benzene dimers.

Figure 7 plots the stacking interaction energies of the benzene-monosubstituted benzene dimers as a function of the magnitude of the dipole moment of the monosubstituted benzenes (detailed data on the dimers is available in the Appendix Table 12). At the end of this chapter, the CCSD(T)/CBS values for a set of benzene dimers is calculated and compared back to the MP2/6-31G*(0.25) values (section 3.3.5, Table 7). The MP2/6-31G*(0.25) values are found to be within 81-112% of the CCSD(T)/CBS values. As a result, error bars equal to 31% of interaction energy are added to all of the graphs to remind the reader of the accuracy of the MP2/6-31G*(0.25) values with respect to the benzene dimers. A strong correlation exists between the interaction energy and dipole moments ($r=-0.93$). Given that the magnitude of the dipole is representative of the extent of charge separation in the monosubstituted benzene, it appears that the extent of charge separation in the ring corresponds to the strength of stacking interactions. This relationship holds more strongly for planar monosubstituted benzenes ($r=-0.98$). Toluene, which has an out-of-plane C-H $\cdots\pi$ interaction with the benzene ring, shows stronger interactions than would be expected based on its dipole moment (dipole=0.278, Figure 7) due to additional (out-of-plane) stabilizing C-H $\cdots\pi$ interactions.³³

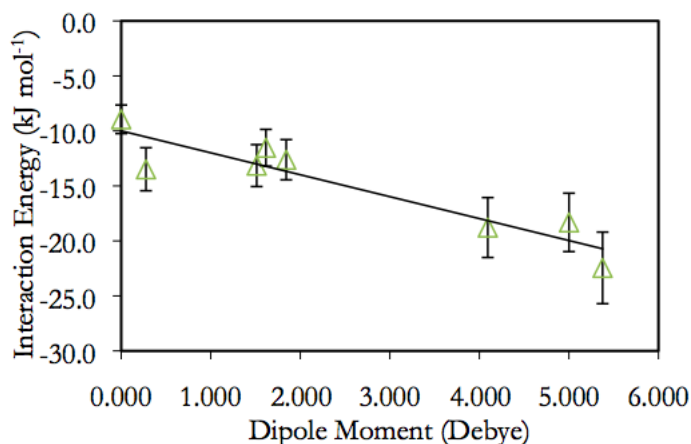


Figure 7: Plot of the stacking interaction energies of the monosubstituted benzene-benzene dimers as a function of the magnitude of the dipole moment of the monosubstituted benzene.

Although charge separation in the benzene monomer (dipole moment) is one possible reason for the observed trends in stacking interactions of monosubstituted benzene-benzene dimers, stabilization due to charge transfer would also cause the same trends. This is because charge transfer interactions are caused by the difference in electrostatic potential (ESP) of the monomer rings and the monomers with the largest charge separation also have the largest difference in ESP from non-polarized benzene. In addition, stabilization due to substituent-ring interactions^{10,12} explain the trends in stacking interactions since unsubstituted benzene stacks the weakest, and more polarizing substituents have the strongest dipoles and stacking interactions (Figure 7). However, on examining the structures of the dimers after the R2 scans (Appendix, Figure 27), direct substituent-ring interactions cannot be identified. Nevertheless, the substituent is always close to the unsubstituted benzene ring, which makes it difficult to definitively comment on the role of substituent-ring interactions. Although electrostatic interactions have also been thought to be behind the trends in stacking interactions in the past,^{4,7,9} they do not explain the trends in stacking interactions in the systems considered here since both electron-donating and electron-withdrawing substituents increase the stacking interactions relative to the benzene dimer. This suggests that electron-electron repulsion over the benzene rings does not cause the trends in stacking interactions. Dipole-induced dipoles is

another interactions which could explain the trends. However, other studies that have broken down the energy components^{11, 46} using SAPT found induction interactions (dipole-induced dipole) to be a very small component of stabilizing interactions that did not vary with the trends in the overall stacking energies. Lastly, dipole-dipole interactions, which are also considered electrostatic, cannot be behind the trends in stacking interactions because only one monomer in the dimer has a dipole moment. To sum up, charge separation in the benzene ring, charge transfer or substituent-ring interactions could all cause the calculated trends in stacking interactions, while electrostatics cannot explain the observed trends.

Previous theoretical work at both the CCSD(T)/CBS¹¹ and the M05-2X/6-31+G(d)¹⁰ levels have found identical trends to those reported here wherein any substituent, whether electron-donating or electron-withdrawing, increases the stacking interactions relative to the unsubstituted benzene dimer. The increased interactions caused by substituted benzenes has been attributed to dispersion interactions, whereas the stronger stacking interactions caused by electron-withdrawing groups relative to electron-donating groups has been attributed to electrostatics.¹¹ Experimental studies have found a different trend where electron-withdrawing groups increase the stacking interactions relative to benzene dimer, whereas electron-donating groups decrease the stacking interactions relative to the benzene dimer.^{3-4,7,9} Since the experimental results suggest that the stacking interactions change according to the electron density over the ring, electrostatics has been used to explain the observed stacking interactions.

The reason for the discrepancy between the experimental and theoretical results is not clear, but shortcomings in both experimental studies (effect of solvent, secondary interactions) and theoretical studies (level of theory and basis set) might be responsible for the different trends. For example, the experimental studies measuring the strength of stacking interactions compare the stacked structures with the non-stacked structures. While the non-stacked structures will vary depending on whether the 1,8-diarylnaphthalene model,⁶⁹ the triptycene model,⁸⁶ or the chemical double mutant cycle⁹² is being used, all of these will have confounding substituents-ring interactions

either due to direct interactions^{86,92} or as a result of conjugation.⁶⁹ If these confounding substituent ring interactions are greater than the effects of the substituent ring interactions the authors are interested in measuring, then the findings of these studies would be difficult to compare to the theoretical studies.

The correlation between the magnitude of the dipole moment of the substituted monomer and stacking interactions has also been noted in the past for some biological stacked structures¹⁷⁻²⁰ and self-assembling stacked systems.³² In certain cases, for example the pyrimidine cytosine, uracil and thymine dimers, the strength of the dipole moment does not necessarily correspond to the strength of the stacking interactions.¹⁷⁻²⁰ In these cases, the dipole moments might not be representative of the charge separation in the rings (as discussed in more detail in the next chapter on nucleobase-benzene dimers). Therefore, the effect of increasing charge separation in the ring shall be examined when the extent of charge separation is not represented by the dipole moment. This will be done by increasing the number of substituents around the benzene ring while keeping the dipole moment of the monomer equal to zero. Specifically, the interactions between the non-zero dipole polysubstituted benzene monomers and benzene will be examined. In addition, the effect of charge transfer and substituent-ring interactions can also not be ruled out at this point and shall be further discussed in the following sections.

3.3.2 Polysubstituted benzene-benzene dimers

In the previous section, it was noted that the stacking interactions of the monosubstituted benzene-benzene dimers increase with an increase in the magnitude of the dipole moment of the monosubstituted benzene. This section examines the stacking interactions of polysubstituted benzene-benzene dimers (Figure 6) where the effect of electron-withdrawing cyano and fluoro substituents, and the electron-donating amino substituent on the polysubstituted benzenes is examined. This will allow the effect of charge separation in the ring to be studied when the increase in charge separation does not necessarily correspond to increasing dipoles (where all of the zero-dipole polysubstituted benzene monomers are considered). For example, the difference in the charge

separation in 1,4-difluorobenzene and hexafluorobenzene is seen in Figure 8 even though both have a dipole moment of zero.

The effect of increasing charge separation shall also be examined for cases when this increase corresponds to increasing dipole moments as was the case for the monosubstituted benzene-benzene dimers. This shall be done by keeping the number and type of substituents constant, but changing the position of substituents. For example, comparing the stacking interactions of 1,4-dicyanobenzene-benzene, 1,3-dicyanobenzene-benzene and 1,2-dicyanobenzene-benzene dimers.

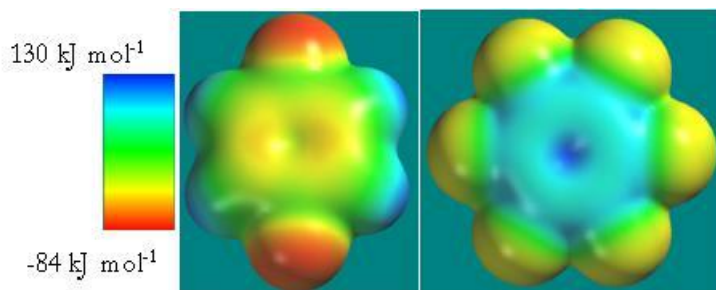


Figure 8: The electrostatic potential map calculated at MP2/6-31G* for 1,4-difluorobenzene (left) and hexafluorobenzene (right).

Figure 9 plots the stacking interaction energies of the polysubstituted benzene-benzene dimers as a function of the number of substituents. For both electron-withdrawing and electron-donating groups, the stacking interactions become stronger with increasing number of substituents, irrespective of the dipole moments. This suggests that stacking interactions are indeed dependent on the extent of charge separation in the benzene ring, even when the increase in charge separation does not correspond to increasing dipole moments. Charge transfer could be behind the increasing stacking stabilization with increasing charge separation. This is because increasing charge separation of the polysubstituted benzene ring increases the difference in ESP between the two molecules and thereby increases the potential for charge transfer. Alternatively, stronger stacking with increasing number of substituents could also be caused by substituent-ring interactions,^{10,12} which may be dominated by dispersion interactions.¹³ Stronger stacking with increasing number of substituents

cannot be a consequence of electrostatics (electron-electron repulsion) because increasing number of electron-donating substituents would be expected to weaken the electrostatic interactions.

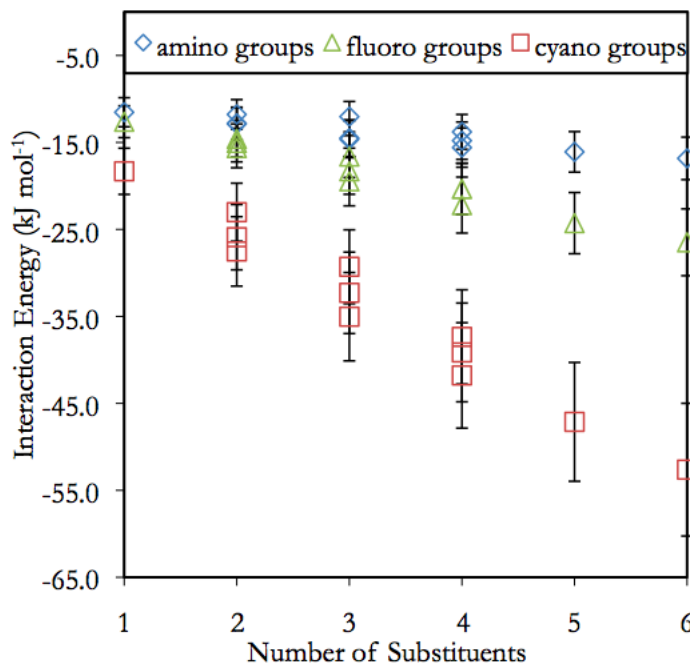


Figure 9: The stacking interactions of the polysubstituted benzene-benzene dimers showing an increase in the stacking interactions with increasing number of substituents.

An increase in the charge separation in the benzene ring is associated with an increase in the stacking interactions when the charge separation arises from an increase in the number of substituents (Figure 9). Increasing charge separation also corresponds to increasing stacking interactions when the difference in charge separation is caused by a different type of substituent. For instance, the cyano substituent causes the strongest stacking interactions ($-18.3 \text{ kJ mol}^{-1}$) followed by the fluoro substituent ($-12.6 \text{ kJ mol}^{-1}$) while the amino substituent causes the weakest stacking interactions ($-11.5 \text{ kJ mol}^{-1}$), which is in accordance with their dipole moments. In addition, the increase in stacking interactions as a result of increasing number of substituents is the greatest for the polycyanobenzenes ($m = -6.97 \text{ kJ mol}^{-1} \text{ substituent}^{-1}$), followed by the polyfluorobenzenes ($m = -2.87 \text{ kJ mol}^{-1} \text{ substituent}^{-1}$), while the polyaminobenzenes ($m = -1.10 \text{ kJ mol}^{-1} \text{ substituent}^{-1}$) lead to the smallest increase.

On examining the stacking interactions of polysubstituted benzenes with the same number and same type of substituents, the stacking interactions are generally found to strengthen with increasing dipole moments (Appendix, Table 13). It was previously noted that the increase in stacking stabilization caused by increasing number of substituents is greater than the increase in stacking stabilization caused by changing dipoles. Exceptions to this trend are found in some of the polyaminobenzene-benzene dimers where the stacking interactions of polyaminobenzene dimers with a large dipole (ex, 1,2-diaminobenzene-benzene, $\Delta E = -12.8 \text{ kJ mol}^{-1}$) can sometimes be stronger than a polyaminobenzene dimer with more substituents but a smaller dipole (ex, 1,3,5-triaminobenzene-benzene, $\Delta E = -12.0 \text{ kJ mol}^{-1}$). This is seen because the polyaminobenzene dimers show the smallest increase in stacking interactions with increasing number of substituents.

Previous studies have explained the increase in stacking interactions of polysubstituted benzene-benzene systems with increasing number of substituents on the basis of electrostatics,^{6,8} charge transfer,⁶ and substituent-ring interactions.¹² The studies that use electrostatic arguments have always considered an electron-rich ring stacked with an electron-deficient ring.^{6,8} These studies find that increasing the number of electron-withdrawing groups on the electron deficient ring strengthens the stacking interactions. This strengthening of stacking interactions has been explained on the basis of stronger quadrupole-quadrupole interactions⁶ and on the basis of stronger interactions between the electron-rich and electron-deficient cores of the two rings.⁸ However, Gung et al.⁶ noted that the same trend can also be explained on the basis of charge transfer. The only study to not propose electrostatics as a possible explanation found that both increasing the number of electron-donating groups and electron-withdrawing groups make the stacking interactions stronger.¹² Given the opposite effects of electron-donating and withdrawing groups on electrostatic interactions, this cannot be the correct explanation and substituent-ring interactions were suggested to be responsible for increased stacking interactions¹² and dispersion could be the force behind the substituent-ring interactions.¹³ On examining the structures of the polysubstituted benzene-benzene dimers after the R2 scans, it is found that the substituents never interact directly with the benzene monomer.

However, the substituents are always close to the benzene ring and therefore substituent-ring interactions cannot be ruled out. Interestingly, the rings show a greater degree of overlap with increasing number of substituents (Appendix, Figures 28 and 29), which would be expected to cause increased charge transfer stabilization because of greater orbital overlap.¹

To conclude, electron-electron repulsion cannot be the dominant force that increases the stacking stabilization with increasing number of substituents since both electron-withdrawing groups and electron-donating groups have the same effect. This trend holds true irrespective of the dipole or quadrupole moments as shown. Charge separation in the ring, charge transfer and substituent-ring interactions can all potentially cause the increase in stacking stabilization with increasing number of substituents. The next section examines the stacking interactions of polysubstituted benzene-monosubstituted benzene dimers in an attempt to determine which of these three forces is dominant.

3.3.3 Polysubstituted benzene-monosubstituted benzene dimers

In the previous section, it was shown that electrostatics cannot be the dominant force responsible for the strengthened stacking interactions caused by an increase in the number of substituents. It was argued that charge separation, charge transfer and substituent-ring interactions can all be responsible for the increase in stacking interactions with increasing substituents, but which of these interactions is dominant, if any, remains unclear. Furthermore, an increase in charge separation in the ring caused by different types of substituents and by increasing the dipoles was found to make the stacking interactions stronger.

The stacking interactions of polycyanobenzenes and polyaminobenzenes are again studied in this section. Specifically, the polycyanobenzenes and the polyaminobenzenes are stacked with cyanobenzene and aminobenzene, and their stacking interactions are compared back to those of benzene. The cyano substituent is chosen because it is a strong electron withdrawing group while the amino group is chosen because it is an electron donating while benzene serves as a control. Cyanobenzene is more electron deficient than benzene, while aminobenzene is more electron rich than benzene. Cyanobenzene has the most charge separation, followed by aminobenzene while

benzene has the least charge separation as indicated by their dipole moments (5.001 D, 1.616 D and 0.000 D respectively using the Mulliken charges at MP2/6-31G(d)). Therefore, comparing the stacking stabilization of aminobenzene, cyanobenzene and benzene will help determine whether it is charge transfer, or separation of charge in the benzene ring which is responsible for the *increase* in stacking stabilization with increasing number of substituents since the two properties will cause different trends as discussed below. Lastly, the effect of dipoles will also be examined to see if the increase in charge separation due to dipoles again corresponds with increasing stacking interactions, as seen in the previous two sections.

Figure 10 plots the stacking interactions of aminobenzene, benzene and cyanobenzene with polycyanobenzene as the number of cyano groups is increased. The stacking stabilization always increases with increasing number of cyano groups. For two or less than two cyano groups, cyanobenzene stacks the strongest, followed by aminobenzene and benzene. Given that cyanobenzene has the most charge separation, followed by aminobenzene and benzene, these results suggest that charge separation in the molecule dominates the stacking interactions. Alternatively, the same trends can also be explained by substituent-ring interactions where the substituent that causes more charge separation in the benzene ring also has the greater stacking stabilization, as shown for the monosubstituted benzene-benzene and polysubstituted benzene-benzene dimers. For three or four cyano substituents, it can be seen that cyanobenzene and aminobenzene experience almost the same stacking stabilization while benzene continues to stack the weakest. This implies that the difference in charge separation between cyanobenzene and aminobenzene is no longer the dominant force in determining the stacking stabilization energies. Instead, charge transfer interactions become increasingly important, as the polycyanobenzenes become increasingly electron deficient and the difference in ESP between the monomers increases. For four or more cyano substituents, aminobenzene always stacks stronger than cyanobenzene, while benzene continues to stack the weakest. Therefore, charge transfer (resulting from difference in ESP of the monomers) is the dominant force for determining the relative trends of aminobenzene and cyanobenzene, while charge

separation in the substituted benzene ring or substituent-ring interactions are dominant in determining the relative stacking interactions of benzene and cyanobenzene. The nature of the force responsible for increasing the stacking stabilization with increasing number of substituents shall be further examined below.

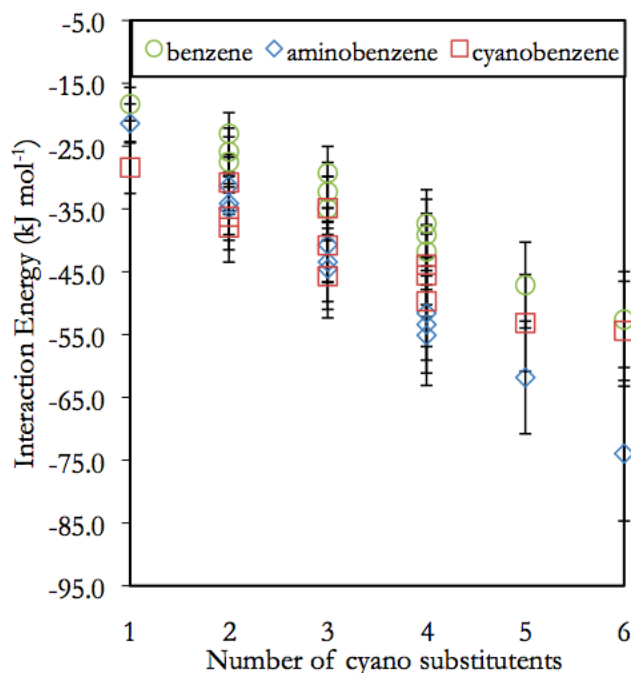


Figure 10: The stacking interaction energies of the polycyanobenzene-monosubstituted benzene dimers as a function of the number of cyano substituents.

In order to examine the dominant force in increasing the stacking interactions, the difference in stacking stabilization between zero-dipole di-, tri-, tetra- and hexa-cyanobenzenes is examined. Figure 11 plots the increase in stacking stabilization energies associated with increasing number substituents of zero-dipole tricyanobenzene, tetracyanobenzene and hexacyanobenzene dimers in comparison to the zero-dipole polycyanobenzene dimers with the next fewer number of cyano substituents. In almost all cases, aminobenzene shows the greatest increase in stacking stabilization, followed by benzene, while cyanobenzene shows the smallest increase in stacking stabilization. This trend suggests that charge transfer is the dominant force in these stacking interactions.

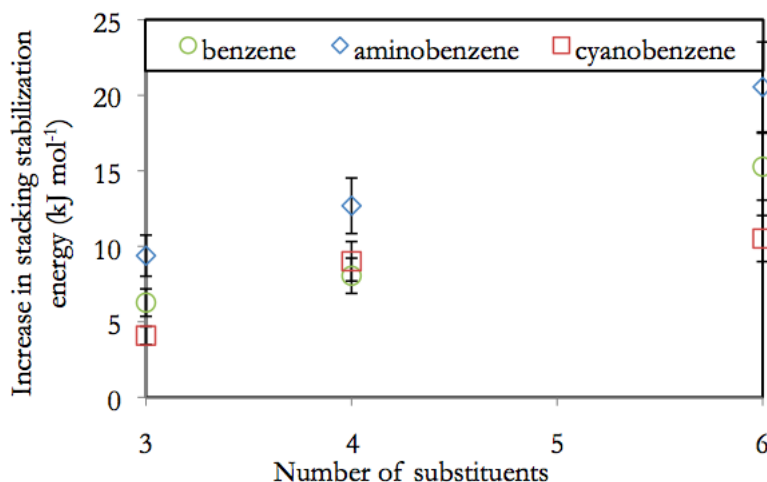


Figure 11: Increase in stacking stabilization energy of zero-dipole tri-, tetra- and hexa-cyanobenzene in comparison to the zero-dipole polycyanobenzene with the next fewest number of cyano substituents.

Lastly, the change in stacking stabilization with increasing dipoles shall be examined. The difference in stacking energies on going from a zero-dipole polycyanobenzene to the maximum-dipole polycyanobenzene with the same number of substituents was calculated (Figure 12). In all cases, an increase in the stacking interaction with increasing dipole moments is seen as had been noted in the last two sections. Among the different monosubstituted benzenes, cyanobenzene shows the greatest increase in stacking stabilization, followed by benzene, while aminobenzene shows the smallest increase in stacking stabilization with increasing dipole moments. This is not the trend expected based on dipole-dipole interactions, wherein cyanobenzene would be expected to show the greatest stacking stabilization, followed by aminobenzene, while benzene (with no dipole) would show the smallest stacking stabilization. In order to explain the unexpected trends, the structures of the polycyanobenzene dimers are examined. In all cases, the substituents are found to be away from each other, which implies that in the polycyanobenzene-cyanobenzene dimers, the dipole moment vectors in the monomers are anti-parallel (average torsional angle=165.9°), whereas, in the polycyanobenzene-aminobenzene dimers, the dipoles are parallel (average torsional angle=59.8°).

The anti-parallel dipole moment vectors have the negative center of charge of one monomer on top of the positive center of charge of the other monomer and vice-versa. This is energetically favourable as noted by the literature on stacking of natural nucleobases.^{20,34-36} The parallel dipoles, on the other hand, have the center of negative charge of one monomer on top of the center of negative charge of the other monomer, which is energetically unfavourable and explains why the polycyanobenzene-aminobenzene dimers show the smallest increase in stacking stabilization with increasing dipole moments. In all of the dimers, the substituents are always far away from each other and repulsion between the substituents could be the reason why the dipoles are parallel. The same trends have been noted by Sinnokrot and Sherrill for monosubstituted benzene dimers.¹¹

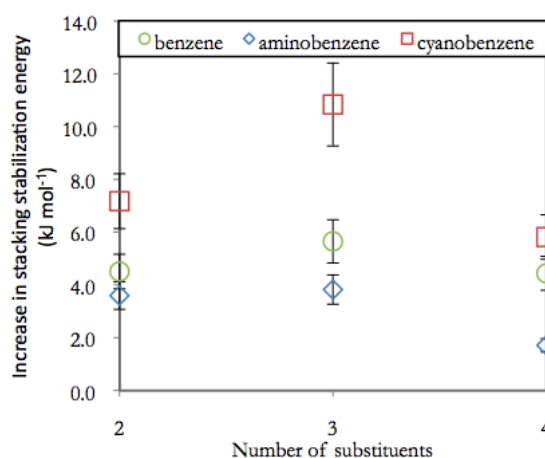


Figure 12: The increase in stacking stabilization energies on going from a zero-dipole polycyanobenzene to the maximum dipole polycyanobenzene with the same number of substituents.

Figure 14 plots the stacking interactions of the polyaminobenzene dimers against the number of amino substituents. Stacking interactions are found to always increase with increasing number of substituents. Cyanobenzene always stacks the strongest, followed by aminobenzene, while benzene stacks the weakest. Cyanobenzene would be expected to stack the strongest based on the charge separation in the monomer, charge transfer (caused by difference in ESP of the monomers) and substituent-ring interactions. Aminobenzene would be expected to stack stronger than benzene based on the extent of charge separation and substituent-ring interactions, while benzene would be

expected to stack stronger than aminobenzene based on charge transfer. Therefore, charge separation in the benzene ring or substituent-ring interaction dominates over charge transfer in dimers containing aminobenzene and benzene monomers. In the polycyanobenzene dimers, it was shown that charge transfer dominates the relative stacking interactions of cyanobenzene and aminobenzene for four or more cyano substituents. However, the same trend will not be visible in the polyaminobenzenes since the trends expected based on charge transfer, charge separation in the benzene ring and substituent-ring interactions are all the same, making it difficult to study the effects of charge transfer.

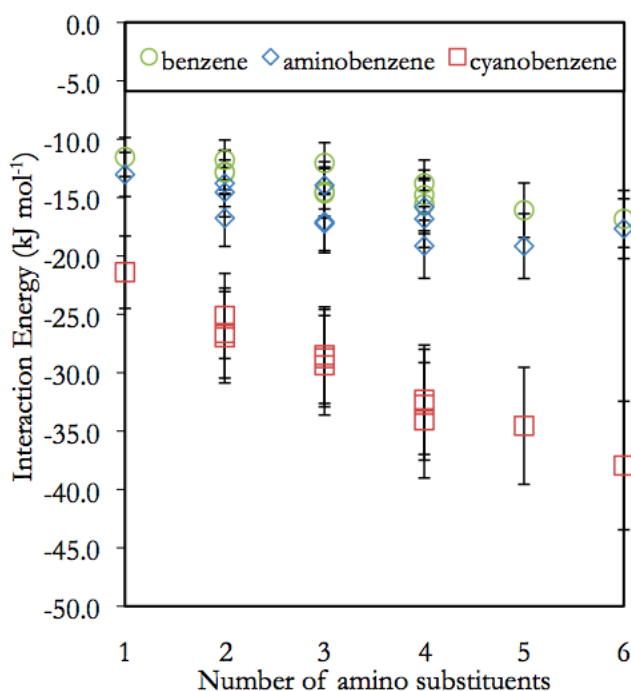


Figure 13: Stacking stabilization energies of polyaminobenzene-monosubstituted benzene dimers plotted as a function of number of amino substituents.

In order to examine the nature of the dominant force in polyaminobenzene dimers, the increase in stacking stabilization for zero-dipole tri-, tetra- and hexa-aminobenzene in comparison to the zero-dipole polyaminobenzene with the next fewer number of substituents is examined (Figure 14). Cyanobenzene shows the greatest increase in stacking interactions, followed by benzene, while aminobenzene shows the smallest increase in stacking interactions with increasing number of

substituents. Therefore, charge transfer appears to be the dominant force in increasing the stacking stabilization as the number of amino substituents is increased.

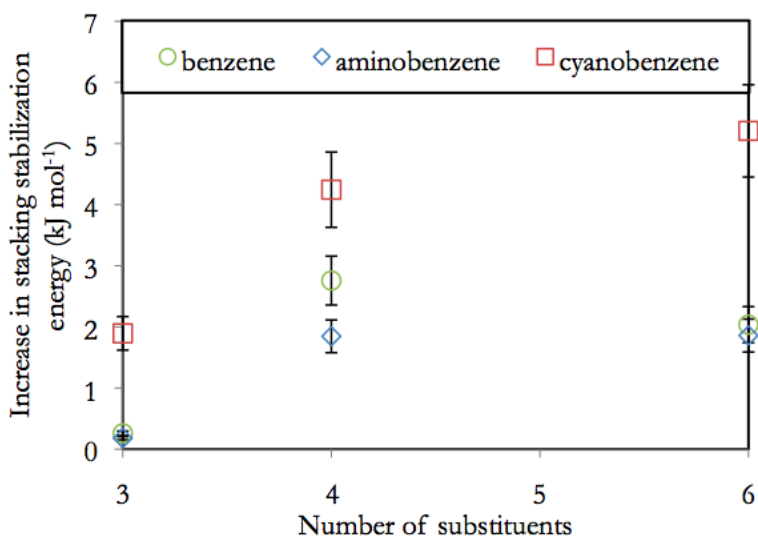


Figure 14: Increase in stacking stabilization with increasing number of substituents for zero-dipole polyaminobenzene containing dimers with benzene, aminobenzene and cyanobenzene. For example, for 3 substituents, the difference in stacking energy with 1,4-diaminobenzene minus the stacking energy with 1,3,5-triaminobenzene is shown for benzene, aminobenzene and cyanobenzene.

Figure 15 plots the difference in stacking interactions of dimers of zero-dipole polyaminobenzene and maximum dipole polyaminobenzene for a given number of amino substituents. The difference in stacking interaction is plotted as a function of the number of amino substituents. In all cases, stacking interactions increase with increasing dipole moment. Since the amino substituent causes less charge separation than the cyano substituent, the average increase in stacking interactions with increasing dipole moments is smaller in the polyaminobenzene dimers (1.5 kJ mol^{-1}) than the polycyanobenzene dimers (5.3 kJ mol^{-1}). For the different polyaminobenzene-monosubstituted benzene dimers, aminobenzene dimers generally shows the greatest increase in stacking stabilization with increasing dipoles, followed by benzene, while cyanobenzene dimers show the smallest increase in stacking interactions with increasing dipole moments. This trend is the reverse of the trend seen in the polycyanobenzene dimers and not what would be expected based on

the charge separation in the monosubstituted benzenes (cyanobenzene>aminobenzene>benzene). In order to explain this trend, the structures of the polyaminobenzene dimers shall again be examined. It is noted that the substituents prefer to be far away from each other, as was the case for the polycyanobenzene dimers. This means that the dipole moments in the polyaminobenzene-cyanobenzene dimers are parallel, while the dipole moments in the polyaminobenzene-aminobenzene dimers are anti-parallel. The energetically unfavourable parallel dipoles have a smaller increase in stacking stabilization due to increased dipole moments, while the energetically favourable anti-parallel dipoles have a larger increase in stacking stabilization. For information on the structures associated with these dimers, please refer to Tables 14 and 15, as well as Figures 30 and 31 in the Appendix.

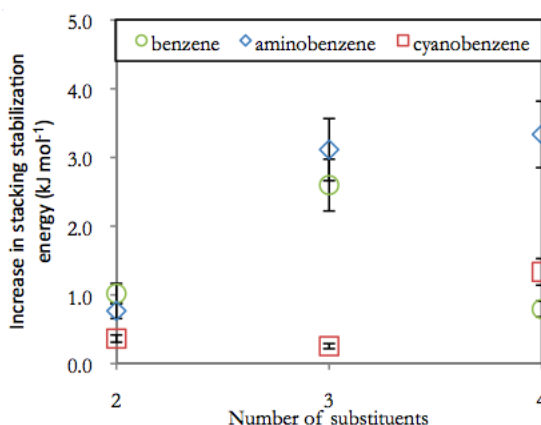


Figure 15: The increase in stacking stabilization energy on going from a zero-dipole polyaminobenzene to the maximum dipole polyaminobenzene with the same number of substituents.

The trends in this section suggest that there are two different kinds of forces responsible for stacking interactions. When the difference in ESP of the monomers is small, then substituent-ring interactions or charge separation in the ring is responsible for stacking interactions. However, when the difference in the ESP of the monomers becomes large, charge transfer interactions dominate the trends in stacking interactions. A similar idea has been proposed before by Gung et al. who suggested that charge transfer interactions occur once a threshold has been crossed.³ Even though charge transfer dominates the stacking interactions in our systems only after a certain point, it has been shown that the increase in stacking stabilization resulting from increased number of substituents is

dominated by charge transfer. Therefore, our results suggest that charge transfer stabilization gradually increases with increasing number of substituents and does not take place suddenly after a threshold is crossed, but does become the dominant force once the difference in ESP of the monomers is large enough.

Previous theoretical studies have examined the stacking interactions of hexafluorobenzene with various monosubstituted benzenes.^{5,10} One of these studies which used the MP2/aug-cc-pVDZ level of theory, found the same trends in stacking interactions, wherein aminobenzene stacks the strongest, followed by cyanobenzene, while benzene stacks the weakest.⁵ The other study examined the stacking interactions of hexafluorobenzene with various monosubstituted benzenes at the M05-2X/6-31+G(d) level of theory.¹⁰ It found that aminobenzene stacks the strongest, followed by benzene, while cyanobenzene stacks the weakest. The trends between cyanobenzene and aminobenzene in both of these studies were explained on the basis of electrostatics, while the stronger interaction of cyanobenzene over benzene was explained on the basis of dispersion interactions in the former study and electrostatics in the latter study. The difference in the relative interactions of cyanobenzene and benzene can be explained on the basis of different conformations and different levels of theory. The former study examines both the parallel displaced and sandwich conformations, with the parallel displaced conformation being more stable. The latter study only examines the sandwich configuration. On comparing only the sandwich configuration, both studies find that cyanobenzene stacks weaker than benzene. However, although the former study finds that cyanobenzene stacks weaker by 2.97 kJ mol⁻¹, the latter study finds that cyanobenzene stacks weaker by 5.36 kJ mol⁻¹. This can be attributed to the differences in the level of theory.

Experimental studies that have examined the stacking interactions of pentafluorophenyls have found that electron rich phenyls resulting from substituents such as dimethylaniline stack stronger than the electron deficient phenyls resulting from substituents such as the nitro group.^{3,6,8-9} This trend is slightly different from our theoretical results which find that electron rich benzenes stack the strongest, but the stacking interaction of unsubstituted benzene is weaker than the stacking

interactions of electron deficient benzenes with greater charge separation. The experimental trend has been explained on the basis of electrostatics. This section has shown that electrostatics does *not* appear to be the dominant interaction, but rather the charge transfer resulting from the difference in electrostatic potential which is the dominant force dictating an increase in the stacking interactions with increasing number of substituents.

3.3.4 Hexasubstituted benzene-polysubstituted benzene dimers

In this section, the stacking interactions of hexacyanobenzene-polycyanobenzene, hexaaminobenzene-polyaminobenzene, hexaaminobenzene-polycyanobenzene and hexacyanobenzene-polyaminobenzene dimers are studied. Zero-dipole polycyanobenzenes and polyaminobenzenes are studied to examine the effect of increasing number of substituents while the effect of dipoles is studied by examining the change in stacking interactions of tricyanobenzenes and triaminobenzenes with different monomer dipoles. Previous sections have shown that charge transfer dictates the change in stacking interactions with change in the number of substituents. This section will test this hypothesis.

Figure 16 plots the stacking stabilization energies as a function of the number of substituents after the R1/ α scans (since the trends after the R1/ α scans differ slightly from the R2 scans, the two trends are examined separately). Increasing the number of substituents causes a decrease in stacking stabilization for the hexacyanobenzene-polycyanobenzene and hexaaminobenzene-polyaminobenzene dimers, but an increase in stacking stabilization for the hexacyanobenzene-polyaminobenzene and hexaaminobenzene-polycyanobenzene dimers. For the hexacyanobenzene-polycyanobenzene and hexaaminobenzene-polyaminobenzene dimers, charge transfer interactions decrease with increasing number of substituents. Since it has been suggested in the last section that charge transfer dominates the change in stacking stabilization with the number of substituents, the decrease in stacking stabilization with increasing number of substituents is probably a result of decreased charge transfer. Hexacyanobenzene-polycyanobenzene dimers show a bigger decrease in stacking stabilization with increasing number of substituents than the hexaaminobenzene-

polyaminobenzene dimers. This difference can be attributed to the fact that the cyano substituent causes more charge separation than the amino substituent. Therefore, the decrease in charge transfer associated with the addition of each substituent is greater for the hexacyanobenzene-polycyanobenzene dimers. Conversely, stacking stabilization increases with increasing number of substituents for the hexacyanobenzene-polyaminobenzene and hexaaminobenzene-polycyanobenzene dimers and the change in stacking stabilization with the number of substituents can again be explained on the basis of charge transfer. Also, the increase in stacking stabilization per substituent is greater for the hexaaminobenzene-polycyanobenzene dimers than the hexacyanobenzene-polyaminobenzene dimers, which can again be attributed to the fact that the cyano substituent causes more charge separation than the amino substituent.

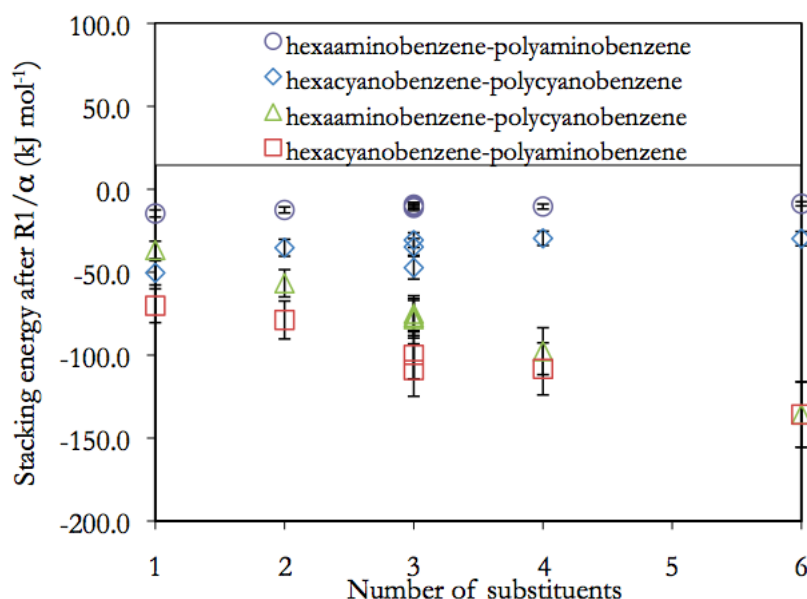


Figure 16: Stacking stabilization energies after R1/ α scans of the hexasubstituted benzene-polysubstituted benzene dimers plotted as a function of the number of substituents.

On looking at the charge transfer interactions after the R2 scans (Figure 17), the stacking interactions of the hexaaminobenzene-polyaminobenzene dimers no longer decrease with increasing number of substituents, but rather stay nearly constant. The hexacyanobenzene-polycyanobenzenes show a decrease in stacking stabilization with increasing number of substituents, although the

decrease in stacking stabilization is not as large. This suggests that the R2 scans result in a more favourable orientation where the substituent-ring interactions might be dominant (Appendix, Figure 32 and Figure 33). The hexacyanobenzene-polyaminobenzene and hexaaminobenzene-polycyanobenzene dimers continue to show an increase in stacking stabilization with increasing number of substituents.

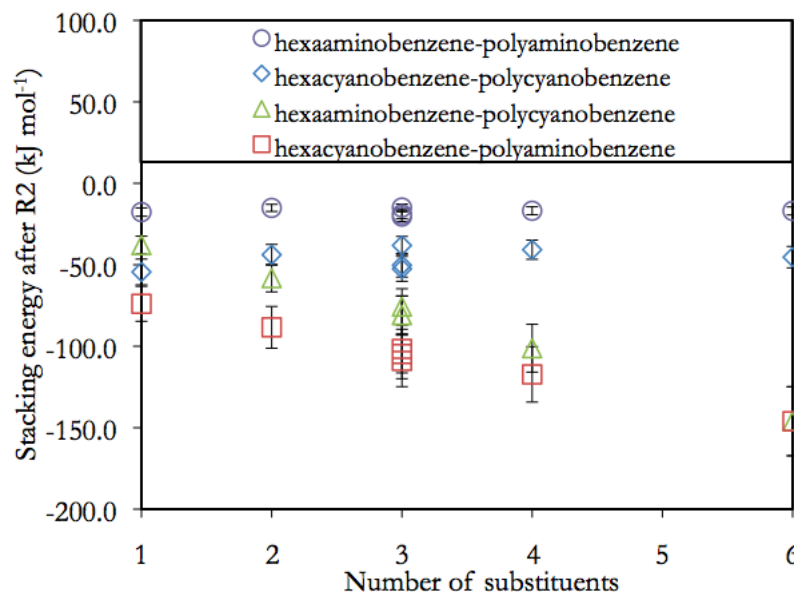


Figure 17: Stacking stabilization energies of hexasubstituted benzene-polysubstituted benzene dimers after the R2 scans plotted as a function of number of substituents.

In order to examine the effect of dipoles, the increases in stacking interactions between the zero-dipole and maximum dipole dimers of tricyanobenzene and triaminobenzene are examined. In all cases, an increase in dipole moment corresponds to an increase in stacking stabilization. For the triaminobenzenes, hexacyanobenzene showed an increase of 7.4 kJ mol⁻¹, while hexaaminobenzene shows an increase of 5.6 kJ mol⁻¹. Therefore, the cyano substituent causes the greater increase in stacking stabilization due to greater charge separation. For the tricyanobenzenes, hexacyanobenzene showed an increase of 14.4 kJ mol⁻¹, whereas hexaaminobenzene showed an increase of 5.2 kJ mol⁻¹. Again, the cyano substituents cause the greater increase in stacking stabilization relative to the amino substituents. Given that dipole-dipole interactions cannot be responsible for the trends (there is no

dipole on hexacyanobenzene or hexaaminobenzene), it is the stronger charge separation and the resulting dispersion interactions caused by cyano groups that are responsible for the trends in stacking interactions. Also, the increase in stacking stabilization with increasing dipoles is greater for the tricyanobenzenes (9.8 kJ mol^{-1}) than for the triaminobenzenes (6.5 kJ mol^{-1}).

This section has, for the first time, shown that the stacking stabilization decreases with an increase in the number of substituents. Therefore, substituent-ring interactions have been ruled out and charge transfer has been reaffirmed to be the dominant interaction changing the stacking stabilization with changing number of substituents.

3.3.5 Effect of HF, MP2 and CCSD(T) levels of theory on stacking interactions.

It has been shown in this chapter that electrostatics is not the dominant interaction in stacking stabilization. Furthermore, charge separation in the ring/substituent-ring interactions are dominant when the number and type of substituents (electron withdrawing or electron donating) on the two benzene rings is the same, while charge transfer dominates when the number and the type of substituents are different. Given that electrostatics and charge transfer do not appear to be the source of stabilization caused by charge separation in the ring/substituent-ring interactions, dispersion interactions might be the source of stabilization (as proposed earlier for substituent-ring interactions)¹³. In this section, I shall examine the stacking interactions of aminobenzene, benzene and cyanobenzene with each of benzene, hexacyanobenzene and hexaaminobenzene at the HF level and MP2 level using the 6-31G*(0.25), aug-cc-pVDZ, and aug-cc-pVTZ basis sets. This will be done to test our conclusions on the role of electrostatics, dispersion (charge separation in the ring/substituent-ring interactions) and charge transfer based on the trends in stacking interactions. Finally, using the above mentioned calculations and calculations at the CCSD(T)/6-31G*(0.25) level of theory, the stacking stabilizations at the CCSD(T)/CBS level are calculated using the method proposed by Helgaker et al.³⁷⁻³⁸ to test the validity of the MP2/6-31G*(0.25) level of theory used in

this study. Similar methods for CCSD(T)/CBS extrapolations for stacked structures have been used before in the literature.^{1,28,39}

Tables 3, 4 and 5 give the HF and MP2 stacking energies at the 6-31G*(0.25), aug-cc-PVDZ and aug-cc-pVTZ basis sets respectively. For all basis sets, the interaction energies at the HF level are nearly always repulsive. Other studies have also shown that HF gives repulsive interactions energies and does not correctly account for stacking interactions.^{14,40-41} Furthermore, the trends in stacking interactions at the HF level do not correctly predict the total MP2 stacking stabilization. For example, when the benzene dimers are considered with HF, benzene has the strongest stacking stabilization energy, followed by cyanobenzene, while aminobenzene has the weakest stacking stabilization. However, at the MP2 level, cyanobenzene has the strongest stacking stabilization, followed by aminobenzene and benzene, which is in accordance with the dipole moments of the monomers. This supports our conclusion that electrostatics is not the dominant interaction in these stacked structures since otherwise HF should correctly predict the trends in the stacking stabilization. Instead, electron correlation is found to be responsible for the trends in stacking stabilization in nearly all of the dimers.

Table 4: HF and MP2 binding energy for the 6-31G*(0.25) basis set. All energies are in kJ mol⁻¹.

Monomer 1	Monomer 2	ΔE HF/6-31G*(0.25)	ΔE MP2/6-31G*(0.25)	$\Delta\Delta E$ (MP2-HF)
benzene	aminobenzene	19.0	-11.5	-30.5
benzene	Benzene	10.6	-8.9	-19.5
benzene	cyanobenzene	17.9	-18.3	-36.2
hexaaminobenzene	aminobenzene	22.7	-17.7	-40.3
hexaaminobenzene	Benzene	42.8	-16.8	-59.6
hexaaminobenzene	cyanobenzene	49.8	-37.9	-87.8
hexacyanobenzene	aminobenzene	30.9	-74.0	-104.9
hexacyanobenzene	Benzene	12.0	-52.6	-64.7
hexacyanobenzene	cyanobenzene	38.4	-54.4	-92.8

Table 5: HF and MP2 binding energy for the aug-cc-pVDZ basis set. All energies are in kJ mol⁻¹.

Monomer 1	Monomer 2	ΔE HF/aug-cc-pVDZ	ΔE MP2/aug-cc-pVDZ	$\Delta\Delta E$ (MP2-HF)
benzene	aminobenzene	13.4	-17.7	-31.1
benzene	benzene	8.6	-13.2	-21.8
benzene	cyanobenzene	12.2	-23.9	-36.1
hexaaminobenzene	aminobenzene	8.7	-26.4	-35.1
hexaaminobenzene	benzene	24.9	-28.4	-53.3
hexaaminobenzene	cyanobenzene	22.0	-50.0	-72.0
hexacyanobenzene	aminobenzene	5.3	-81.0	-86.3
hexacyanobenzene	benzene	-0.4	-58.5	-58.1
hexacyanobenzene	cyanobenzene	19.7	-60.2	-79.9

Table 6: HF and MP2 binding energy for the aug-cc-pVTZ basis set. All energies are in kJ mol⁻¹.

Monomer 1	Monomer 2	ΔE HF/aug-cc-pVTZ	ΔE MP2/aug-cc-pVTZ	$\Delta\Delta E$ (MP2-HF)
benzene	aminobenzene	12.6	-18.8	-31.4
benzene	benzene	8.3	-14.1	-22.3
benzene	cyanobenzene	12.0	-25.5	-37.5
hexaaminobenzene	aminobenzene	8.6	-26.9	-35.5
hexaaminobenzene	benzene	24.5	-30.2	-54.6
hexaaminobenzene	cyanobenzene	21.9	-52.3	-74.2
hexacyanobenzene	aminobenzene	5.3	-86.7	-92.0
hexacyanobenzene	benzene	-0.3	-61.7	-61.5
hexacyanobenzene	cyanobenzene	19.9	-65.1	-84.9

This section has shown that correlation is responsible for stabilizing the stacked dimers. The role of electron correlation in stabilizing stacking interactions has been noted previously in the literature.^{14,40-41} In addition, electron correlation is found to determine the trends between the different dimers. Previous computational studies on the benzene dimers have not analysed the stacking interactions along these lines, and therefore a direct comparison with those studies is not possible. Previous studies used to analyse stacking interactions of benzene dimers include SAPT

(DFT-SAPT and SAPT2),^{11,42} effective fragment potential,³¹ and dividing the stacking energy into electrostatic, induction, exchange and dispersion in a different way from any of the previously listed methods (ref. 45).^{14,45} The majority of the stabilization due to electron correlation in all of these methods has been attributed to dispersion (with a minor component being attributed to induction⁴⁶). However, based on the trends seen here, I propose that charge transfer between the molecules in conjunction with dispersion could be responsible for stabilization associated with electron correlation. Similar to this study, all of these studies have found that correlation is the biggest stabilizing contributor to stacking interactions,^{1,11,14-16,24,31,34,43} although the different studies do not agree on the nature of the interaction that dominates the trends. In the monosubstituted benzene-benzene dimer study by Sinnokrot and Sherrill, which used SAPT,¹¹ electrostatics and dispersion were both responsible for determining the trends in stacking interactions for electron-withdrawing groups, while dispersion interactions were found to be responsible for the trends in stacking interactions caused by electron-donating groups. Similar results were found using the EFP2 method on the same monosubstituted benzene-benzene dimers by Smith et al.³¹ Tsuzuki et al. calculated the stacking interaction energies of the toluene dimer,¹⁵ nitrobenzene dimer and the nitrobenzene-benzene dimer¹⁶ using the approach as described in reference 44. In all of these cases, electron correlation is found to be responsible for the increase in stacking interactions relative to the benzene dimer. Tsuzuki et al. also studied the stacking interactions of the hexafluorobenzene-benzene dimer¹ and found that electrostatic interactions were responsible for the biggest increase in stacking interactions relative to the benzene dimer. The different results of this study can be attributed to the different approach used to calculate the electrostatic interaction in the dimers. In summary, the nature of stabilizing interactions can vary between different methods.

The present study has used MP2/6-31G*(0.25) level of theory to study the stacking interactions. MP2 overestimates the stacking interactions, while the incomplete basis set destabilizes the stacking interactions, and this cancellation of errors is the reason MP2/6-31G*(0.25) has been

successfully used in the past to study stacked structures.²⁸ A CCSD(T)/CBS extrapolation is done for nine dimers studied in this section (Table 7) in order to compare the performance of MP2/6-31G*(0.25) method in cases where charge transfer is not dominant (benzene-monosubstituted benzene) and in cases where charge transfer is dominant (hexaaminobenzene and hexacyanobenzene dimers). Table 7 gives the stacking stabilization energies at the CCSD(T)/CBS limit. As can be seen, the MP2/6-31G*(0.25) energies are within 81-110% of the CCSD(T)/CBS energies. Furthermore, the trends at the MP2/6-31G*(0.25) level for the benzene, hexacyanobenzene and hexaaminobenzene dimers are the same as the trends at the CCSD(T)/CBS limit. Lastly, there is no trend in the MP2/6-31G*(0.25) and CCSD(T)/CBS energies between dimers where charge transfer is not dominant vs. dimers where charge transfer is dominant. These results reaffirm the choice of the MP2/6-31G*(0.25) level of theory for calculating the energies of dimers considered in this thesis.

Table 7: Results from the CCSD(T)/CBS extrapolation. All energies are in kJ mol⁻¹. The aug-cc-pVTZ calculations for the hexaaminobenzene-aminobenzene and hexaaminobenzene-cyanobenzene dimers were calculated using the RI approximation with Turbomole V5-9-1 18.⁴⁵

Monomer 1	Monomer 2	CCSD(T) /CBS	MP2/ 6-31G*(0.25)	Percentage (100* (MP2/6-31G*(0.25) /(CCSD(T)/CBS))
Benzene	Aminobenzene	-9.9	-8.9	90.3%
Benzene	Benzene	-18.3	-18.3	100.1%
Benzene	Cyanobenzene	-13.1	-11.5	88.0%
Hexaaminobenzene	Aminobenzene	-21.6	-17.7	81.8%
Hexaaminobenzene	Benzene	-20.8	-16.8	80.8%
Hexaaminobenzene	Cyanobenzene	-38.7	-37.9	98.1%
Hexacyanobenzene	Aminobenzene	n/a	-74.0	n/a
Hexacyanobenzene	Benzene	-47.1	-52.6	111.7%
Hexacyanobenzene	Cyanobenzene	n/a	-54.4	n/a

3.4 Conclusion

Electrostatics has been ruled out as being dominant in stacking stabilization since it cannot explain the trends. In addition, HF energies (electrostatic + exchange interactions) are always repulsive and never give the correct trends in stacking stabilization suggesting that electrostatics is not responsible for stacking interactions. The trends in stacking stabilization are successfully explained by electron correlation (dispersion, induction and charge transfer). Dispersion interactions dominate the trends in stacking stabilization when both monomers are lightly substituted while charge transfer dominates the trends in stacking stabilization when the one of the monomers is heavily substituted. In addition, charge transfer interactions have been shown to be dominant in changing the relative stacking stabilization between benzene, cyanobenzene and aminobenzene with changing number of substituents.

This chapter finds that the MP2/6-31G*(0.25) level of theory is accurate for studying dimers where charge transfer interactions are not dominant and in dimers where charge transfer interactions are dominant. Previous studies had never examined the validity of the MP2/6-31G*(0.25) level of theory under the two different circumstances and this supports the use of MP2/6-31G*(0.25) level of theory for studying stacking interactions.

To conclude, on being stacked with lightly substituted monomers, the trends between lightly and heavily substituted benzene monomers are dominated by different stabilization forces, with the former being dominated by dispersion and the latter by charge transfer.

References:

- 1 Tsuzuki, S.; Uchimaru, T.; Mikami, M. *Journal of Physical Chemistry A* **2006**, *110*, 2027.
- 2 Sinnokrot, M. O.; Sherrill, C. D. *Journal of Physical Chemistry A* **2004**, *108*, 10200.
- 3 Gung, B. W.; Patel, M.; Xue, X. W. *Journal of Organic Chemistry* **2005**, *70*, 10532.
- 4 Gung, B. W.; Xue, X.; Reich, H. J. *J. Org. Chem.* **2005**, *70*, 3641.
- 5 Gung, B. W.; Amicangelo, J. C. *Journal of Organic Chemistry* **2006**, *71*, 9261.
- 6 Gung, B. W.; Xue, X. W.; Zou, Y. *Journal of Organic Chemistry* **2007**, *72*, 2469.
- 7 Cozzi, F.; Cinquini, M.; Annuziata, R.; Siegel, J. S. *Journal of the American Chemical Society* **1993**, *115*, 5330.
- 8 Cozzi, F.; Siegel, J. S. *Pure and applied chemistry* **1995**, *67*, 683.
- 9 Cockroft, S. L.; Perkins, J.; Zonta, C.; Adams, H.; Spey, S. E.; Low, C. M. R.; Vinter, J. G.; Lawson, K. R.; Urch, C. J.; Hunter, C. A. *Organic & Biomolecular Chemistry* **2007**, *5*, 1062.

- 10 Wheeler, S. E.; Houk, K. N. *J. Am. Chem. Soc.* **2008**.
- 11 Sinnokrot, M. O.; Sherrill, C. D. *Journal of the American Chemical Society* **2004**, *126*, 7690.
- 12 Ringer, A. L.; Sinnokrot, M. O.; Lively, R. P.; Sherrill, C. D. *Chemistry-a European Journal* **2006**, *12*, 3821.
- 13 Ringer, A. L.; Sherrill, C. D. *Journal of the American Chemical Society* **2009**, *131*, 4574.
- 14 Tsuzuki, S.; Honda, K.; Uchimaru, T.; Mikami, M.; Tanabe, K. *Journal of the American Chemical Society* **2002**, *124*, 104.
- 15 Tsuzuki, S.; Honda, K.; Uchimaru, T.; Mikami, M. *Journal of Chemical Physics* **2005**, *122*, 8.
- 16 Seiji, T.; Kazumasa, H.; Tadafumi, U.; Masuhiro, M. *The Journal of Chemical Physics* **2006**, *125*, 124304.
- 17 Wheaton, C. A.; Dobrowolski, S. L.; Millen, A. L.; Wetmore, S. D. *Chemical Physics Letters* **2006**, *428*, 157.
- 18 Rutledge, L. R.; Durst, H. F.; Wetmore, S. D. *Physical Chemistry Chemical Physics* **2008**, *10*, 2801.
- 19 Rutledge, L. R.; Wheaton, C. A.; Wetmore, S. D. *Physical Chemistry Chemical Physics* **2007**, *9*, 497.
- 20 Rutledge, L. R.; Campbell-Verduyn, L. S.; Wetmore, S. D. *Chemical Physics Letters* **2007**, *444*, 167.
- 21 Zhang, C.; Zhang, X.; Zhang, X.; Fan, X.; Jie, J.; Chang, J. C.; Lee, C.-S.; Zhang, W.; Lee, S.-T. *Advanced Materials* **2008**, *20*, 1716.
- 22 Zhang, X.; Zhang, X.; Shi, W.; Meng, X.; Lee, C.; Lee, S. *Angewandte Chemie International Edition* **2007**, *46*, 1525.
- 23 Xu, J.; Wen, L.; Zhou, W.; Lv, J.; Guo, Y.; Zhu, M.; Liu, H.; Li, Y.; Jiang, L. *Journal of Physical Chemistry C* **2009**, *113*, 5924.
- 24 Lee, E. C.; Kim, D.; Jurecka, P.; Tarakeshwar, P.; Hobza, P.; Kim, K. S. *Journal of Physical Chemistry A* **2007**, *111*, 3446.
- 25 Seo, J.-I.; Kim, I.; Lee, Y. S. *Chemical Physics Letters* **2009**, *474*, 101.
- 26 Kroon-Batenburg, L. M. J.; van Duijneveldt, F. B. *Journal of Molecular Structure: THEOCHEM* **1985**, *121*, 185.
- 27 Spomer, J.; Leszczynski, J.; Hobza, P. *Journal of Physical Chemistry* **1996**, *100*, 5590.
- 28 Hobza, P.; Spomer, J. *Journal of the American Chemical Society* **2002**, *124*, 11802.
- 29 M. J. Frisch, G. W. T., H. B. Schlegel, G. E. Scuseria, M. A. Robb, J. R. Cheeseman, J. A. Montgomery, Jr., T. Vreven, K. N. Kudin, J. C. Burant, J. M. Millam, S. S. Iyengar, J. Tomasi, V. Barone, B. Mennucci, M. Cossi, G. Scalmani, N. Rega, G. A. Petersson, H. Nakatsuji, M. Hada, M. Ehara, K. Toyota, R. Fukuda, J. Hasegawa, M. Ishida, T. Nakajima, Y. Honda, O. Kitao, H. Nakai, M. Klene, X. Li, J. E. Knox, H. P. Hratchian, J. B. Cross, V. Bakken, C. Adamo, J. Jaramillo, R. Gomperts, R. E. Stratmann, O. Yazyev, A. J. Austin, R. Cammi, C. Pomelli, J. W. Ochterski, P. Y. Ayala, K. Morokuma, G. A. Voth, P. Salvador, J. J. Dannenberg, V. G. Zakrzewski, S. Dapprich, A. D. Daniels, M. C. Strain, O. Farkas, D. K. Malick, A. D. Rabuck, K. Raghavachari, J. B. Foresman, J. V. Ortiz, Q. Cui, A. G. Baboul, S. Clifford, J. Cioslowski, B. B. Stefanov, G. Liu, A. Liashenko, P. Piskorz, I. Komaromi, R. L. Martin, D. J. Fox, T. Keith, M. A. Al-Laham, C. Y. Peng, A. Nanayakkara, M. Challacombe, P. M. W. Gill, B. Johnson, W. Chen, M. W. Wong, C. Gonzalez, and J. A. Pople In *Gaussian, Inc.* Wallingford CT, 2004.
- 30 Arnstein, S. A.; Sherrill, C. D. *Physical Chemistry Chemical Physics* **2008**, *10*, 2646.
- 31 Smith, T.; Slipchenko, L. V.; Gordon, M. S. *Journal of Physical Chemistry A* **2008**, *112*, 5286.
- 32 Chen, Z.; Lohr, A.; Saha-Moller, C. R.; Wurthner, F. *Chem Soc Rev* **2009**, *38*, 564.
- 33 Tsuzuki, S.; Honda, K.; Uchimaru, T.; Mikami, M.; Tanabe, K. *Journal of the American Chemical Society* **2000**, *122*, 3746.
- 34 Rutledge, L. R.; Campbell-Verduyn, L. S.; Hunter, K. C.; Wetmore, S. D. *Journal of Physical Chemistry B* **2006**, *110*, 19652.

- 35 Hobza, P.; Sponer, J. *Chemical Reviews (Washington, D. C.)* **1999**, *99*, 3247.
- 36 Sponer, J.; Leszczynski, J.; Hobza, P. *Journal of Molecular Structure* **2001**, *573*, 43.
- 37 Halkier, A.; Helgaker, T.; Jorgensen, P.; Klopper, W.; Koch, H.; Olsen, J.; Wilson, A. K. *Chemical Physics Letters* **1998**, *286*, 243.
- 38 Halkier, A.; Helgaker, T.; Jorgensen, P.; Klopper, W.; Olsen, J. *Chemical Physics Letters* **1999**, *302*, 437.
- 39 Rutledge, L. R.; Wetmore, S. D. *Journal of Chemical Theory and Computation* **2008**, *4*, 1768.
- 40 Hobza, P.; Selzle, H. L.; Schlag, E. W. *Journal of the American Chemical Society* **1994**, *116*, 3500.
- 41 Sinnokrot, M. O.; Valeev, E. F.; Sherrill, C. D. *Journal of the American Chemical Society* **2002**, *124*, 10887.
- 42 Pitonak, M.; Riley, K. E.; Hobza, P. N. P. *ChemPhysChem* **2008**, *9*, 1636.
- 43 Tsuzuki, S.; Honda, K.; Uchimaru, T.; Mikami, M. *Journal of Chemical Physics* **2004**, *120*, 647.
- 44 The electrostatic interaction is calculated as the interaction between the distributed multipoles (upto hexadecapole), the induction interaction is calculated as the interactions between the multipoles of one monomer with the polarizable sites of the other monomer, the exchange energy is calculated as the difference between the HF energy at a large basis set such as aug(d)-6-311G(d) and the electrostatic and induction energy components while the dispersion energy is calculated as the difference between the CCSD(T)/CBS extrapolation and the HF energy.
- 45 Ahlrichs, R.; Bär, M.; Häser, M.; Horn, H.; Kölmel, C. *Chemical Physics Letters* **1989**, *162*, 165.
- 46 Induction interactions occur when the permanent charges on one molecule perturb the charge distribution on the neighbouring molecule. These have been shown to play a very minor role in stacking interactions^{11,14,31,42,45} and therefore have not been given much importance in the thesis.

4. Stacking of nucleobase-benzene dimers

4.1 Introduction

In the previous chapter, it was shown that the dominant force responsible for stacking interactions varies with the difference in substitution of the rings. When the difference in the number and type of substituents of the rings is small, dispersion interactions are dominant in determining the trends. When the difference is large, charge transfer interactions are dominant in determining the trends in stacking interactions between the dimers.

Previous work has studied the stacking interactions between the nucleobases,¹⁻¹² and between the nucleobases and other biological molecules such as amino acid side-chains.¹³⁻¹⁴ Both experimental and theoretical studies have found that the polarizability of the monomers affect stacking interactions, with increase in polarizability corresponding to an increase in stacking interactions.¹³⁻¹⁷ Polarizability in turn has been found to be related to the surface area (size) of the molecules.¹³ In addition, the role of dipole-dipole (electrostatic) interactions has also been noted in the literature.^{7,10,13-14,18} Finally, experimental studies have found hydrophobic interactions to be important for stacking interactions,¹⁹⁻²⁰ although they will not play a role in our gas-phase calculations. The literature on nucleobase stacking has not yet examined the role of charge transfer interactions in stabilizing stacked neutral monomers. The literature examining the stacking interactions of cationic methylated adenine with the histidine and tryptophan amino acid side-chains has noted the possibility of charge transfer influencing stacking interactions.¹³

In this chapter, the stacking interactions of nucleobase-benzene dimers are studied. The five common natural nucleobases, namely adenines, cytosines, guanines, thymine and uracils are examined (Figure 18). The substituents around the benzene ring are varied in the same fashion as the benzene chapter so that the results can be compared. The nucleobases are first stacked with monosubstituted benzenes where both electron-donating ($-NH_2$, $-OH$, $-CH_3$) and electron-

withdrawing (-CN, -CONH₂, -F, -NO₂) substituents are considered. In addition, the unsubstituted benzene is also studied as a reference. Next, each of the nucleobases is stacked with polysubstituted benzenes (Figure 9) where the effects of electron-donating amino groups and electron-withdrawing fluoro groups are examined. The fluoro groups are examined because previous experimental work have examined the effects of various fluoro substituted rings with the natural nucleobases.²⁰

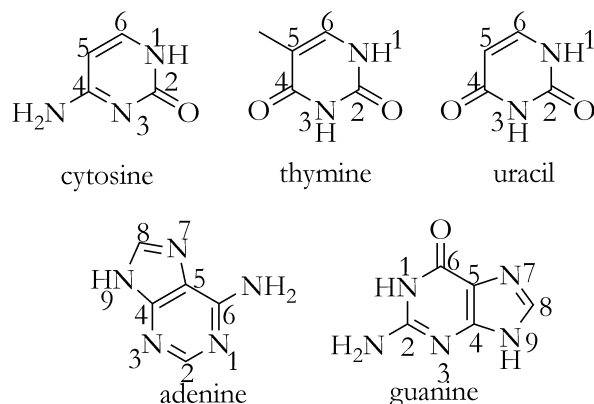


Figure 18: The five natural nucleobases (adenine, guanine, cytosine, thymine and uracil) and the numbering of their ring atoms.

4.2 Computational methodology

The methodology for examining these dimers is the same as for the benzene dimers discussed in section 2.2. The only two differences are the structure chosen to be $\alpha=0^\circ$ and the monomer kept constant during the scans. For $\alpha=0^\circ$, the torsional angle between the hydrogen at the glycosidic bond on the nucleobase, the centers of mass of the nucleobase and benzene, and the substituent indicated by the circles in Figure 9 is set to zero. In addition, the nucleobase is always kept fixed during the R1/ α and R2 scans for these systems. For some of the substituted benzenes which are asymmetrical, the monomers are flipped and the potential energy surface of the flipped monomers are examined. These flipped monomers have the suffix “-fl” attached to them in the data tables in the Appendix and their energies are also plotted in all of the graphs.

4.3 Results and Discussion

4.3.1 Nucleobase-monosubstituted benzene dimers

The stacking energies of the one-ring molecules (pyrimidines and benzene) are examined separately from the stacking interaction of the two ring molecules (purines). Breaking down the analysis into smaller subgroups will make for a more systematic examination of the systems and therefore aid in the analysis. A breakdown based on ring size is chosen since ring size is the fundamental difference between the structures. Both electron-donating ($-\text{NH}_2$, $-\text{OH}$, and $-\text{CH}_3$) and electron-withdrawing groups ($-\text{CN}$, $-\text{CONH}_2$, $-\text{F}$ and $-\text{NO}_2$) are considered on the monosubstituted benzenes. In addition, unsubstituted benzene is also studied as a reference. The stacking stabilization energies for pyrimidine-monosubstituted benzenes and benzene-monosubstituted benzenes are plotted as a function of the dipole moments of the monosubstituted benzenes in Figure 19a. Both electron-donating and electron-withdrawing substituents are found to increase the stacking stabilization energy relative to unsubstituted benzene. This suggests that electrostatics cannot be the dominant interaction in determining the stacking stabilization energies.

For charge transfer to be the dominant interaction between the natural nucleobases and monosubstituted benzenes, the stacking interactions between the dimers should increase with increasing difference in the ESP of the monomers. This is not found to be the case. For example, uracil has two strong electron-withdrawing carbonyl groups (Figure 18 and Figure 20), but still stacks the strongest with monosubstituted benzenes containing electron-withdrawing groups like nitrobenzene (Dipole = 5.376D, Figure 19a).

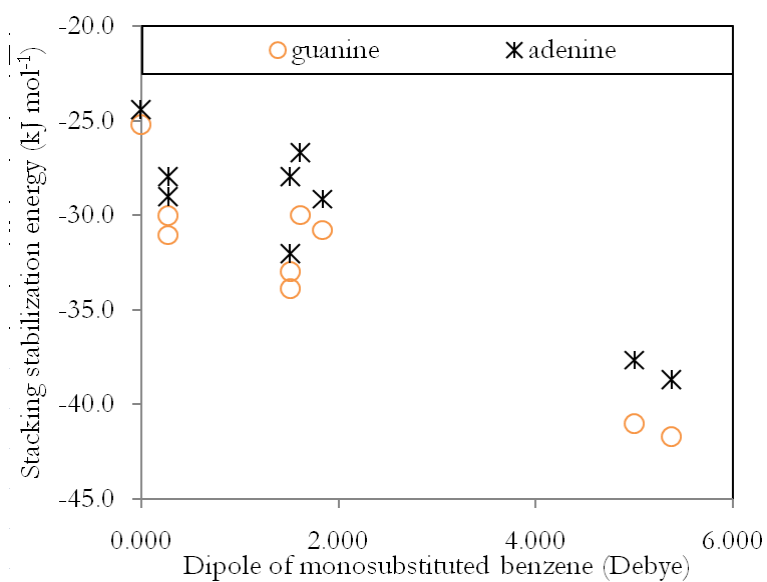
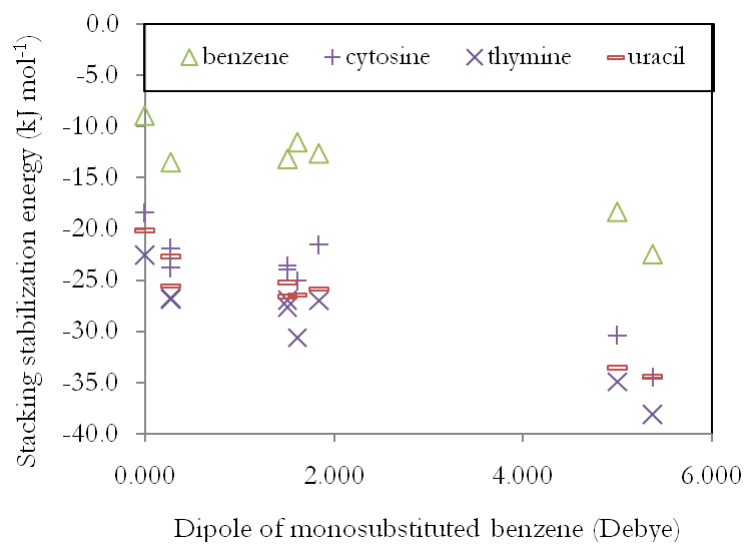


Figure 19: (a) Stacking stabilization energies of the pyrimidine-monosubstituted dimers and benzene-monosubstituted dimers plotted as a function of the dipole moments of the monosubstituted benzenes. (b) Stacking stabilization energies of the purine-monosubstituted benzene dimers plotted as a function of the dipole moments of the monosubstituted benzenes.

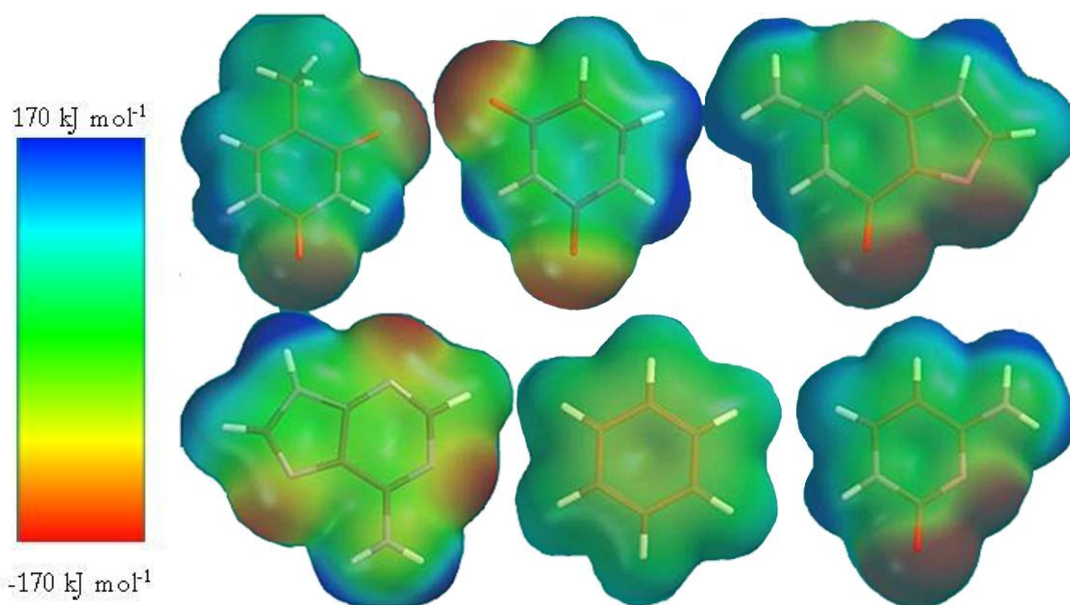


Figure 20: Electrostatic potential maps of the different nucleobases. (Top row, left to right: thymine, uracil and guanine. Bottom row, left to right: adenine, benzene and cytosine)

A high degree of correlation can be seen between the dipole moments of the monosubstituted benzenes and their stacking stabilization energies for each set of dimers (Table 8). On examining the increase in stacking stabilization with increasing dipole moments of the monosubstituted benzenes, benzene shows the smallest increase followed by thymine, cytosine, and uracil (Table 8). Therefore, the rate of increase in the stacking stabilization with increasing dipole moments of the monosubstituted benzenes has a positive correlation with the dipole moments of the monomers for benzene, thymine and cytosine, but not for uracil (Table 8).

In order to examine why the uracil dimers are an exception, the uracil-monosubstituted benzene data is evaluated further (Figure 19a). Uracil shows a stronger stacking interaction with benzenecarboxamide than would be expected based on the dipole of benzenecarboxamide (Figure 19a, dipole moment = 4.094 D). Therefore, the rate of increase in the stacking interactions with an increase in the dipole moments are examined without the benzenecarboxamide outlier. In this case, it is now found that benzene has the smallest increase, followed by uracil, thymine and cytosine (Table

8), in accordance with the dipole moments of the molecules. This trend can be explained on the basis of (electrostatic) dipole-dipole interactions. Dipole-dipole interactions have also been noted in the nucleobase literature in the past,^{7,10,13-14,18} and can be seen in the anti-parallel dipole orientation (Table 8).

Table 8: The dipole moments of the different monomers, dipole alignments and their coefficients of correlation and slopes (with and without benzenecarboxamide) when the stabilization energy of their dimers with monosubstituted benzenes are plotted as a function of the dipole moment of the monosubstituted benzenes (Figure 19).

Monomer	Dipole at MP2/6-31G* (Debye)	Coefficient of correlation (r)	Dipole alignment * (°)	Slope (kJ mol ⁻¹ Debye ⁻¹)	Slope without benzenecarboxamide (kJ mol ⁻¹ Debye ⁻¹)
Benzene	0.0000	-0.93	n/a	-2.0	-2.0
Cytosine	7.3552	-0.93	153.6	-2.5	-2.7
Thymine	4.9599	-0.95	151.7	-2.4	-2.3
Uracil	5.0295	-0.94	133.2	-2.6	-2.3
Adenine	2.4591	-0.93	139.1	-2.3	-2.4
Guanine	7.3335	-0.93	141.4	-2.9	-2.9

* The dipole alignment is the angle between the dipoles plotted from the center of masses.

Benzenecarboxamide shows stronger stacking interactions than expected based on its dipole. The reason for this discrepancy could be because the carboxamide group has a carbonyl and amino group, both of which cause charge separation in the molecule. However, the extent of charge separation caused by these groups may not necessarily be reflected in the dipole moment of benzenecarboxamide. In order to test this idea, the relative stacking interactions of the pyrimidines are examined. One would expect the thymine ring to be have the most charge separation, followed by uracil, while cytosine would be expected to have the least charge separation (Figure 20). As expected based on charge separation, thymine has the strongest stacking interactions, followed by uracil, while cytosine has the smallest stacking interactions (Figure 19a). The same trend has been seen in previous studies which examined the stacking interactions of natural nucleobases with each

other and the protein side-chains histidine, phenylalanine, tyrosine and tryptophan.^{7,14} Substituent-ring interactions could also explain the stacking interaction energies, since the substituents cause the charge separation in the ring, which in turn would cause increased dispersion interactions with the other ring. In terms of dipoles, cytosine has the largest dipole (7.355 D), followed by uracil (5.030 D), while thymine has the smallest dipole moment (4.960 D) at MP2/6-31G(d). Therefore, like benzenecarboxamide, the extent of charge separation of the pyrimidine rings is not reflected in their dipole moments. This suggests that in addition to dipole-dipole electrostatic interactions, the extent of charge separation also plays a role in determining stacking stabilization energies. In terms of polarizabilities, cytosine has the greatest polarizability (108.3 au), followed by thymine (97.6 au), while uracil has the smallest polarizability (95.7 au) at the MP2/aug-cc-pVDZ level of theory. One possible reason why the polarizabilities do not reflect the extent of charge separation could be because it is the dipole polarizability that was calculated,²¹ and therefore it is not surprising that the polarizabilities of the pyrimidines correspond to their dipole moments. Thus, the stacking interactions follow the extent of charge separation in the pyrimidines, even when charge separation is not reflected in the dipole moments or the polarizabilities.

The stacking interactions of the purines are plotted as a function of the dipole moments of the monosubstituted benzenes in Figure 19b. The trends in stacking stabilization of the monosubstituted benzenes are the same between the purines and pyrimidines, suggesting that electrostatics and charge transfer are not the dominant interactions determining the trends of the purine-monosubstituted benzene dimers. Guanine shows a greater increase in stacking stabilization with increasing dipole moments than adenine (Table 8). This can be explained on the basis of both the extent of charge separation and dipole-dipole interactions since guanine has a larger dipole moment (7.334 D) than adenine (2.459 D) (Table 8). Guanine has an exocyclic carbonyl substituent and an amino substituent, which would imply that it has more charge separation than adenine, which has only one exocyclic amino substituent. Guanine also seems to undergo more dipole-dipole

stabilization as suggested above. In terms of the polarizabilities, guanine (123.4 au) and adenine (124.5 au) have nearly the same polarizabilities at MP2/aug-cc-pVDZ and therefore this property cannot explain the difference in stacking stabilization.

It has so far been established that electrostatics and charge transfer cannot explain the stacking interactions of the monosubstituted benzene-nucleobase dimers examined in this section. However it can be concluded that when the dipole moments and polarizability of the molecules differ from the degree of charge separation, the latter dominates the stacking interactions. However, the role of substituent-ring interactions cannot be ruled out since the same trends would be expected based on the extent of charge separation and substituent-ring interactions.

4.3.2 Nucleobase-polysubstituted benzene dimers

In this section, the stacking interactions of the natural nucleobase-polysubstituted benzene dimers are examined and compared to the benzene-polysubstituted benzene dimers for fluoro and amino substituents. It was shown in the previous section that an increase in the dipole moment causes an increase in the stacking stabilization, particularly when the magnitude of the dipole represents the extent of charge separation in the molecules. In the case of the polysubstituted benzenes, increasing dipoles corresponds to increasing charge separation only when the number and type of substituents is kept constant. Figure 21a plots the difference in stacking stabilization energy between the zero-dipole polyaminobenzene and maximum dipole polyaminobenzene dimers with the same number of amino substituents for the pyrimidine and benzene dimers. Cytosine shows the greatest increase in stacking stabilization energy with increasing dipole moments (6.6 kJ mol^{-1}), followed by uracil (4.2 kJ mol^{-1}), thymine (2.3 kJ mol^{-1}) and benzene (1.3 kJ mol^{-1}). Therefore, the increase in stacking stabilization energy follows the trends in dipole moments for the pyrimidines and benzene, suggesting that dipole-dipole interactions are responsible for the relative increase in stacking stabilization energies. For the purines (Figure 21b), guanine shows a greater increase in stacking

stabilization energy (2.0 kJ mol^{-1}) than adenine (1.5 kJ mol^{-1}) and this difference can again be explained on the basis of the stronger dipole moment of guanine, which gives further evidence of the presence of dipole-dipole interactions.

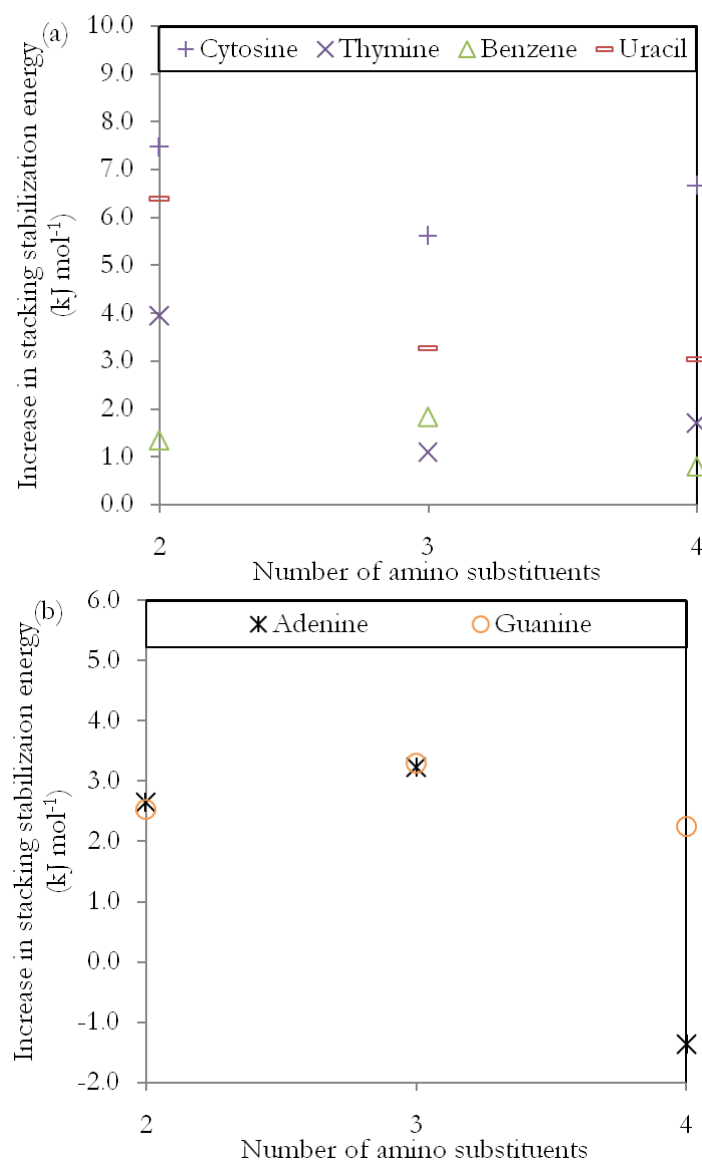


Figure 21: Increase in stacking stabilization energy on going from a zero-dipole polyaminobenzene to the maximum dipole polyaminobenzene with the same number of amino substituents plotted as a function of the number of amino substituents for (a) pyrimidines-polyaminobenzene and benzene polyaminobenzene dimers, and (b) purine-polyaminobenzene dimers.

On examining the increase in stacking stabilization energies on going from a zero-dipole polyfluorobenzene dimer to the maximum dipole polyfluorobenzene dimer with the same number of fluoro substituents for pyrimidines and benzene (Figure 22a), cytosine again shows the greatest increase in stacking stabilization energies (4.6 kJ mol^{-1}), followed by uracil (2.9 kJ mol^{-1}), thymine (2.8 kJ mol^{-1}) and benzene (2.7 kJ mol^{-1}). Therefore, increase in stacking stabilization energy again follows the trends in dipoles of the pyrimidines and benzene. On examining the increase in stacking stabilization energies for the purine-polyfluorobenzene dimers, guanine shows a greater increase (2.0 kJ mol^{-1}) than adenine (-0.7 kJ mol^{-1}) and this difference can again be explained on the basis of the greater dipole moment of guanine. The decrease in stacking stabilization energies of adenine (-0.7 kJ mol^{-1}) suggests that dipole-dipole interactions are not the dominant interaction and this can be attributed to the small dipole moment of adenine (2.459 D). Other secondary interactions might be responsible for the small decrease in stacking stabilization observed for the adenine-polyfluorobenzene dimers.

In conclusion, it appears that dipole-dipole interactions can be seen in nearly all of the polyfluorobenzene and polyaminobenzene dimers, but only when the type and number of substituents remain constant around the polysubstituted benzene ring.

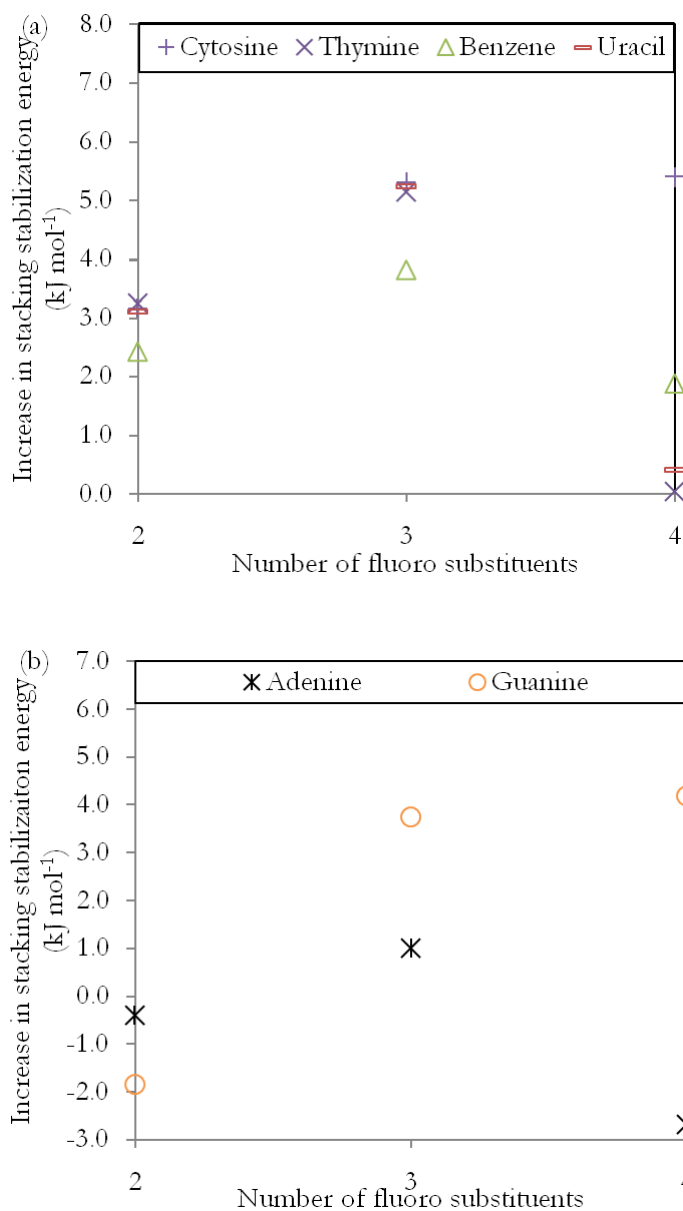


Figure 22: Increase in stacking stabilization energy on going from a zero-dipole polyfluorobenzene to the maximum dipole polyfluorobenzene with the same number of substituents for (a) pyrimidines and benzene dimers, and (b) purine dimers.

The stacking stabilization energies of purine-polyaminobenzene and benzene-polyaminobenzene dimers are plotted as a function of the number of amino substituents in Figure 23. On examining the stacking stabilization energies after $R1/\alpha$ scans (Figure 23a), the stacking

interactions of all of the molecules are found to increase with increasing number of amino substituents. Furthermore, the increase in stacking stabilization is the greatest for uracil ($m=-2.52 \text{ kJ mol}^{-1} \text{ substituent}^{-1}$), followed by thymine ($m=-2.15 \text{ kJ mol}^{-1} \text{ substituent}^{-1}$), benzene ($m=-1.28 \text{ kJ mol}^{-1} \text{ substituent}^{-1}$) and cytosine ($m=-1.22 \text{ kJ mol}^{-1} \text{ substituent}^{-1}$) after the R1/ α scans. The relative trends between the different molecules remain the same after the R2 scans with the exception of benzene and cytosine. Cytosine now shows a greater increase in stacking stabilization ($m=-2.41 \text{ kJ mol}^{-1} \text{ substituent}^{-1}$) than benzene ($m=-1.28 \text{ kJ mol}^{-1} \text{ substituent}^{-1}$).

Figure 24 shows the stacking interactions of pyrimidine-polyfluorobenzene dimers as a function of the number of fluoro substitutions. On examining the change in stacking stabilization with increasing number of substituents after the R1/ α scans (Figure 24a), it is found that the stacking interactions of cytosine and benzene increase ($m=-2.45$ and $-2.94 \text{ kJ mol}^{-1} \text{ substituent}^{-1}$ respectively), the stacking interactions of thymine stay nearly constant ($m=-0.02 \text{ kJ mol}^{-1} \text{ substituent}^{-1}$) while the stacking interactions of uracil decrease with increasing number of substituents ($m=1.05 \text{ kJ mol}^{-1} \text{ substituent}^{-1}$). The relative trends in stacking interactions between the molecules stay the same after the R2 scans (Figure 24b).

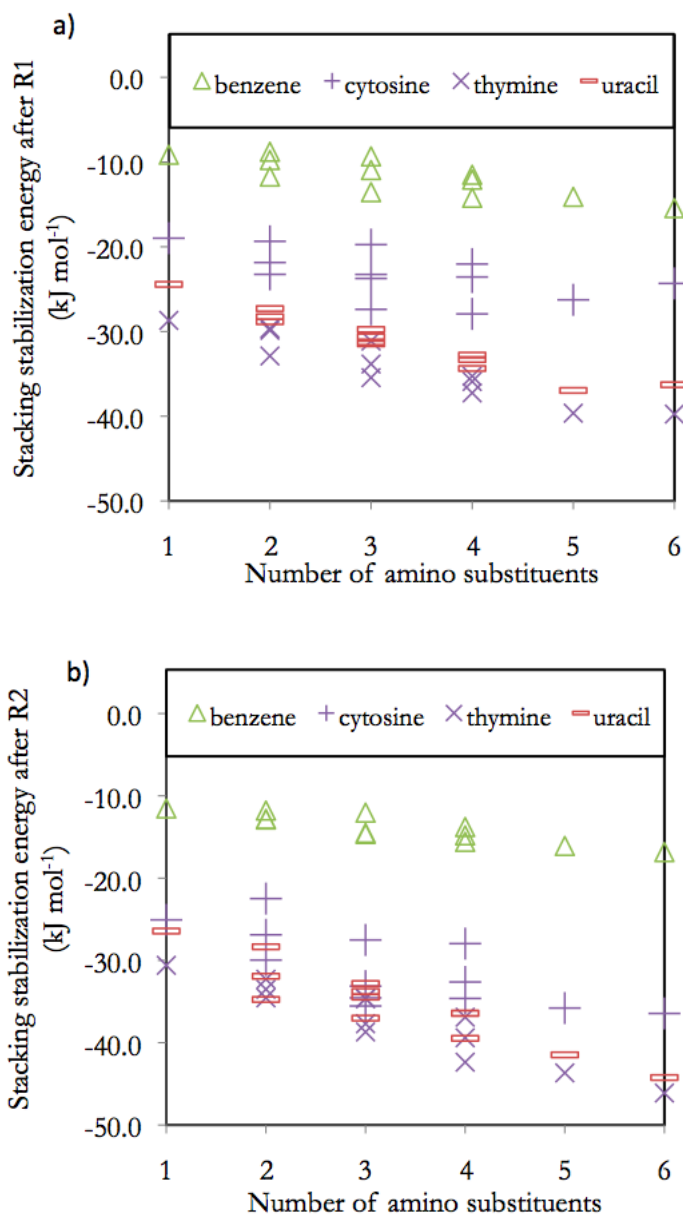


Figure 23: (a) The stacking stabilization energies of the pyrimidine-polyaminobenzene and benzene-polyaminobenzene dimers after the R1/ α scans plotted as a function of the number of amino substituents. (b) The stacking stabilization energies of the pyrimidine-polyaminobenzene and benzene-polyaminobenzene dimers after the R2 scans plotted as a function of the number of amino substituents.

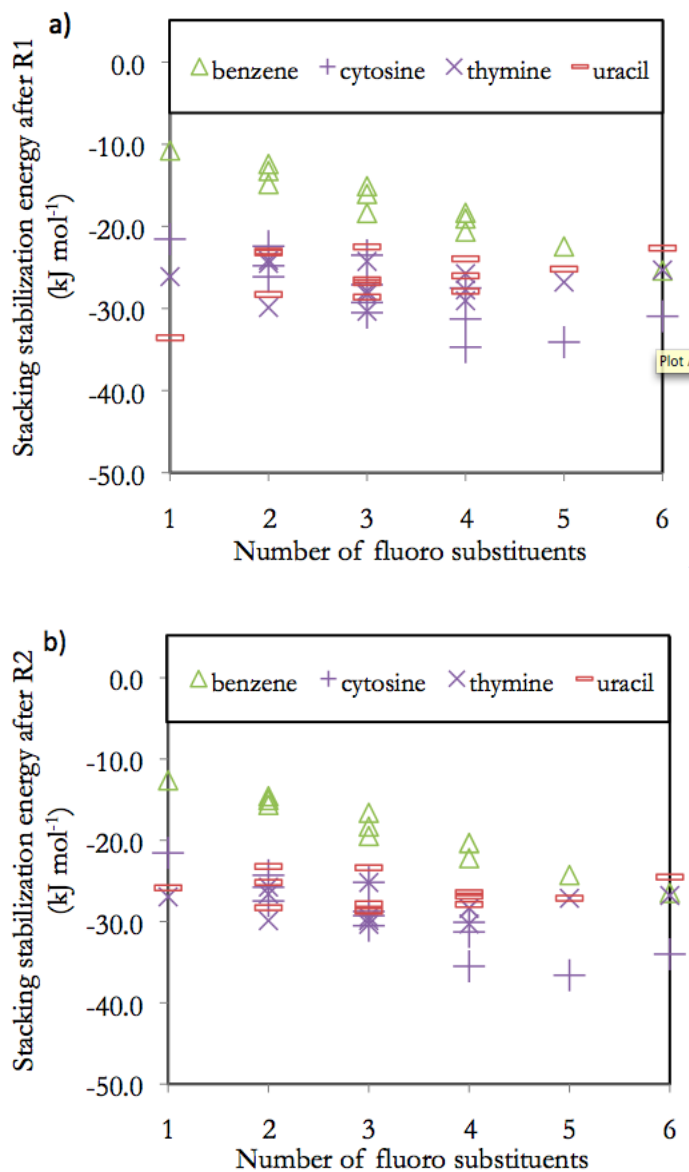


Figure 24: (a) The stacking stabilization energies of the pyrimidine-polyfluorobenzene and benzene-polyfluorobenzene dimers after the R1/ α scans plotted as a function of the number of fluoro substituents. (b) The stacking stabilization energies of the pyrimidine-polyfluorobenzene and benzene-polyfluorobenzene dimers after the R2 scans plotted as a function of the number of fluoro substituents.

Given that an increase in number of substituents can cause a decrease in the stacking stabilization as seen for the uracil-polyfluorobenzene dimers, dispersion cannot be the dominant interactions in determining the change in stacking interactions with changing number of substituents. This is because stacking interactions would only be expected to increase with increasing number of substituents were dispersion interactions (due to charge separation in the monomers) dominant in changing the stacking interactions with changing number of substituents. In order to explain the different trends in stacking stabilization associated with increasing number of substituents, let us examine the substituents present on the different pyrimidines (Figure 18). As a result of the two carboxyl groups, uracil has the most positive ESP, followed by thymine while cytosine would have the most negative ESP over the ring (Figure 20). Benzene also has a negative ESP over the ring (Figure 20). Therefore, electrostatics or charge transfer could explain why uracil shows the greatest increase in stacking interactions with increasing number of electron-donating amino substituents, followed by thymine, cytosine and benzene, and why the reverse trend is seen for increasing number of electron-withdrawing fluoro substituents.

In order to determine whether electrostatics or charge transfer is responsible for the change in stacking stabilizations, the interaction energy of all of the zero-dipole uracil-polyfluorobenzenes and uracil-polyaminobenzenes are examined (Table 9). The stacking interactions of only the zero-dipole systems are examined so that the effect of dipole-dipole interactions can be separated from the effect of changing number of substituents. For the uracil-polyfluorobenzene dimers, neither the HF interaction nor the MP2 interaction alone account for the trends in stacking stabilization. The destabilization due to HF does not always increase with increasing number of substituents, suggesting that electrostatic repulsion alone is not responsible for the decrease in stacking stabilization with increasing number of substituents. Instead decreases in both the HF energy and correlation energy can be seen with increasing number of substituents. For the polyaminobenzenes, the stacking interactions are dominated by the correlation energy, which shows an increase with increasing

number of substituents. The HF component, on the other hand, stays nearly constant with increasing number of amino substituents. The trends for the polyaminobenzenes and polyfluorobenzenes suggest that the increase in stacking stabilization with increasing number of substituents is caused by increased charge transfer interactions and not by increased electrostatic interactions. The decrease in stacking stabilization seen with increasing number of substituents results from small changes in stabilization due to either electrostatics or correlation (charge transfer).

Table 9: Stacking stabilization energies of zero-dipole uracil-polyfluorobenzenes and uracil-polyaminobenzenes at the HF/6-31G*(0.25) and MP2/6-31G*(0.25) level and the stacking stabilization due to electron correlation at the MP2/6-31G*(0.25) level.

Monomer1	Monomer2	ΔE_{HF} (kJ mol ⁻¹)	ΔE_{MP2} (kJ mol ⁻¹)	$\Delta\Delta E_{(\text{MP2-HF})}$ (kJ mol ⁻¹)
uracil	1,4-difluorobenzene	7.3	-25.2	-32.5
uracil	1,3,5-trifluorobenzene	11.1	-23.4	-34.5
uracil	1,2,4,5-tetrafluorobenzene	6.7	-26.5	-33.2
uracil	hexafluorobenzene	11.2	-24.5	-35.7
uracil	1,4-diaminobenzene	2.0	-28.3	-30.4
uracil	1,3,5-triaminobenzene	2.7	-33.8	-36.5
uracil	1,2,4,5-tetraaminobenzene	3.0	-36.4	-39.5
uracil	hexaaminobenzene	2.8	-44.2	-47.1

Figure 25 plots the stacking interactions of the purine-polyaminobenzene dimers after the R1/ α scans and after the R2 scans. As can be seen, the stacking interactions always increase with increasing number of substituents. After the R1/ α scans, the stacking interactions of adenine increase more ($m=-1.24$ kJ mol⁻¹ substituent⁻¹) than the stacking interactions of guanine ($m=-0.64$ kJ mol⁻¹ substituent⁻¹) with increasing number of substituents. The same relative trends are seen after the R2 scans, with adenine showing a greater increase in stacking stabilization ($m=-2.03$ kJ mol⁻¹ substituent⁻¹) than guanine ($m=-1.79$ kJ mol⁻¹ substituent⁻¹).

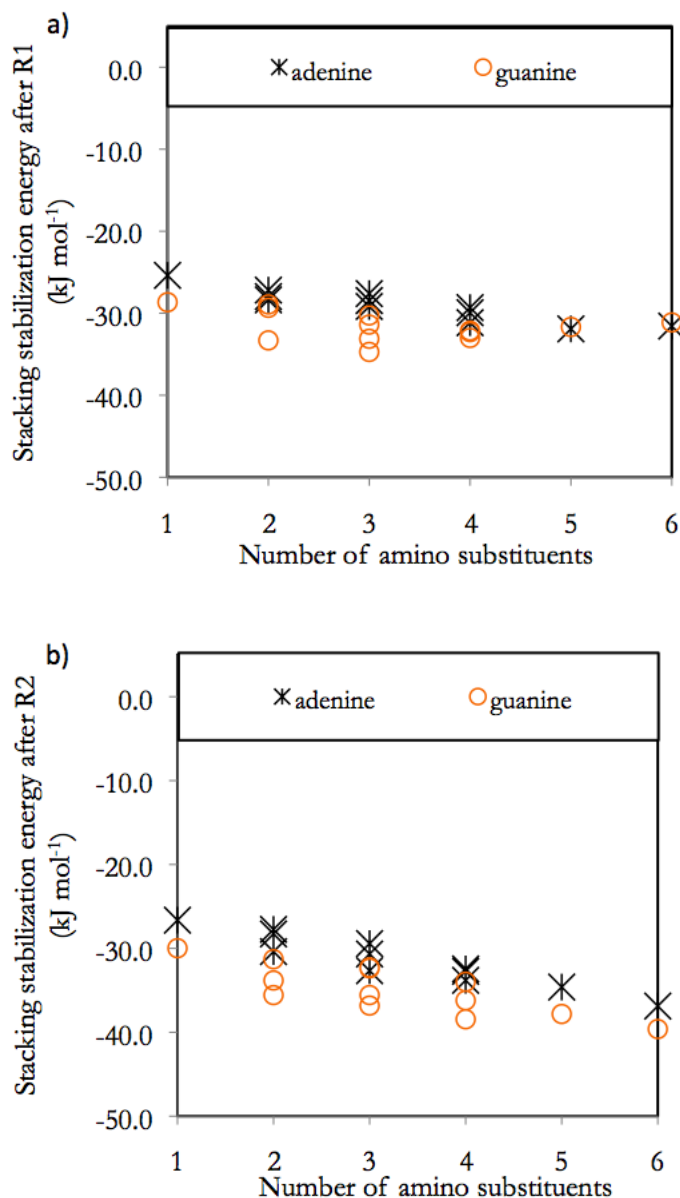


Figure 25: (a) The stacking stabilization energies of the purine-polyaminobenzene dimers after the R1/ α scans plotted as a function of the number of amino substituents. (b) The stacking stabilization energies of the purine-polyaminobenzene dimers after the R2 scans plotted as a function of the number of amino substituents.

Figure 26 plots the stacking interactions of the purine-polyfluorobenzene dimers as a function of the number of fluoro substituents after the R1/ α and R2 scans. After the R1/ α scans,

adenine shows a greater increase in stacking stabilization ($m=-2.84 \text{ kJ mol}^{-1} \text{ substituent}^{-1}$) than guanine ($m=-1.75 \text{ kJ mol}^{-1} \text{ substituent}^{-1}$) with increasing number of fluoro substitutions. After the R2 scans, the increase in stacking interactions with increasing number of fluoro substitutions is almost the same for adenine and guanine ($m=-2.20$ and $-2.08 \text{ kJ mol}^{-1} \text{ substituent}^{-1}$ respectively).

Since adenine has one electron-donating amino group while guanine has an electron-withdrawing carbonyl group and an electron-donating amino group, adenine would be expected to show a greater increase in stacking stabilization with increasing number of fluoro substitutions. In contrast, guanine would be expected to show a greater increase in stacking stabilization with increasing number of amino substitutions on the basis of electrostatics and charge transfer. Adenine, however, shows a greater increase in stacking stabilization with increasing number of both amino and fluoro substituents. This suggests that charge transfer and electrostatics are not the dominant interactions in determining the relative increase in stacking interactions between the two purines. Additionally, charge separation in the ring also does not appear to be the dominant interaction in determining the relative increase in stacking interactions between the two purines, since guanine has more charge separation. Substituent-ring interactions also cannot explain the difference in stacking stabilization with increasing number of substituents since both guanine and adenine would be expected to show the same increase in stacking interaction with increasing number of substituents. The slightly greater increase in stacking stabilization of adenine with increasing number of substituents could be as a result of the slightly greater polarizability of adenine vis-à-vis guanine (124.5 vs 123.4 au respectively at the MP2/aug-cc-pVDZ level of theory).

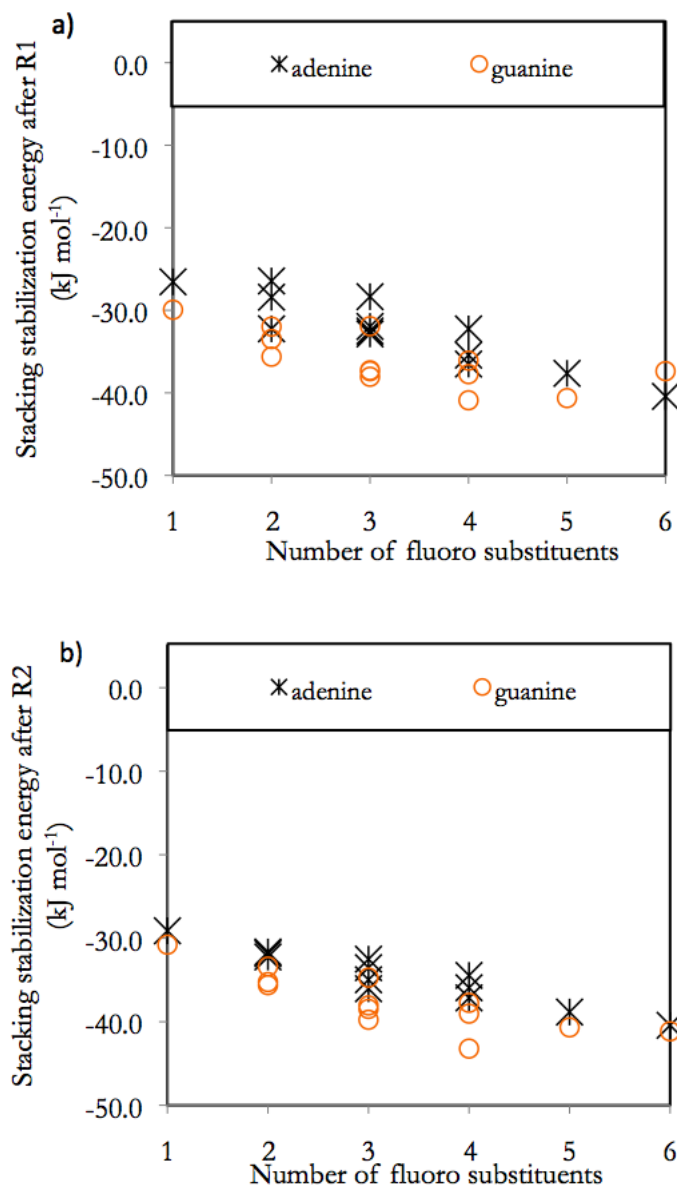


Figure 26: (a) The stacking stabilization energies of the purine-polyfluorobenzene dimers after the R1/ α scans plotted as a function of the number of fluoro substituents. (b) The stacking stabilization energies of the purine-polyfluorobenzene dimers after the R2 scans plotted as a function of the number of fluoro substituents.

The two-ring purines differ from the single-ring molecules examined in this thesis so far because the trends in stacking stabilization with increasing number of substitutions has always been

dominated by charge transfer interactions for the latter. This difference could be due to the larger number of electrons in the two ring systems. As a result, the substituents do not perturb the electrons in the rings to the same extent as the single-ring molecules. Therefore, the polarizabilities of the two ring molecules, and not the effect of substituents, determine the trends in stacking interactions.

Evidence has been provided in this chapter for the role of charge transfer interactions in stabilizing stacked structures of the nucleobases. It has been suggested that uracil is the best electron acceptor among the pyrimidines, followed by thymine and cytosine. The calculated and experimental (in DMSO) electron affinities of the pyrimidines support this argument where uracil has the greatest electron affinity, followed by thymine, while cytosine has the smallest electron affinity.²²⁻²³ Furthermore, the data also shows that guanine is a better electron acceptor than adenine and the calculated and experimental (in DMSO) electron affinities of the two purines support this argument.²²⁻²³

4.4 Conclusions

This thesis chapter has shown that charge transfer interactions, which were determined to dominate the stacking energy of benzene dimers with a large difference in ESP, also dominate the stacking interactions of single-ring nucleobases (pyrimidines) when the difference in ESP of the benzene monomers is large. In addition, the role of charge separation in determining the relative strength of stacking interactions in cases where the difference in ESP is small between the monomers has again been noted. Lastly, the role of dipole-dipole interactions in determining the relative orientation of monomers and their effect on stacking interactions is seen.

This is also the first study to suggest that the effect of substituents on stacking interactions differs between the single-ring pyrimidines and the two ring purines. The effect of substituents on stabilization due to charge transfer interactions in the single-ring molecules is not seen for the two

ring pyrimidine, as specifically, adenine shows a greater increase in stacking interactions with increasing amino and fluoro substituents. Instead, the difference in stacking stabilization with increasing number of substituents between the purine-polysubstituted benzene dimers could be a result of the different polarizabilities of the purines. However, the true dominant force for purines is yet to be determined.

References:

- (1) Hobza, P.; Sponer, J.; Polasek, M. *Journal of the American Chemical Society* **1995**, *117*, 792.
- (2) Sponer, J.; Leszczynski, J.; Hobza, P. *Journal of Physical Chemistry* **1996**, *100*, 5590.
- (3) Hobza, P.; Kabelac, M.; Sponer, J.; Mejzlik, P.; Vondrasek, J. *Journal of Computational Chemistry* **1997**, *18*, 1136.
- (4) Sponer, J.; Hobza, P. *Chemical Physics Letters* **1997**, *267*, 263.
- (5) Hobza, P.; Sponer, J. *Chemical Physics Letters* **1998**, *288*, 7.
- (6) Kratochvil, M.; Engkvist, O.; Sponer, J.; Jungwirth, P.; Hobza, P. *Journal of Physical Chemistry A* **1998**, *102*, 6921.
- (7) Hobza, P.; Sponer, J. *Chemical Reviews (Washington, D. C.)* **1999**, *99*, 3247.
- (8) Sponer, J.; Hobza, P.; Leszczynski, J. *Journal of Computational Chemistry* **2000**, *5*, 171.
- (9) Hobza, P.; Sponer, J. *Journal of the American Chemical Society* **2002**, *124*, 11802.
- (10) Sponer, J.; Leszczynski, J.; Hobza, P. *Biopolymers* **2002**, *61*, 3.
- (11) Jurecka, P.; Sponer, J.; Hobza, P. *Journal of Physical Chemistry B* **2004**, *108*, 5466.
- (12) Pitonak, M.; Riley, K. E.; Hobza, P. N. P. *ChemPhysChem* **2008**, *9*, 1636.
- (13) Rutledge, L. R.; Campbell-Verduyn, L. S.; Hunter, K. C.; Wetmore, S. D. *Journal of Physical Chemistry B* **2006**, *110*, 19652.
- (14) Rutledge, L. R.; Campbell-Verduyn, L. S.; Wetmore, S. D. *Chemical Physics Letters* **2007**, *444*, 167.
- (15) Rosemeyer, H.; Seela, F. *Journal of the Chemical Society, Perkin Transactions 2* **2002**, 746.
- (16) Rutledge, L. R.; Wheaton, C. A.; Wetmore, S. D. *Physical Chemistry Chemical Physics* **2007**, *9*, 497.
- (17) Wheaton, C. A.; Dobrowolski, S. L.; Millen, A. L.; Wetmore, S. D. *Chemical Physics Letters* **2006**, *428*, 157.
- (18) Sponer, J.; Leszczynski, J.; Hobza, P. *Journal of Molecular Structure* **2001**, *573*, 43.
- (19) Guckian, K. M.; Schweitzer, B. A.; Ren, R. X. F.; Sheils, C. J.; Tahmassebi, D. C.; Kool, E. T. *Journal of the American Chemical Society* **2000**, *122*, 2213.
- (20) Kool, E. T.; Morales, J. C.; Guckian, K. M. *Angewandte Chemie International Edition* **2000**, *39*, 990.
- (21) M. J. Frisch, G. W. T., H. B. Schlegel, G. E. Scuseria, M. A. Robb, J. R. Cheeseman, J. A. Montgomery, Jr., T. Vreven, K. N. Kudin, J. C. Burant, J. M. Millam, S. S. Iyengar, J. Tomasi, V. Barone, B. Mennucci, M. Cossi, G. Scalmani, N. Rega, G. A. Petersson, H. Nakatsuji, M. Hada, M. Ehara, K. Toyota, R. Fukuda, J. Hasegawa, M. Ishida, T. Nakajima, Y. Honda, O. Kitao, H. Nakai, M. Klene, X. Li, J. E. Knox, H. P. Hratchian, J. B. Cross, V. Bakken, C. Adamo, J. Jaramillo, R. Gomperts, R. E. Stratmann, O. Yazyev, A. J. Austin, R. Cammi, C. Pomelli, J. W. Ochterski, P. Y. Ayala, K. Morokuma, G. A. Voth, P. Salvador, J. J. Dannenberg, V. G. Zakrzewski, S. Dapprich, A. D. Daniels, M. C. Strain, O. Farkas, D. K. Malick, A. D. Rabuck, K. Raghavachari, J. B. Foresman, J. V. Ortiz, Q. Cui, A. G. Baboul, S. Clifford, J. Cioslowski, B. B. Stefanov, G. Liu, A. Liashenko, P. Piskorz, I. Komaromi, R. L.

- Martin, D. J. Fox, T. Keith, M. A. Al-Laham, C. Y. Peng, A. Nanayakkara, M. Challacombe, P. M. W. Gill, B. Johnson, W. Chen, M. W. Wong, C. Gonzalez, and J. A. Pople In *Gaussian, Inc.* Wallingford CT, 2004.
- (22) Wesolowski, S. S.; Leininger, M. L.; Pentchev, P. N.; Schaefer, H. F. *Journal of the American Chemical Society* **2001**, *123*, 4023.
- (23) Wiley, J. R.; Robinson, J. M.; Ehdaie, S.; Chen, E. C. M.; Chen, E. S. D.; Wentworth, W. E. *Biochemical and Biophysical Research Communications* **1991**, *180*, 841.

5. Global Conclusions and Future Work

5.1 Global Conclusions

The Introduction mentioned that the goal of this thesis is to bring together the different viewpoints in the literature on the source of stacking interactions. The stacking application papers mention the importance of charge transfer and dipole-dipole interactions in stabilizing stacked structures,¹⁻⁶ the theoretical literature on biological molecules emphasise the importance of dipole-dipole interactions and polarizability of the monomers,⁷⁻¹¹ the experimental literature on benzene systems mention the importance of electrostatics,¹²⁻¹⁸ and in some cases charge transfer,¹⁹⁻²¹ while the theoretical literature on benzene systems has so far not given a global explanation that explains all of the trends seen.²²⁻²⁷ This thesis has examined stacking interactions in more depth than has been done in the past, and the results are found to agree most closely with the findings of the stacking application papers wherein two different kinds of forces (charge transfer and dipole-dipole interactions) have been identified. In addition, the extent of charge separation in the ring is found to be important. Charge separation is found to be important when the difference in the ESP of the interacting monomers is small. Charge transfer is dominant when the difference in ESP of the stacked rings is large, while dipole-dipole interactions are present in all of the studied dimers. This answers the question set-out in the Chapter 1 regarding whether the nature of interactions change between heavily-substituted phenyl dimers (>3 substituents) and lightly-substituted phenyl dimers (≤ 3 substituents).

The stabilization due to dispersion can be strengthened by increasing the extent of charge separation in the ring or by increasing the ring size. Charge transfer can be increased by increasing the difference in ESP of the two rings. The stabilization due to charge transfer is seen in the electron correlation. This has been deduced by examining the stacking stabilization energies at HF and MP2

level of theory. These results will no doubt prove valuable for studies interested in designing self-assembling stacked structures.

This thesis also provides valuable structural information on stacked structures. It is shown that dipoles are anti-parallel when both stacked rings have an electron-withdrawing substituent or when both rings have an electron-donating substituent. However, in cases where one ring has only electron-donating substituents while the other ring has only electron-withdrawing substituents, the dipole orientation is no longer anti-parallel. This deviation has been shown to have an associated energetic cost. While these results do a good job illustrating the potential energy surface of the dimers in the gas phase, they are not optimizations and therefore cannot predict exactly how the molecules will behave in solution.

5.2 Future Work

The biggest unanswered question in this thesis is: why does the effect of substituents differ between the two-ring purines and one-ring pyrimidines? While the one-ring pyrimidines show the same substituent effects as benzene, the two-ring purines do not show the same substituent effects. It might be that the substituents on two-ring systems do not have the same stacking interaction trends because one or two substituents are not enough to change the charge transfer interactions involving the bigger ring systems, and substituent effects will be seen only when more substituents are added to the ring. Another reason why substituent effects cannot be seen could be because the opposite molecule has only one ring and substituent effects will become visible if the two-ring systems are stacked with other two ring systems.

Another interesting question to address in future work is which orbitals are involved in the electron correlation, and whether my hypothesis of intramolecular electron correlation vs

intermolecular electron correlation can be confirmed. Furthermore, it will be interesting to see if it is the ring carbons or the substituent atoms or both that take part in the electron correlation.

This study has so far concerned itself with gas-phase calculations. It would be interesting to determine the effect of external solvents on the two different forces involved in- π/π stacking interactions, given that the experimental applications of stacking are always in a solvent.

The last important question that needs to be investigated is why experimental benzene studies differ from theory. Experimental studies have never confirmed charge transfer interactions by showing decreasing stacking energies with increasing number of substituents as has been shown in the hexasubstituted benzene-polysubstituted benzene systems. Further experimental studies would help confirm or refute the charge transfer hypothesis proposed in this study.

References

- (1) Zhang, C.; Zhang, X.; Zhang, X.; Fan, X.; Jie, J.; Chang, J. C.; Lee, C.-S.; Zhang, W.; Lee, S.-T. *Advanced Materials* **2008**, *20*, 1716.
- (2) Zhang, X.; Zhang, X.; Shi, W.; Meng, X.; Lee, C.; Lee, S. *Angewandte Chemie International Edition* **2007**, *46*, 1525.
- (3) Yamamoto, Y.; Fukushima, T.; Suna, Y.; Ishii, N.; Saeki, A.; Seki, S.; Tagawa, S.; Taniguchi, M.; Kawai, T.; Aida, T. *Science* **2006**, *314*, 1761.
- (4) Schmidt-Mende, L.; Fechtenkötter, A.; Mullen, K.; Moons, E.; Friend, R. H.; MacKenzie, J. D. *Science* **2001**, *293*, 1119.
- (5) Xu, J.; Wen, L.; Zhou, W.; Lv, J.; Guo, Y.; Zhu, M.; Liu, H.; Li, Y.; Jiang, L. *Journal of Physical Chemistry C* **2009**, *113*, 5924.
- (6) Yamauchi, Y.; Yoshizawa, M.; Fujita, M. *Journal of the American Chemical Society* **2008**, *130*, 5832.
- (7) Rutledge, L. R.; Campbell-Verduyn, L. S.; Hunter, K. C.; Wetmore, S. D. *Journal of Physical Chemistry B* **2006**, *110*, 19652.
- (8) Rutledge, L. R.; Campbell-Verduyn, L. S.; Wetmore, S. D. *Chemical Physics Letters* **2007**, *444*, 167.
- (9) Hobza, P.; Sponer, J. *Chemical Reviews (Washington, D. C.)* **1999**, *99*, 3247.
- (10) Sponer, J.; Leszczynski, J.; Hobza, P. *Journal of Molecular Structure* **2001**, *573*, 43.
- (11) Sponer, J.; Leszczynski, J.; Hobza, P. *Biopolymers* **2002**, *61*, 3.
- (12) Cockroft, S. L.; Perkins, J.; Zonta, C.; Adams, H.; Spey, S. E.; Low, C. M. R.; Vinter, J. G.; Lawson, K. R.; Urch, C. J.; Hunter, C. A. *Organic & Biomolecular Chemistry* **2007**, *5*, 1062.
- (13) Cockroft, S. L.; Hunter, C. A.; Lawson, K. R.; Perkins, J.; Urch, C. J. *J. Am. Chem. Soc.* **2005**, *127*, 8594.

- (14) Adams, H.; Blanco, J. L. J.; Chessari, G.; Hunter, C. A.; Low, C. M. R.; Sanderson, J. M.; Vinter, J. G. *Chemistry-a European Journal* **2001**, 7, 3494.
- (15) Adams, H.; Hunter, C. A.; Lawson, K. R.; Perkins, J.; Spey, S. E.; Urch, C. J.; Sanderson, J. M. *Chemistry-a European Journal* **2001**, 7, 4863.
- (16) Gung, B. W.; Xue, X.; Reich, H. J. *J. Org. Chem.* **2005**, 70, 3641.
- (17) Cozzi, F.; Siegel, J. S. *Pure and applied chemistry* **1995**, 67, 683.
- (18) Cozzi, F.; Cinquini, M.; Annuziata, R.; Siegel, J. S. *Journal of the American Chemical Society* **1993**, 115, 5330.
- (19) Gung, B. W.; Xue, X. W.; Zou, Y. *Journal of Organic Chemistry* **2007**, 72, 2469.
- (20) Gung, B. W.; Amicangelo, J. C. *Journal of Organic Chemistry* **2006**, 71, 9261.
- (21) Gung, B. W.; Patel, M.; Xue, X. W. *Journal of Organic Chemistry* **2005**, 70, 10532.
- (22) Arnstein, S. A.; Sherrill, C. D. *Physical Chemistry Chemical Physics* **2008**, 10, 2646.
- (23) Sinnokrot, M. O.; Sherrill, C. D. *Journal of Physical Chemistry A* **2006**, 110, 10656.
- (24) Ringer, A. L.; Sinnokrot, M. O.; Lively, R. P.; Sherrill, C. D. *Chemistry-a European Journal* **2006**, 12, 3821.
- (25) Sinnokrot, M. O.; Sherrill, C. D. *Journal of the American Chemical Society* **2004**, 126, 7690.
- (26) Sinnokrot, M. O.; Sherrill, C. D. *Journal of Physical Chemistry A* **2004**, 108, 10200.
- (27) Sinnokrot, M. O.; Sherrill, C. D. *Journal of Physical Chemistry A* **2003**, 107, 8377.

Appendix

Table 10: Sample results from the R1 and α potential energy surface scans (for 1,2,4-triaminobenzene and benzonitrile dimer).

R1(Å) across						
α (°) down	3.1	3.2	3.3	3.4	3.5	3.6
0	-2.5	-12.1	-17.9	-21.1	-22.4	-22.6
30	-12.2	-19.0	-22.9	-24.6	-24.9	-24.3
60	-18.7	-23.9	-26.5	-27.2	-26.8	-25.7
90	-19.7	-24.4	-26.6	-27.1	-26.5	-25.2
120	-14.3	-20.1	-23.1	-24.2	-24.1	-23.2
150	-17.6	-22.6	-24.9	-25.6	-25.0	-23.8
180	-18.4	-22.9	-25.0	-25.5	-24.9	-23.6
210	-20.6	-24.5	-26.2	-26.4	-25.5	-24.1
240	-25.3	-28.4	-29.4	-28.9	-27.6	-25.8
270	-21.6	-25.9	-27.8	-28.0	-27.2	-25.7
300	-12.1	-19.0	-22.9	-24.6	-24.8	-24.2
330	-11.5	-18.7	-22.8	-24.7	-25.1	-24.6

Table 11: Sample results from the R2 potential energy surface scans (for 1,2,4-triaminobenzene and benzonitrile dimer).

x across (Å)							
y down (Å)	-1.5	-1	-0.5	0	0.5	1	1.5
-1.5	-17.4	-19.6	-22.4	-22.7	-20.7	-20.3	-22.4
-1.0	-17.2	-21.6	-25.0	-23.2	-18.6	-18.0	-21.8
-0.5	-18.3	-23.7	-27.7	-26.2	-21.7	-20.8	-23.4
0.0	-19.7	-24.3	-28.7	-29.4	-27.2	-25.8	-25.2
0.5	-20.0	-22.6	-26.1	-28.3	-28.3	-26.8	-24.3
1.0	-18.9	-19.7	-21.5	-23.7	-24.9	-24.4	-22.5
1.5	-16.9	-17.1	-17.9	-19.9	-22.0	-23.0	-22.2

Table 12: Summary of information from potential energy surface scans of the benzene-monomosubstituted benzene dimers at the counterpoise corrected MP2/6-31G*(0.25) level of theory. All energies are in kJ mol⁻¹, dipoles in Debye and distances are in Å.

Monomer	Dipole of monomer	R1	α	ΔE	R2		ΔE
					x	y	
Benzene	0.000	3.900	30.0	-7.4	-1	-1	-8.9
Toluene	0.277	3.700	30.0	-10.6	0.5	1	-13.5
Phenol	1.513	3.700	0.0	-10	-1	0.5	-13.2
Aminobenzene	1.616	3.700	0.0	-9.1	-1	0.5	-11.5
Fluorobenzene	1.843	3.700	30.0	-10.8	0	1.5	-12.6
Benzenecarboxamide	4.094	3.500	30.0	-17.6	1	0	-18.8
Cyanobenzene	5.001	3.600	0.0	-16.9	0.5	0.5	-18.3
Nitrobenzene	5.376	3.400	30.0	-21.8	0	0.5	-22.5

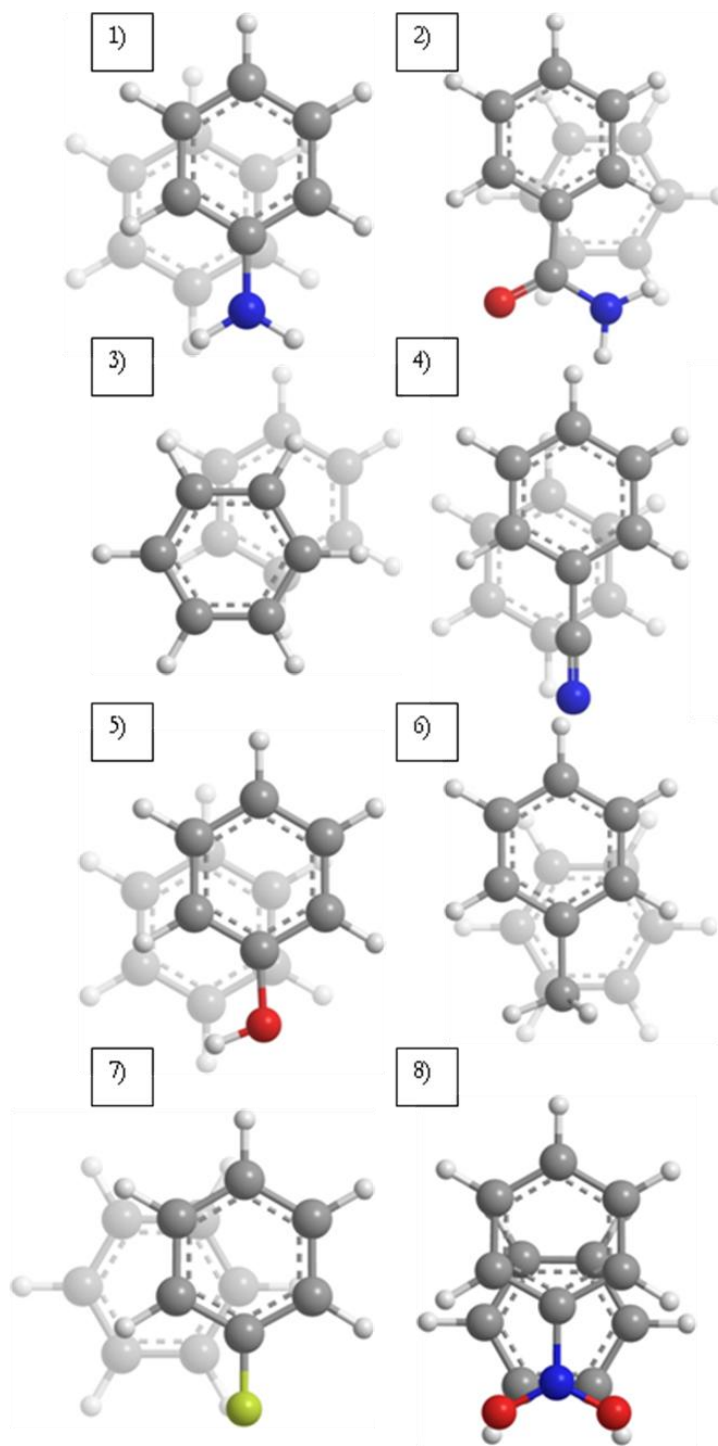


Figure 27: The dimer conformation corresponding to the most stable structure after the R2 scans for the benzene-monomonsubstituted benzenes. The carbon attached to the substituent is over the benzene ring in all cases except for fluorobenzene (5) where the carbon atom is close to the ring. The different dimers are $C_6H_6-C_6H_5X$ where $X = -NH_2$, $-CONH_2$, $-H$, $-CN$, $-OH$, $-CH_3$, $-F$, $-NO_2$ for structures 1-8 respectively.

Table 13: Summary of information from potential energy surface scans of the benzene-polysubstituted benzene dimers at the counterpoise corrected MP2/6-31G*(0.25) level of theory. All energies are in kJ mol⁻¹ and all distances are in Å.

Monomer	R1	α	ΔE	R2		ΔE
				x	y	
Hexaaminobenzene	3.500	0.0	-15.4	0	1	-16.8
Pentaaminobenzene	3.500	0.0	-14.1	0.5	0.5	-16.1
1,2,3,4-Tetraaminobenzene	3.500	0.0	-14.2	-0.5	0	-15.6
1,2,3,5-Tetraaminobenzene	3.600	0.0	-12.1	1.5	-1	-13.8
1,2,4,5-Tetraaminobenzene	3.600	0.0	-11.5	0	-1.5	-14.8
1,2,3-Triaaminobenzene	3.500	0.0	-13.6	0	0.5	-14.6
1,2,4-Triaminobenzene	3.600	0.0	-10.9	-1	0.5	-14.5
1,3,5-Triaminobenzene	3.700	0.0	-9.3	0	-1.5	-12.0
1,2-Diaminobenzene	3.600	0.0	-11.7	0.5	-1	-12.8
1,3-Diaminobenzene	3.700	0.0	-9.8	0	1	-12.9
1,4-Diaminobenzene	3.700	0.0	-8.8	1	1	-11.8
Aminobenzene	3.700	0.0	-9.1	-1	0.5	-11.5
Hexafluorobenzene	3.500	0.0	-25.4	0.5	0.5	-26.5
Pentafluorobenzene	3.500	0.0	-22.4	0.5	0.5	-24.3
1,2,3,4-Tetrafluorobenzene	3.500	0.0	-20.6	-0.5	0	-22.2
1,2,3,5-Tetrafluorobenzene	3.600	0.0	-19.0	0	0.5	-20.4
1,2,4,5-Tetrafluorobenzene	3.600	0.0	-18.3	0	1	-20.3
1,2,3-Trifluorobenzene	3.500	0.0	-18.4	0	0.5	-19.5
1,2,4-Trifluorobenzene	3.600	0.0	-16.1	1	0.5	-18.3
1,3,5-Trifluorobenzene	3.700	0.0	-15.1	-1	0.5	-16.6
1,2-Difluorobenzene	3.600	0.0	-14.8	1	0	-15.6
1,3-Difluorobenzene	3.700	0.0	-13.3	0	1	-15.1
1,4-Difluorobenzene	3.700	30.0	-12.4	-1.5	0	-14.6
Fluorobenzene	3.700	30.0	-10.8	0	1.5	-12.6
Hexacyanobenzene	3.400	30.0	-49.4	1	0	-52.6
Pentacyanobenzene	3.400	30.0	-43.7	-0.5	-0.5	-47.1
1,2,3,4-Tetracyanobenzene	3.400	0.0	-40.2	-0.5	0	-41.8
1,2,3,5-Tetracyanobenzene	3.500	30.0	-36.4	-0.5	0.5	-39.1
1,2,4,5-Tetracyanobenzene	3.500	30.0	-34.5	-1	0	-37.4
1,2,3-Tricyanobenzene	3.400	0.0	-35.0	0.5	0	-35.0
1,2,4-Tricyanobenzene	3.500	30.0	-29.6	-0.5	0.5	-32.3
1,3,5-Tricyanobenzene	3.600	30.0	-26.9	-0.5	-1.5	-29.3
1,2-Dicyanobenzene	3.400	0.0	-27.3	0	0.5	-27.5
1,3-Dicyanobenzene	3.500	0.0	-22.9	0	0.5	-25.9
1,4-Dicyanobenzene	3.600	30.0	-20.2	-1	0.5	-23.0
Cyanobenzene	3.600	0.0	-16.9	0.5	0.5	-18.3

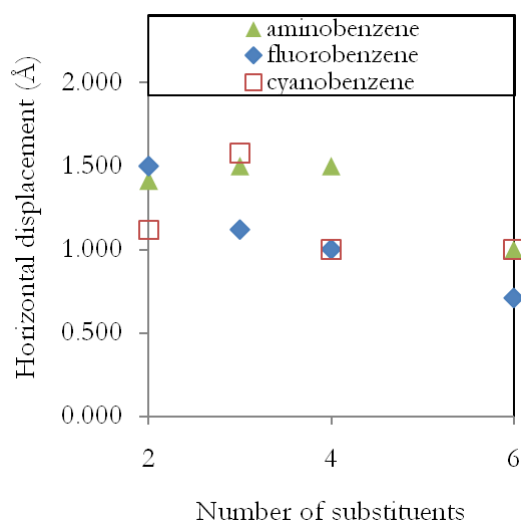


Figure 28: Figure showing the effect of increasing number of substitutions on horizontal displacements for all the zero dipole polysubstituted benzenes in the benzene-polysubstituted benzene dimers. The horizontal displacements represent the distance between the centers of the ring. The overlap between the rings increases with increasing number of amino, fluoro and cyano substituents.

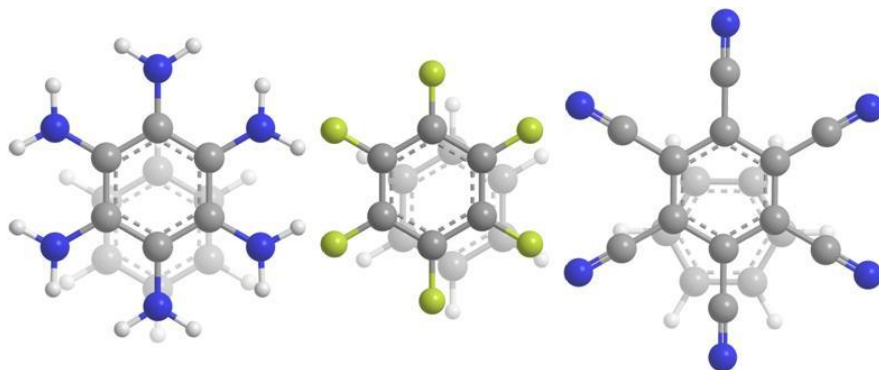


Figure 29: Final structures of the hexaminobenzene-benzene dimer, hexafluorobenzene-benzene dimer and the hexacyanobenzene-benzene dimer. The rings show a considerable degree of overlap in the dimers.

Table 14: Summary of information from potential energy surface scans of the cyanobenzene-polycyanobenzene dimers and cyanobenzene-polyaminobenzene dimers at the counterpoise corrected MP2/6-31G*(0.25) level of theory. All energies are in kJ mol⁻¹ and all distances are in Å.

Monomer	R1	α	ΔE	R2		ΔE
				x	y	
Hexacyanobenzene	3.300	30.0	-50.4	-0.5	0	-54.4
Pentacyanobenzene	3.300	180.0	-53.2	0	0	-53.2
1,2,3,4-Tetracyanobenzene	3.300	210.0	-49.5	0.5	-0.5	-49.7
1,2,3,5-Tetracyanobenzene	3.300	270.0	-45.6	0	0	-45.6
1,2,4,5-Tetracyanobenzene	3.300	180.0	-40.0	0	0.5	-43.9
1,2,3-Tricyanobenzene	3.300	180.0	-43.5	0	0.5	-45.7
1,2,4-Tricyanobenzene	3.300	210.0	-40.8	0	0	-40.8
1,3,5-Tricyanobenzene	3.400	60.0	-32.5	-0.5	0	-34.9
1,2-Dicyanobenzene	3.400	210.0	-36.0	0.5	0	-38.0
1,3-Dicyanobenzene	3.300	180.0	-36.2	0	0	-36.2
1,4-Dicyanobenzene	3.400	150.0	-28.1	0.5	0.5	-30.8
Cyanobenzene	3.400	150.0	-28.3	0	0.5	-28.4
Hexaaminobenzene	3.300	30.0	-36.6	0	1.5	-37.9
Pentaaminobenzene	3.300	180.0	-33.5	0.5	-0.5	-34.5
1,2,3,4-Tetraaminobenzene	3.400	90.0	-30.8	-1	0	-34.1
1,2,3,5-Tetraaminobenzene	3.300	300.0	-30.1	-0.5	1.5	-32.3
1,2,4,5-Tetraaminobenzene	3.300	180.0	-31.8	0	0.5	-32.7
1,2,3-Triaaminobenzene	3.400	270.0	-27.2	1	0.5	-28.8
1,2,4-Triaminobenzene	3.300	240.0	-29.4	0	0	-29.4
1,3,5-Triaminobenzene	3.400	30.0	-25.6	-0.5	-0.5	-28.5
1,2-Diaminobenzene	3.400	300.0	-27.0	0	0	-27.0
1,3-Diaminobenzene	3.300	180.0	-25.1	0	0	-25.1
1,4-Diaminobenzene	3.400	60.0	-23.2	-1	0	-26.6
Aminobenzene	3.400	240.0	-21.2	0.5	-0.5	-21.4

Table 15: Summary of information from potential energy surface scans of the aminobenzene-polycyanobenzene dimers and aminobenzene-polyaminobenzene dimers at the counterpoise corrected MP2/6-31G*(0.25) level of theory. All energies are in kJ mol⁻¹ and all distances are in Å.

Monomer	R1	α	ΔE	R2		ΔE
				x	y	
Hexacyanobenzene	3.200	30.0	-70.2	0	-0.5	-74.0
Pentacyanobenzene	3.200	150.0	-61.8	0	0	-61.8
1,2,3,4-Tetracyanobenzene	3.300	300.0	-54.4	0	-0.5	-55.1
1,2,3,5-Tetracyanobenzene	3.300	270.0	-51.6	0	0	-51.6
1,2,4,5-Tetracyanobenzene	3.300	90.0	-50.6	0.5	0	-53.4
1,2,3-Tricyanobenzene	3.300	120.0	-43.4	0.5	0	-44.5
1,2,4-Tricyanobenzene	3.300	150.0	-42.1	-0.5	0	-43.4
1,3,5-Tricyanobenzene	3.400	30.0	-38.3	0	-0.5	-40.7
1,2-Dicyanobenzene	3.300	300.0	-34.7	0	-0.5	-34.9
1,3-Dicyanobenzene	3.400	120.0	-32.1	-0.5	0.5	-34.1
1,4-Dicyanobenzene	3.500	90.0	-28.6	1	0	-31.3
Cyanobenzene	3.400	240.0	-21.2	0.5	-0.5	-21.4
Hexaaminobenzene	3.500	30.0	-14.6	2.5	-1.5	-17.7
Pentaaminobenzene	3.500	180.0	-14.9	0	2.5	-19.2
1,2,3,4-Tetraaminobenzene	3.500	240.0	-14.9	-2	0.5	-19.1
1,2,3,5-Tetraaminobenzene	3.500	270.0	-12.9	0	-2.5	-16.8
1,2,4,5-Tetraaminobenzene	3.500	180.0	-13.4	0	0.5	-15.8
1,2,3-Triaaminobenzene	3.500	120.0	-14.0	2	1	-17.1
1,2,4-Triaaminobenzene	3.500	240.0	-14.3	-2	1.5	-17.2
1,3,5-Triaaminobenzene	3.600	30.0	-9.3	0	-2.5	-14.0
1,2-Diaminobenzene	3.500	120.0	-13.8	0.5	0	-14.5
1,3-Diaminobenzene	3.500	180.0	-14.0	0	2.5	-16.8
1,4-Diaminobenzene	3.600	120.0	-10.5	0	1	-13.8
Aminobenzene	3.500	240.0	-12.0	0.5	0.5	-13.0

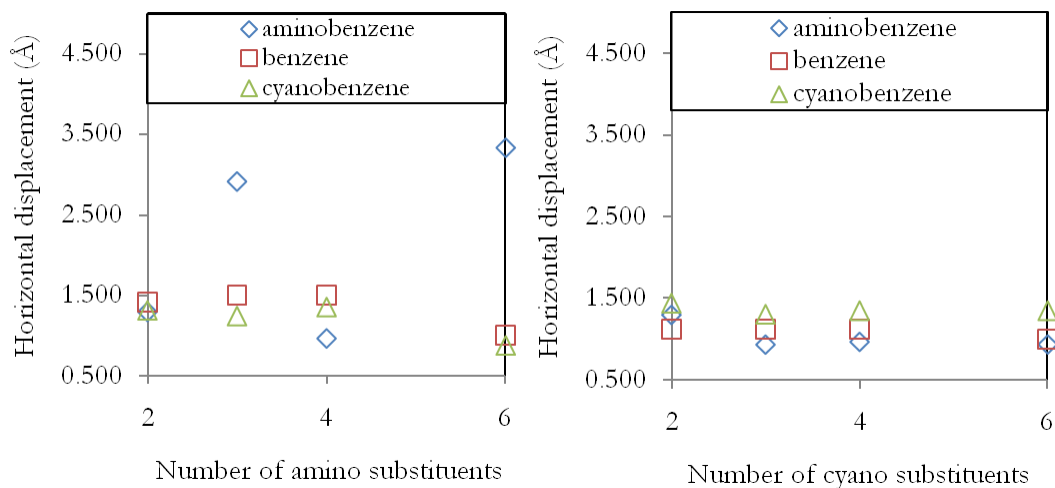


Figure 30: Figure showing the effect of increasing number of substitutions on horizontal displacements for all the zero dipole polysubstituted benzenes in the monosubstituted benzene-polysubstituted benzene dimers. The horizontal displacements represent the distance between the centers of the ring. The overlap between the rings generally increases with increasing number of amino, fluoro and cyano substituents.

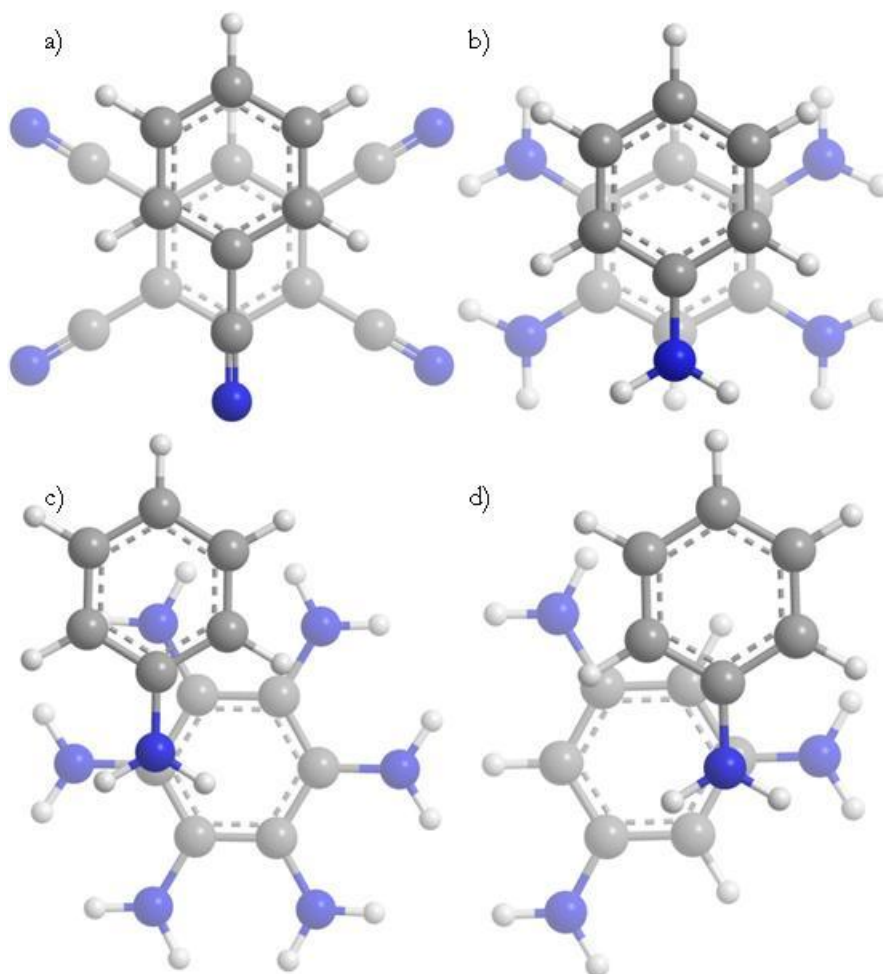


Figure 31: Representative pictures of the structures found in monosubstituted benzene-polysubstituted benzene dimers. Structures a) and b) are 1,2,4,5-tetraaminobenzene-aminobenzene and 1,2,4,5-tetracyanobenzene-cyanobenzene respectively. They represent the typical structure with the rings overlapping and the most polarized carbon atom of the monosubstituted benzene over the benzene ring. In addition, the polycyanobenzenes-cyanobenzenes typically have the carbon atom of the cyano substituent overlapping with ring of the other benzene monomer. Structures c) and d) are hexaminobenzene-aminobenzene and 1,3,5-triaminobenzene-aminobenzene respectively, the two exceptions which are exceptions to the above mentioned trend because substituent-ring interactions dominate over charge transfer interactions.

Table 16: Summary of information from potential energy surface scans of the hexacyanobenzene-polycyanobenzene dimers and hexacyanobenzene-polyaminobenzene dimers at the counterpoise corrected MP2/6-31G*(0.25) level of theory. All energies are in kJ mol⁻¹ and all distances are in Å.

Monomer	R1	α	ΔE	R2		ΔE
				x	y	
Hexacyanobenzene	3.400	30.0	-29.8	-2	-3	-45.3
1,2,4,5-Tetracyanobenzene	3.400	30.0	-29.6	-1.5	0	-40.7
1,2,3-Tricyanobenzene	3.300	0.0	-47.3	-2	-2	-52.5
1,2,4-Tricyanobenzene	3.400	30.0	-34.7	1.5	2.5	-50.3
1,3,5-Tricyanobenzene	3.500	30.0	-30.6	0	1.5	-38.1
1,4-Dicyanobenzene	3.400	30.0	-35.3	-0.5	1.5	-43.9
Cyanobenzene	3.300	30.0	-50.4	-0.5	0	-54.4
Hexaaminobenzene	3.100	30.0	-135.8	-1	0	-146.0
1,2,4,5-Tetraaminobenzene	3.200	30.0	-108.3	-1	0	-117.3
1,2,3-Triaminobenzene	3.100	30.0	-109.0	0	0	-109.0
1,2,4-Triaminobenzene	3.200	30.0	-99.8	0.5	0.5	-104.7
1,3,5-Triaminobenzene	3.200	30.0	-99.8	-0.5	0.5	-101.6
1,4-Diaminobenzene	3.300	30.0	-78.8	-1	0.5	-88.4
Aminobenzene	3.200	30.0	-70.2	0	-0.5	-74.0

Table 17: Summary of information from potential energy surface scans of the hexaaminobenzene-polyaminobenzene dimers and hexaaminobenzene-polycyanobenzene dimers at the counterpoise corrected MP2/6-31G*(0.25) level of theory. All energies are in kJ mol⁻¹ and all distances are in Å.

Monomer	R1	α	ΔE	R2		ΔE
				x	y	
Hexaaminobenzene	3.500	30.0	-8.8	-5	0	-17.0
1,2,4,5-Tetraaminobenzene	3.500	30.0	-10.4	2.5	3	-16.9
1,2,3-Triaaminobenzene	3.500	30.0	-10.3	0	2.5	-20.4
1,2,4-Triaminobenzene	3.500	30.0	-11.2	-1.5	3	-18.9
1,3,5-Triaminobenzene	3.500	30.0	-9.2	-1.5	3	-14.9
1,4-Diaminobenzene	3.500	30.0	-12.5	-1.5	-3	-15.1
Aminobenzene	3.500	30.0	-14.6	2.5	-1.5	-17.7
Hexacyanobenzene	3.100	30.0	-135.8	-1	0	-146.0
1,2,4,5-Tetracyanobenzene	3.200	30.0	-97.6	-1	0	-101.2
1,2,3-Tricyanobenzene	3.200	30.0	-77.0	0	1	-80.8
1,2,4-Tricyanobenzene	3.200	30.0	-78.3	-0.5	-1	-80.9
1,3,5-Tricyanobenzene	3.200	0.0	-75.1	-0.5	0	-75.7
1,4-Dicyanobenzene	3.300	30.0	-56.7	-0.5	-0.5	-58.2
Cyanobenzene	3.300	30.0	-36.6	0	1.5	-37.9

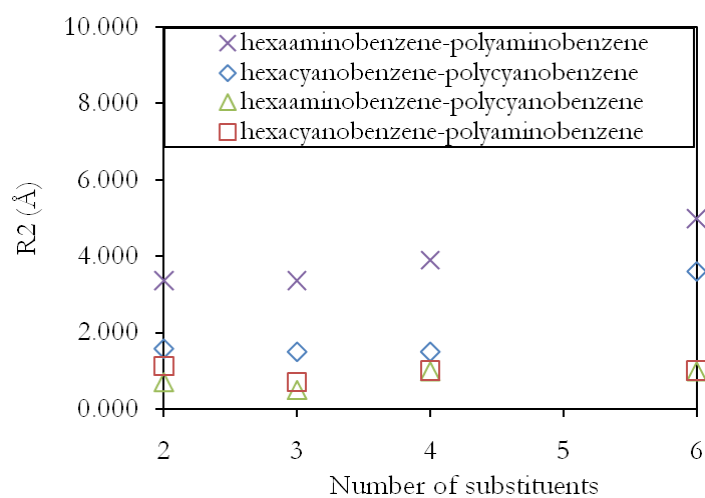


Figure 32: Figure showing the effect of increasing number of substitutions on horizontal displacements for all the zero dipole polysubstituted benzenes in the hexasubstituted benzene-polysubstituted benzene dimers. The horizontal displacements represent the distance between the centers of the ring. The overlap between the rings generally increases with increasing charge transfer interactions.

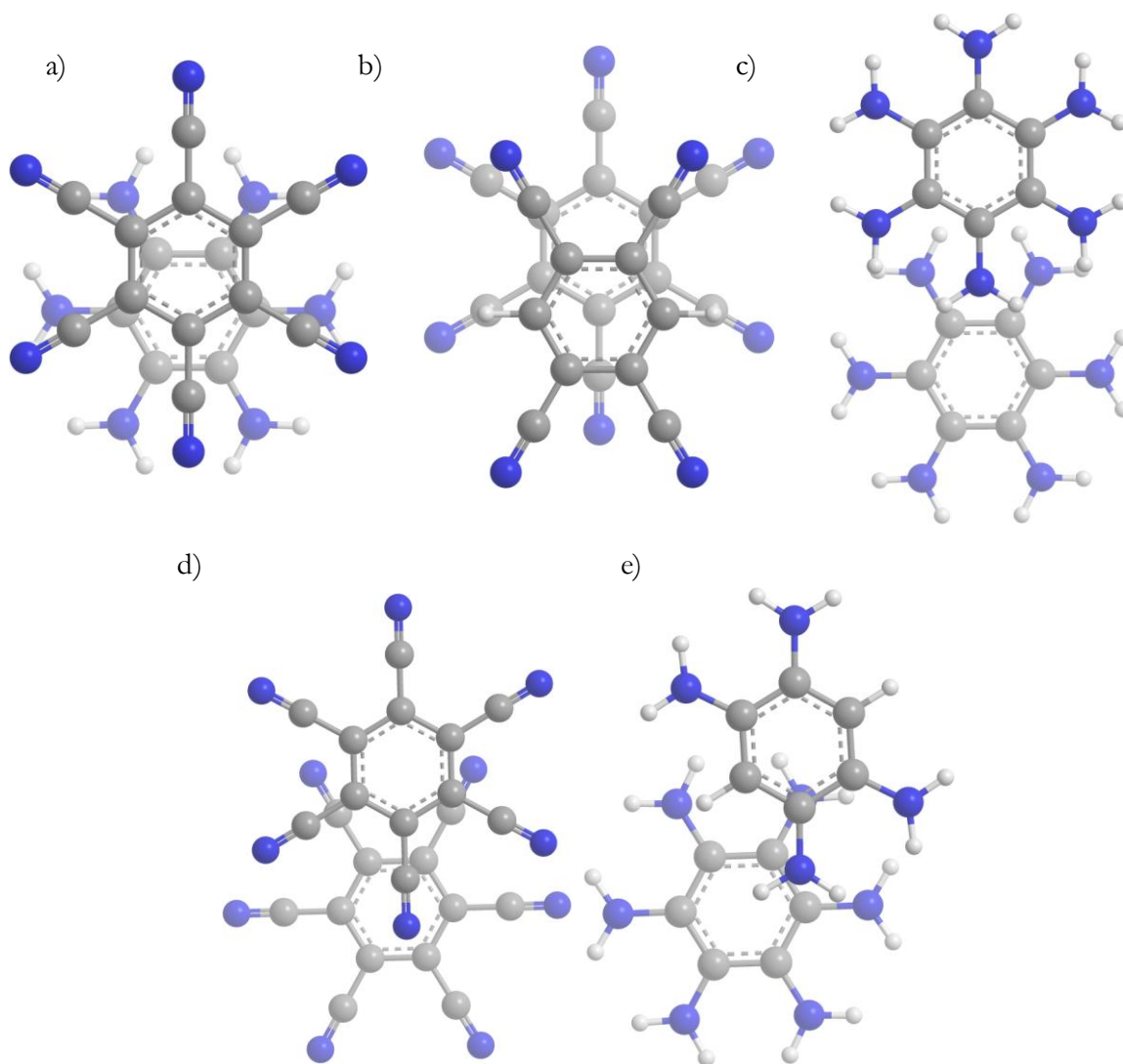


Figure 33: Figures representative of the final horizontal displacement structures for the zero-dipole hexasubstituted benzene-polysubstituted benzene systems. There are five representative figures of the final conformations. a) The hexacyanobenzene-hexaaminobenzene structure shows the overlapping benzene dimers with the most polarized carbon atom over the benzene ring. This structure is representative of hexacyanobenzene-polyaminobenzene and hexaaminobenzene-polycyanobenzene dimers where there are strong charge transfer interactions. b) The hexacyanobenzene-1,2,4,5-tetracyanobenzene dimer with the most polarized carbon atom and the substituents over the benzene ring. This structure is representative of all of the hexacyanobenzene-polycyanobenzene dimers except for the hexacyanobenzene dimer. c) The hexaaminobenzene-hexaaminobenzene dimer with only the substituents interacting with each other. d) The hexacyanobenzene dimer showing no ring overlap and substituent-ring interactions. e) The hexaaminobenzene-1,2,4,5-tetraaminobenzene dimer with no ring overlap and the amino substituent interacting with the ring. This structure is representative of the polyaminobenzene-hexaaminobenzene dimers.

Table 18: Summary of information from potential energy surface scans of the adenine-monomonsubstituted benzene dimers at the counterpoise corrected MP2/6-31G*(0.25) level of theory. All energies are in kJ mol⁻¹, dipoles in Debye and distances are in Å. The “-fl” suffix represents the flipped monomer.

Monomer	Dipole of monomer	R1	α	ΔE	R2		ΔE
					x	y	
Benzene	0.000	3.400	30.0	-24.3	-0.5	0	-24.4
Toluene	0.277	3.400	0.0	-27.9	0	0	-27.9
Toluene-fl	0.277	3.300	150.0	-28.3	0	-0.5	-29.0
Phenol	1.513	3.300	210.0	-29.6	-0.5	0	-32.0
Phenol-fl	1.513	3.400	0.0	-27.8	0.5	0	-27.9
Aminobenzene	1.616	3.400	270.0	-25.4	0	-0.5	-26.6
Fluorobenzene	1.843	3.400	180.0	-26.5	-0.5	0	-29.1
Benzenecarboxamide	4.094	3.400	30.0	-29.6	1	0.5	-34.5
Benzenecarboxamide-fl	4.094	3.400	180.0	-32.3	-1	0	-37.6
Cyanobenzene	5.001	3.400	180.0	-34.5	0.5	-0.5	-37.7
Nitrobenzene	5.376	3.300	180.0	-33.3	1	0	-38.7

Table 19: Summary of information from potential energy surface scans of the cytosine-monomonsubstituted benzene dimers at the counterpoise corrected MP2/6-31G*(0.25) level of theory. All energies are in kJ mol⁻¹, dipoles in Debye and distances are in Å. The “-fl” suffix represents the flipped monomer.

Monomer	Dipole of monomer	R1	α	ΔE	R2		ΔE
					x	y	
Benzene	0.000	3.500	0.0	-15.2	-0.5	1.5	-18.4
Toluene	0.277	3.500	210.0	-20.4	0	-1.5	-21.9
Toluene-fl	0.277	3.500	270.0	-20.6	0	-1	-23.8
Phenol	1.513	3.500	30.0	-21.0	-1	1	-24.0
Phenol-fl	1.513	3.400	180.0	-22.1	-0.5	1.5	-23.6
Aminobenzene	1.616	3.500	90.0	-19.0	-0.5	1.5	-25.1
Fluorobenzene	1.843	3.400	240.0	-21.6	0	0	-21.6
Benzenecarboxamide	4.094	3.400	180.0	-31.0	0.5	0	-32.0
Benzenecarboxamide-fl	4.094	3.400	0.0	-31.1	0	1	-33.5
Cyanobenzene	5.001	3.300	240.0	-30.4	0	0	-30.4
Nitrobenzene	5.376	3.300	270.0	-32.8	-0.5	0	-34.4

Table 20: Summary of information from potential energy surface scans of the guanine-monomonsubstituted benzene dimers at the counterpoise corrected MP2/6-31G*(0.25) level of theory. All energies are in kJ mol⁻¹, dipoles in Debye and distances are in Å. The “-fl” suffix represents the flipped monomer.

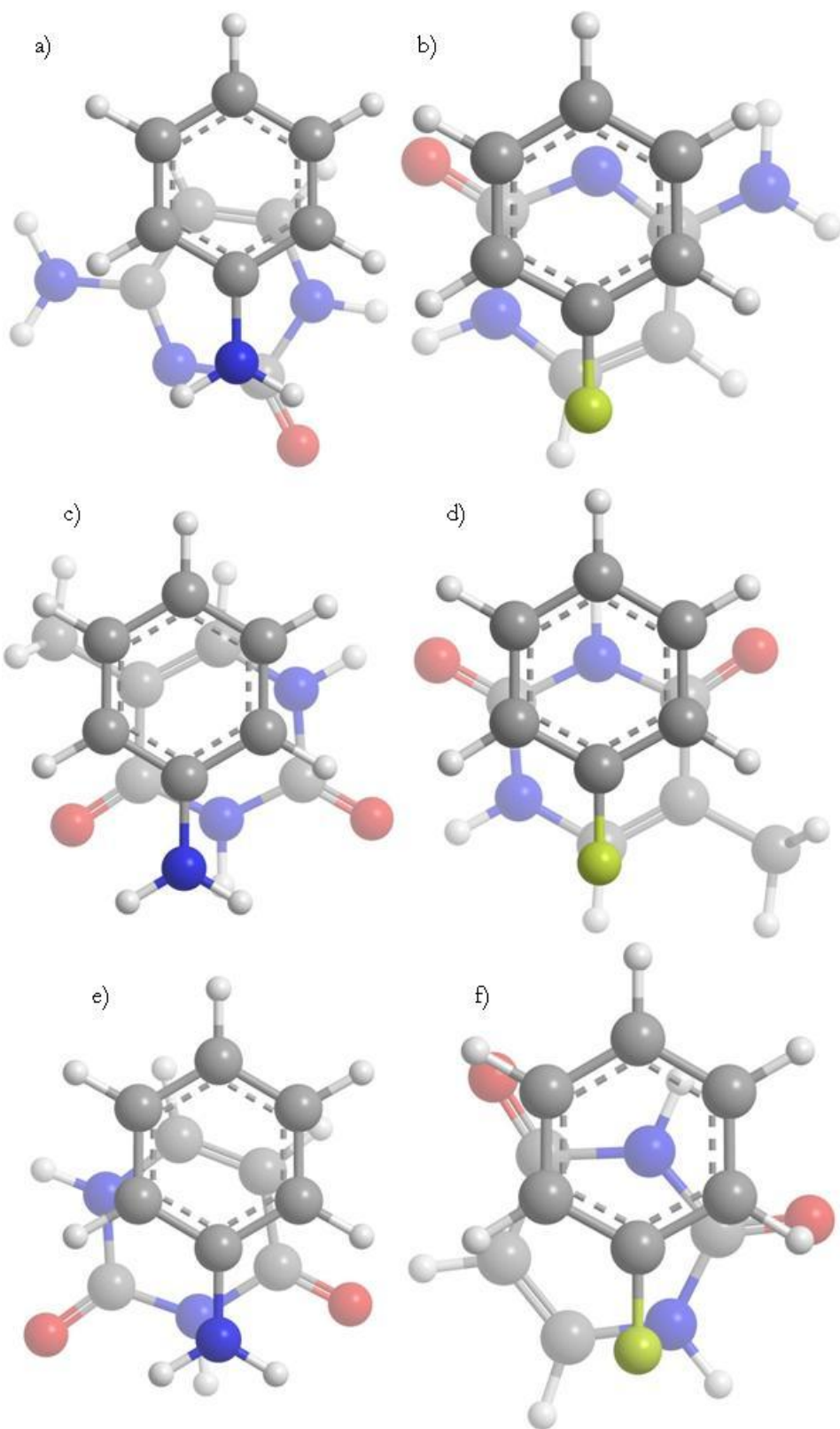
Monomer	Dipole of monomer	R1	α	ΔE	R2		ΔE
					x	y	
Benzene	0.000	3.400	30.0	-24.5	0	0.5	-25.2
Toluene	0.277	3.400	300.0	-29.0	0	-0.5	-31.0
Toluene-fl	0.277	3.400	0.0	-30.0	0	0	-30.0
Phenol	1.513	3.300	0.0	-33.8	0	0	-33.8
Phenol-fl	1.513	3.400	150.0	-29.7	1	-0.5	-33.0
Aminobenzene	1.616	3.400	60.0	-28.7	-0.5	0.5	-30.0
Fluorobenzene	1.843	3.300	330.0	-29.9	0.5	0	-30.8
Benzenecarboxamide	4.094	3.300	150.0	-39.2	-1	1	-41.8
Benzenecarboxamide-fl	4.094	3.300	0.0	-40.4	0	-0.5	-42.4
Cyanobenzene	5.001	3.300	30.0	-39.4	0.5	0	-41.0
Nitrobenzene	5.376	3.300	270.0	-39.3	0	-0.5	-41.7

Table 21: Summary of information from potential energy surface scans of the thymine-monomonsubstituted benzene dimers at the counterpoise corrected MP2/6-31G*(0.25) level of theory. All energies are in kJ mol⁻¹, dipoles in Debye and distances are in Å. The “-fl” suffix represents the flipped monomer.

Monomer	Dipole of monomer	R1	α	ΔE	R2		ΔE
					x	y	
Benzene	0.000	3.500	30.0	-20.8	1	-0.5	-22.5
Toluene	0.277	3.500	30.0	-25.3	1	0	-26.8
Toluene-fl	0.277	3.500	90.0	-25.6	0.5	-0.5	-26.7
Phenol	1.513	3.400	240.0	-26.7	-0.5	0	-27.6
Phenol-fl	1.513	3.400	210.0	-25.8	-0.5	0	-26.9
Aminobenzene	1.616	3.400	60.0	-28.7	0.5	0	-30.6
Fluorobenzene	1.843	3.400	240.0	-26.1	-0.5	0	-27.0
Benzenecarboxamide	4.094	3.400	180.0	-33.4	-0.5	-0.5	-35.2
Benzenecarboxamide-fl	4.094	3.300	240.0	-35.0	0	-0.5	-35.5
Cyanobenzene	5.001	3.300	240.0	-34.0	-0.5	0	-34.9
Nitrobenzene	5.376	3.200	240.0	-38.1	0	0	-38.1

Table 22: Summary of information from potential energy surface scans of the uracil-monosubstituted benzene dimers at the counterpoise corrected MP2/6-31G*(0.25) level of theory. All energies are in kJ mol⁻¹, dipoles in Debye and distances are in Å. The “-fl” suffix represents the flipped monomer.

Monomer	Dipole of monomer	R1	α	ΔE	R2		ΔE
					x	y	
Benzene	0.000	3.500	30.0	-18.7	0	-0.5	-20.1
Toluene	0.277	3.400	0.0	-22.6	0	0	-22.6
Toluene-fl	0.277	3.500	300.0	-24.4	-0.5	0.5	-25.5
Phenol	1.513	3.300	120.0	-26.6	0	0	-26.6
Phenol-fl	1.513	3.300	210.0	-24.8	0	-0.5	-25.2
Aminobenzene	1.616	3.500	300.0	-24.4	-0.5	1	-26.4
Fluorobenzene	1.843	3.300	150.0	-25.4	0	-0.5	-25.8
Benzenecarboxamide	4.094	3.300	180.0	-32.9	1	0	-35.6
Benzenecarboxamide-fl	4.094	3.300	270.0	-33.4	-0.5	0	-35.4
Cyanobenzene	5.001	3.300	150.0	-33.6	0	0	-33.6
Nitrobenzene	5.376	3.200	180.0	-34.5	0	0	-34.5



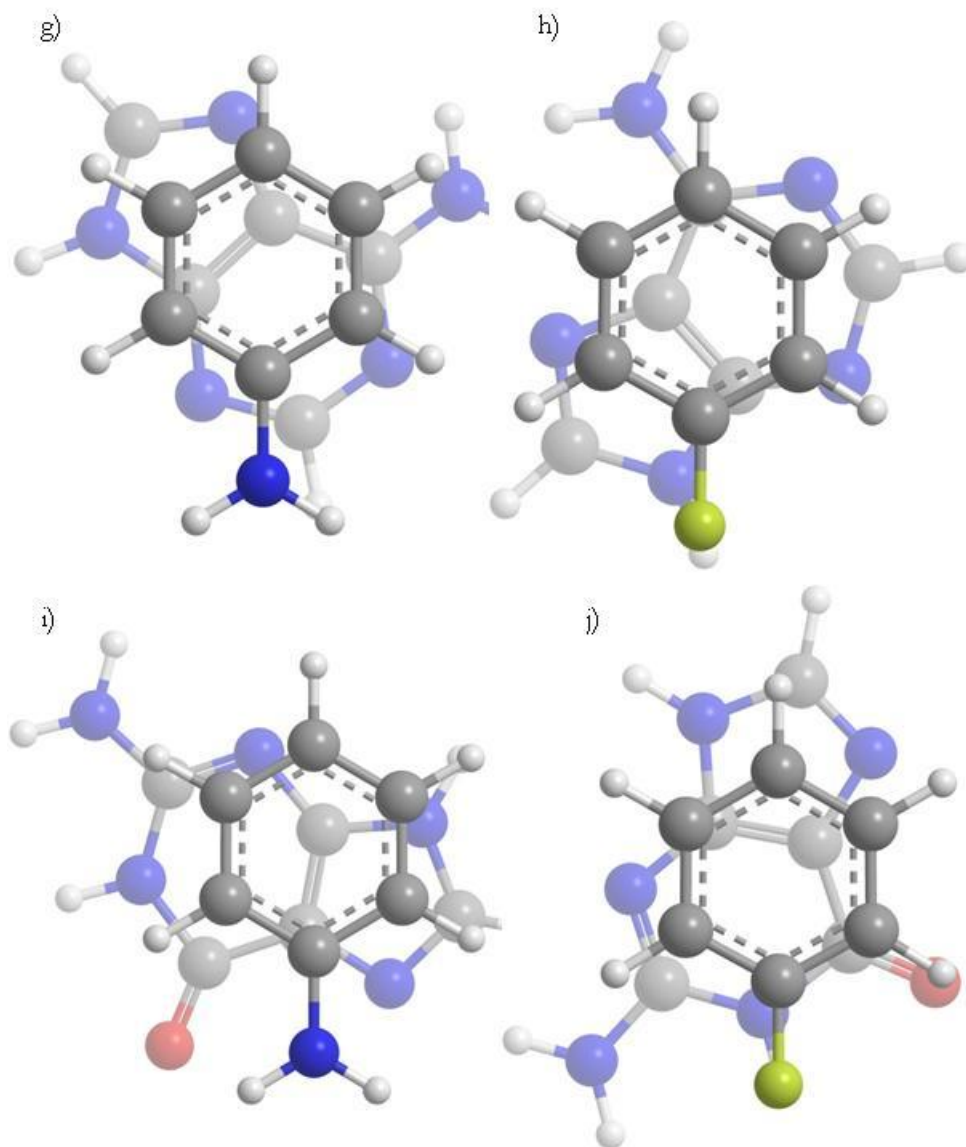


Figure 34: Figure showing the final structures for all the aminobenzene and fluorobenzene dimers. The final structures of all of the monosubstituted benzene-nucleobase dimers were examined and the most polarized carbon atom on the monosubstituted benzene ring was always over the nucleobase ring. Since there was not a large difference between the structures for the monosubstituted benzene-nucleobase dimers, the aminobenzene and fluorobenzene dimers were chosen to represent the stacking interactions of an electron rich and electron deficient monosubstituted benzene. a) Cytosine-aminobenzene, b) cytosine-fluorobenzene, c) thymine-aminobenzene, d) thymine-fluorobenzene, e) uracil-aminobenzene, f) uracil-fluorobenzene, g) adenine-aminobenzene, h) adenine-fluorobenzene, i) guanine-aminobenzene, j) guanine-fluorobenzene.

Table 23: Summary of information from potential energy surface scans of the adenine-polyfluorobenzene and adenine-polyaminobenzene dimers at the counterpoise corrected MP2/6-31G*(0.25) level of theory. All energies are in kJ mol⁻¹ and distances are in Å. The “-fl” suffix represents the flipped monomer.

Monomer	R1	α	ΔE	R2		ΔE
				x	y	
Hexafluorobenzene	3.200	0.0	-40.4	0	0	-40.4
Pentafluorobenzene	3.300	60.0	-37.6	0	0.5	-38.8
1,2,3,4-Tetrafluorobenzene	3.300	210.0	-32.3	-0.5	-0.5	-34.5
1,2,3,5-Tetrafluorobenzene	3.300	150.0	-35.4	-0.5	0	-35.9
1,2,4,5-Tetrafluorobenzene	3.300	90.0	-36.5	0	0.5	-37.1
1,2,3-Trifluorobenzene	3.300	150.0	-28.3	-1	-0.5	-33.5
1,2,4-Trifluorobenzene	3.300	150.0	-32.0	-0.5	0.5	-36.0
1,2,4-Trifluorobenzene-fl	3.300	60.0	-32.9	0	0.5	-35.0
1,3,5-Trifluorobenzene	3.300	180.0	-32.5	0	0	-32.5
1,2-Difluorobenzene	3.400	210.0	-26.4	-1	0	-31.8
1,3-Difluorobenzene	3.400	120.0	-28.4	-0.5	0.5	-31.6
1,4-Difluorobenzene	3.300	120.0	-32.2	0	0	-32.2
Fluorobenzene	3.400	180.0	-26.5	-0.5	0	-29.1
Hexaaminobenzene	3.300	0.0	-31.6	-2	1	-36.9
Pentaaminobenzene	3.300	60.0	-31.9	-0.5	0	-34.6
1,2,3,4-Tetraaminobenzene	3.300	120.0	-31.2	-2.5	0	-32.4
1,2,3,5-Tetraaminobenzene	3.400	30.0	-29.3	-2	0	-32.7
1,2,4,5-Tetraaminobenzene	3.300	60.0	-29.9	-2	0	-33.8
1,2,3-Triaaminobenzene	3.400	0.0	-28.5	-1.5	0.5	-32.7
1,2,4-Triaminobenzene	3.300	60.0	-29.2	-2.5	0.5	-30.7
1,2,4-Triaminobenzene-fl	3.400	270.0	-28.4			
1,3,5-Triaminobenzene	3.400	60.0	-27.6	-0.5	-0.5	-29.4
1,2-Diaminobenzene	3.300	0.0	-28.4	-2	1	-30.4
1,3-Diaminobenzene	3.300	0.0	-28.0	0	-0.5	-28.3
1,4-Diaminobenzene	3.400	60.0	-27.2	-0.5	0	-27.7
Aminobenzene	3.400	270.0	-25.4	0	-0.5	-26.6

Table 24: Summary of information from potential energy surface scans of the cytosine-polyfluorobenzene and cytosine-polyaminobenzene dimers at the counterpoise corrected MP2/6-31G*(0.25) level of theory. All energies are in kJ mol⁻¹ and distances are in Å. The “-fl” suffix represents the flipped monomer.

Monomer	R1	α	ΔE	R2		ΔE
				x	y	
Hexafluorobenzene	3.300	30.0	-31.0	0	-0.5	-34.0
Pentafluorobenzene	3.300	300.0	-34.1	0	-0.5	-36.6
1,2,3,4-Tetrafluorobenzene	3.300	300.0	-34.7	-0.5	0	-35.5
1,2,3,5-Tetrafluorobenzene	3.300	300.0	-31.3	0	0	-31.3
1,2,4,5-Tetrafluorobenzene	3.400	120.0	-27.5	0	-0.5	-30.1
1,2,3-Trifluorobenzene	3.300	240.0	-30.5	0	0	-30.5
1,2,4-Trifluorobenzene-fl	3.400	300.0	-27.1	-0.5	-0.5	-28.8
1,2,4-Trifluorobenzene	3.300	240.0	-29.3	0	0	-29.3
1,3,5-Trifluorobenzene	3.400	180.0	-23.5	0	-0.5	-25.2
1,2-Difluorobenzene	3.300	240.0	-26.1	-0.5	0	-27.5
1,3-Difluorobenzene	3.400	270.0	-24.8	-0.5	0	-25.8
1,4-Difluorobenzene	3.400	330.0	-22.4	0	-0.5	-24.3
Fluorobenzene	3.400	240.0	-21.6	0	0	-21.6
Hexaaminobenzene	3.400	30.0	-24.3	-0.5	1.5	-36.4
Pentaaminobenzene	3.400	90.0	-26.3	0	1.5	-35.8
1,2,3,4-Tetraaminobenzene	3.400	150.0	-27.9	0	1.5	-34.6
1,2,3,5-Tetraaminobenzene	3.400	150.0	-23.6	-0.5	1.5	-32.6
1,2,4,5-Tetraaminobenzene	3.400	150.0	-22.0	1.5	3	-28.0
1,2,3-Triaminobenzene	3.400	90.0	-27.4	0	1	-33.1
1,2,4-Triaminobenzene	3.400	90.0	-23.3	1.5	2.5	-34.5
1,2,4-Triaminobenzene-fl	3.400	150.0	-23.7	0	1.5	-35.5
1,3,5-Triaminobenzene	3.400	60.0	-19.7	-1	1.5	-27.5
1,2-Diaminobenzene	3.500	90.0	-23.3	0	1.5	-30.0
1,3-Diaminobenzene	3.500	90.0	-21.9	0	1	-26.9
1,4-Diaminobenzene	3.400	90.0	-19.4	-0.5	1.5	-22.5
Aminobenzene	3.500	90.0	-19.0	-0.5	1.5	-25.1

Table 25: Summary of information from potential energy surface scans of the guanine-polyfluorobenzene and guanine-polyaminobenzene dimers at the counterpoise corrected MP2/6-31G*(0.25) level of theory. All energies are in kJ mol⁻¹ and distances are in Å. The “-fl” suffix represents the flipped monomer.

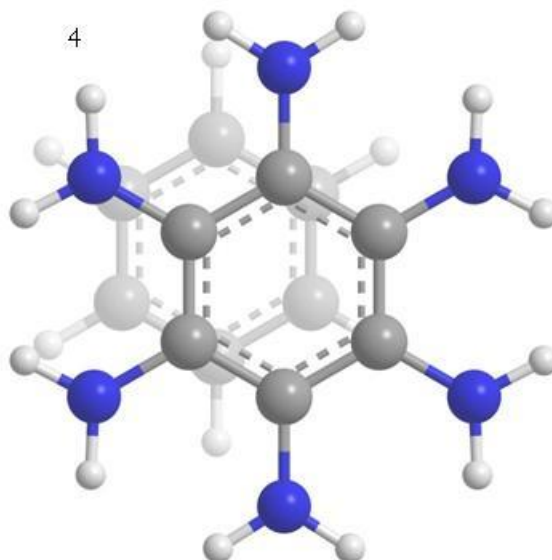
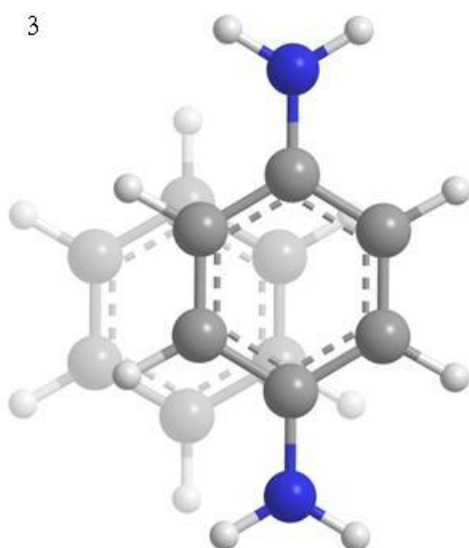
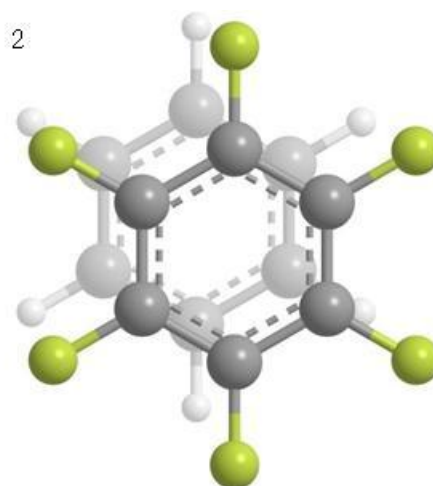
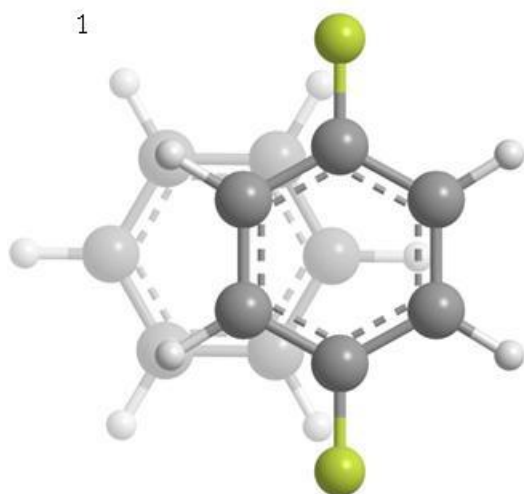
Monomer	R1	α	ΔE	R2		ΔE
				x	y	
Hexafluorobenzene	3.300	30.0	-37.4	0	0.5	-41.1
Pentafluorobenzene	3.300	270.0	-40.6	0	0.5	-40.7
1,2,3,4-Tetrafluorobenzene	3.300	210.0	-40.9	-0.5	0	-43.2
1,2,3,5-Tetrafluorobenzene	3.200	210.0	-37.7	0	0	-37.7
1,2,4,5-Tetrafluorobenzene	3.300	60.0	-36.1	0	0.5	-39.0
1,2,3-Trifluorobenzene	3.300	270.0	-37.4	0	-0.5	-38.5
1,2,4-Trifluorobenzene-fl	3.300	270.0	-38.0	0	0	-38.0
1,2,4-Trifluorobenzene	3.300	210.0	-37.3	-0.5	0.5	-39.8
1,3,5-Trifluorobenzene	3.300	330.0	-31.9	0	0.5	-34.7
1,2-Difluorobenzene	3.300	300.0	-32.0	0	-0.5	-33.4
1,3-Difluorobenzene	3.300	270.0	-35.6	0	0	-35.6
1,4-Difluorobenzene	3.300	90.0	-33.5	0	0.5	-35.3
Fluorobenzene	3.300	330.0	-29.9	0.5	0	-30.8
Hexaaminobenzene	3.400	30.0	-31.1	1	-2	-39.6
Pentaaminobenzene	3.400	90.0	-31.7	1	-2	-37.8
1,2,3,4-Tetraaminobenzene	3.400	60.0	-33.0	-0.5	-1	-38.4
1,2,3,5-Tetraaminobenzene	3.400	90.0	-32.1	0.5	-1	-34.0
1,2,4,5-Tetraaminobenzene	3.400	120.0	-32.3	-0.5	-1	-36.2
1,2,3-Triaminobenzene	3.400	60.0	-33.1	0	-1	-35.6
1,2,4-Triaminobenzene	3.300	60.0	-34.7	-0.5	0	-36.8
1,2,4-Triaminobenzene-fl	3.300	0.0	-31.4	0	-1.5	-32.4
1,3,5-Triaminobenzene	3.300	90.0	-30.3	-2.5	1	-32.3
1,2-Diaminobenzene	3.300	0.0	-33.3	0	-1	-33.8
1,3-Diaminobenzene	3.300	270.0	-28.9	0	-1	-35.6
1,4-Diaminobenzene	3.300	60.0	-29.3	-0.5	0	-31.3
Aminobenzene	3.400	60.0	-28.7	-0.5	0.5	-30.0

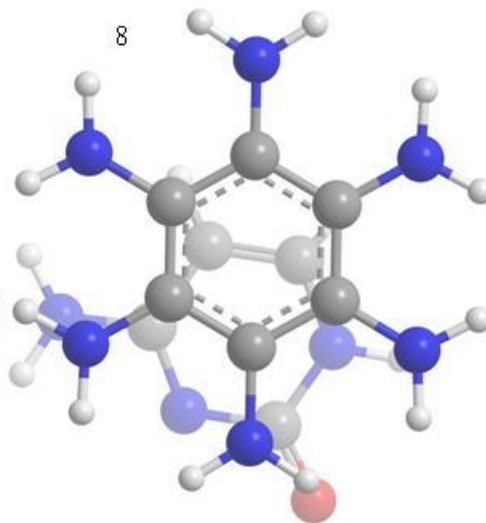
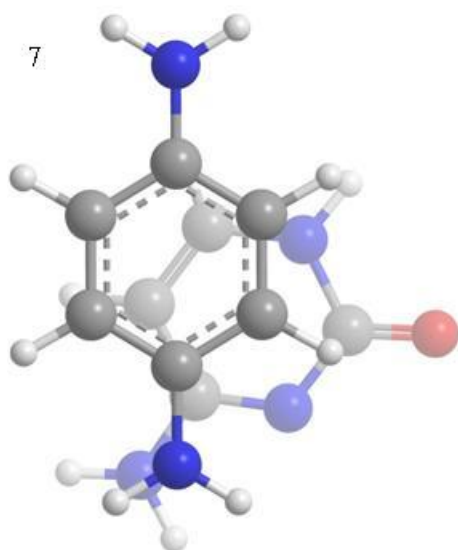
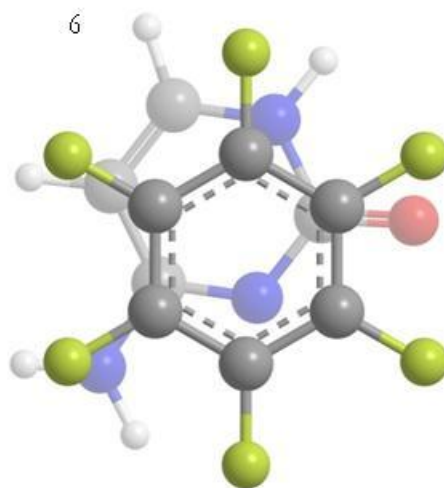
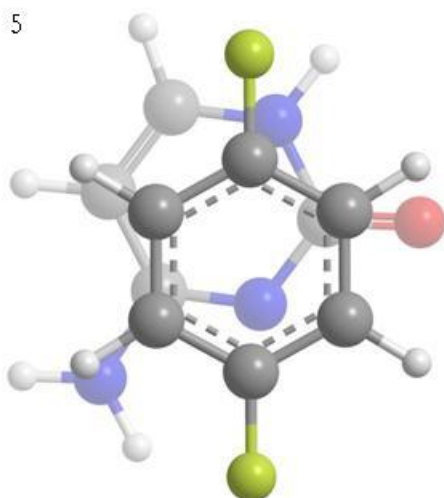
Table 26: Summary of information from potential energy surface scans of the thymine-polyfluorobenzene and thymine-polyaminobenzene dimers at the counterpoise corrected MP2/6-31G*(0.25) level of theory. All energies are in kJ mol⁻¹ and distances are in Å. The “-fl” suffix represents the flipped monomer.

Monomer	R1	α	ΔE	R2		ΔE
				x	y	
Hexafluorobenzene	3.400	30.0	-25.3	-0.5	0.5	-26.8
Pentafluorobenzene	3.400	210.0	-26.8	-0.5	0	-27.1
1,2,3,4-Tetrafluorobenzene	3.300	240.0	-27.7	-0.5	0	-28.4
1,2,3,5-Tetrafluorobenzene	3.400	180.0	-29.1	-0.5	0	-30.3
1,2,4,5-Tetrafluorobenzene	3.400	60.0	-25.8	-0.5	0.5	-28.3
1,2,3-Trifluorobenzene	3.300	240.0	-30.3	0	0	-30.3
1,2,4-Trifluorobenzene-fl	3.300	210.0	-28.3	-0.5	0	-29.9
1,2,4-Trifluorobenzene	3.300	270.0	-27.9	-0.5	0.5	-29.5
1,3,5-Trifluorobenzene	3.400	60.0	-24.3	1	0	-25.2
1,2-Difluorobenzene	3.300	210.0	-29.9	0	0	-29.9
1,3-Difluorobenzene	3.400	270.0	-24.1	-0.5	0.5	-25.8
1,4-Difluorobenzene	3.400	0.0	-24.5	-1	0	-26.6
Fluorobenzene	3.400	240.0	-26.1	-0.5	0	-27.0
Hexaaminobenzene	3.300	30.0	-39.7	1	-0.5	-46.1
Pentaaminobenzene	3.300	90.0	-39.6	1	-0.5	-43.7
1,2,3,4-Tetraaminobenzene	3.400	60.0	-37.2	0.5	-0.5	-42.4
1,2,3,5-Tetraaminobenzene	3.400	30.0	-35.3	1	-1	-39.4
1,2,4,5-Tetraaminobenzene	3.300	150.0	-35.9	1.0	-0.5	-36.9
1,2,3-Triaminobenzene	3.400	90.0	-35.4	0.5	-1	-37.7
1,2,4-Triaminobenzene	3.300	90.0	-33.8	0.5	-0.5	-34.6
1,2,4-Triaminobenzene-fl	3.400	90.0	-33.8	1	-0.5	-38.7
1,3,5-Triaminobenzene	3.400	90.0	-31.1	1	0	-34.7
1,2-Diaminobenzene	3.400	90.0	-32.9	0.5	-0.5	-33.5
1,3-Diaminobenzene	3.400	120.0	-29.9	0.5	-0.5	-34.5
1,4-Diaminobenzene	3.400	0.0	-29.6	1	-0.5	-32.3
Aminobenzene	3.400	60.0	-28.7	0.5	0	-30.6

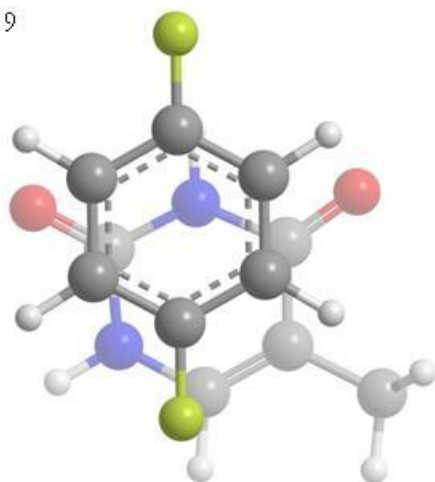
Table 27: Summary of information from potential energy surface scans of the uracil-polyfluorobenzene and uracil-polyaminobenzene dimers at the counterpoise corrected MP2/6-31G*(0.25) level of theory. All energies are in kJ mol⁻¹ and distances are in Å. The “-fl” suffix represents the flipped monomer.

Monomer	R1	α	ΔE	R2		ΔE
				x	y	
Hexafluorobenzene	3.400	30.0	-22.7	-0.5	-0.5	-24.5
Pentafluorobenzene	3.300	180.0	-25.2	0.5	-0.5	-27.1
1,2,3,4-Tetrafluorobenzene	3.300	180.0	-26.0	0.5	0	-26.9
1,2,3,5-Tetrafluorobenzene	3.300	300.0	-27.9	0.5	1.5	-27.9
1,2,4,5-Tetrafluorobenzene	3.400	150.0	-24.0	0.0	-0.5	-26.5
1,2,3-Trifluorobenzene	3.200	240.0	-28.6	0	0	-28.6
1,2,4-Trifluorobenzene-fl	3.300	180.0	-26.8	0.5	-0.5	-28.7
1,2,4-Trifluorobenzene	3.300	270.0	-26.5	-0.5	-0.5	-27.8
1,3,5-Trifluorobenzene	3.400	60.0	-22.5	0.5	1	-23.4
1,2-Difluorobenzene	3.300	210.0	-28.3	0	0	-28.3
1,3-Difluorobenzene	3.400	240.0	-23.2	0	0	-23.2
1,4-Difluorobenzene	3.400	0.0	-23.0	0	-0.5	-25.2
Fluorobenzene	3.300	150.0	-33.6	0	-0.5	-25.8
Hexaaminobenzene	3.300	30.0	-36.3	-0.5	1.5	-44.2
Pentaaminobenzene	3.300	300.0	-37.0	0.5	1.5	-41.5
1,2,3,4-Tetraaminobenzene	3.400	30.0	-33.3	0	1	-39.5
1,2,3,5-Tetraaminobenzene	3.300	300.0	-34.4	0.5	1.5	-36.4
1,2,4,5-Tetraaminobenzene	3.300	120.0	-32.8	1.0	1.5	-36.4
1,2,3-Triaminobenzene	3.400	0.0	-31.5	0.5	1	-37.0
1,2,4-Triaminobenzene	3.300	300.0	-31.2	0.5	1.5	-34.5
1,2,4-Triaminobenzene-fl	3.300	180.0	-29.8	-0.5	1.5	-32.8
1,3,5-Triaminobenzene	3.400	60.0	-30.6	0.5	1	-33.8
1,2-Diaminobenzene	3.400	30.0	-28.8	0.5	0.5	-34.7
1,3-Diaminobenzene	3.400	0.0	-28.2	0.5	1	-31.9
1,4-Diaminobenzene	3.400	120.0	-27.3	-1	2.5	-28.3
Aminobenzene	3.500	300.0	-24.4	-0.5	1	-26.4

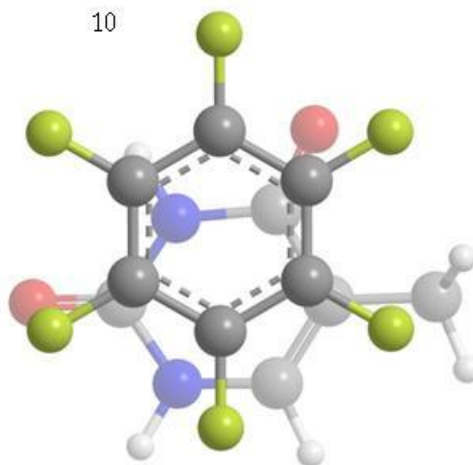




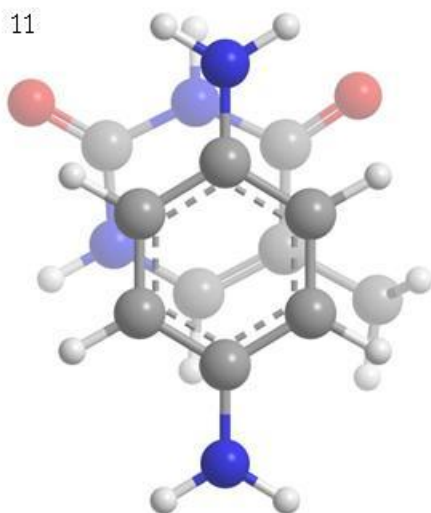
9



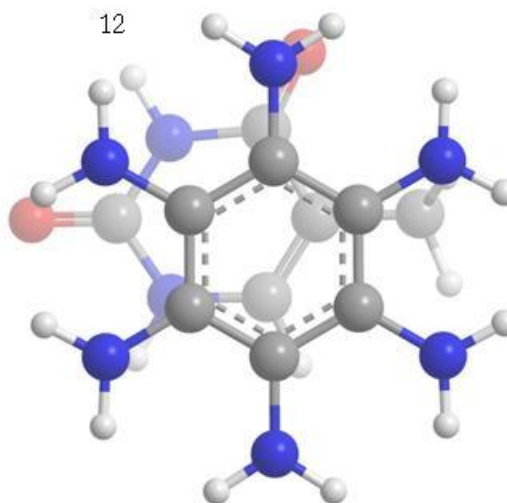
10



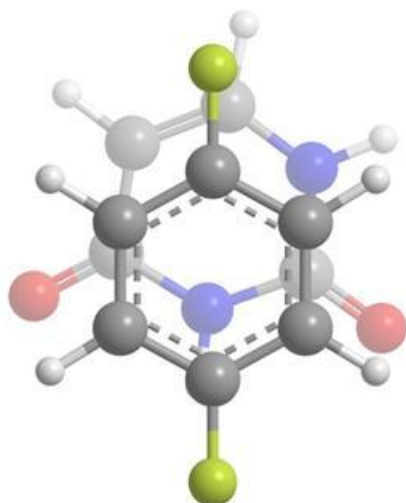
11



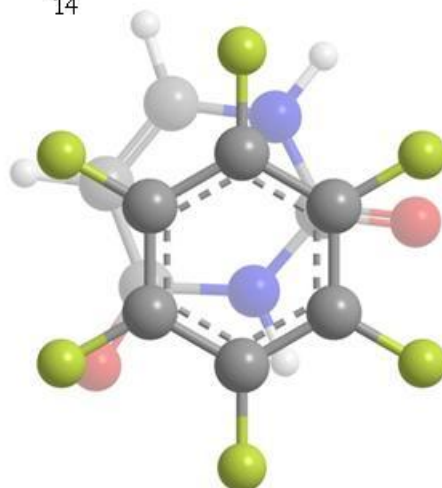
12



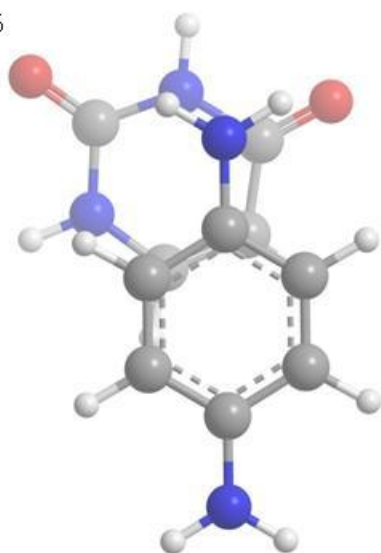
13



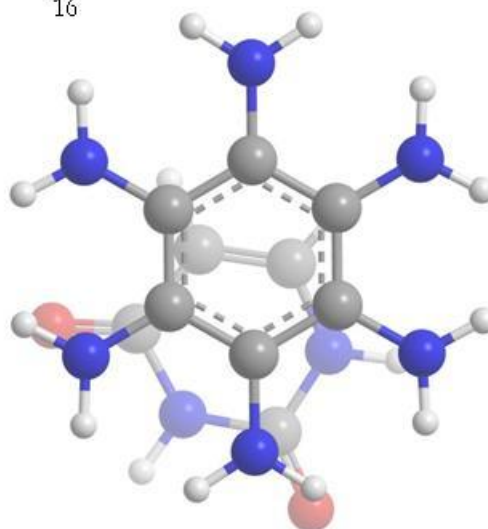
14

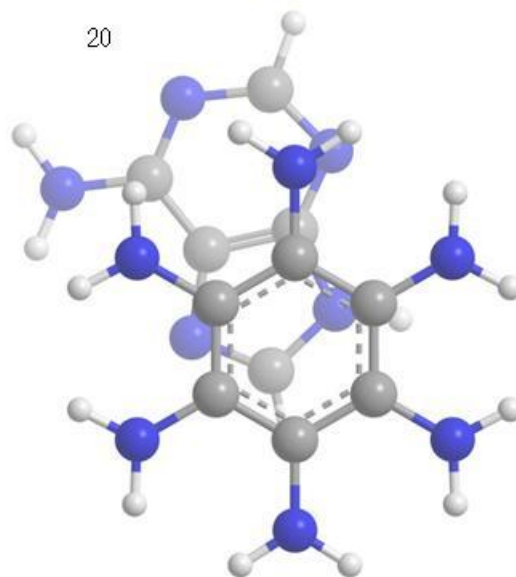
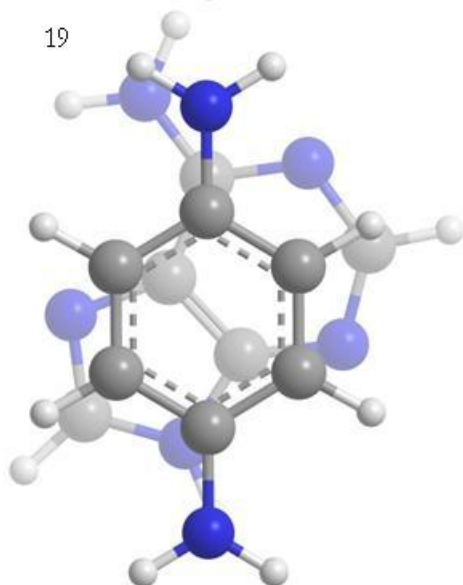
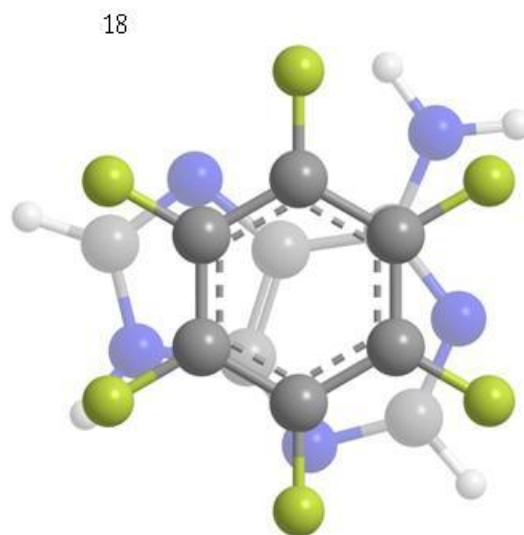
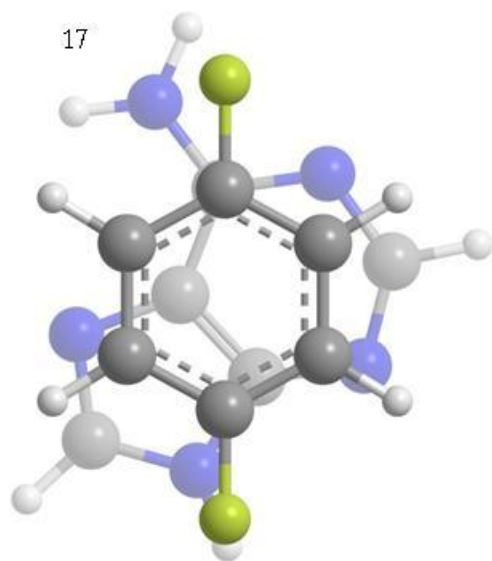


15



16





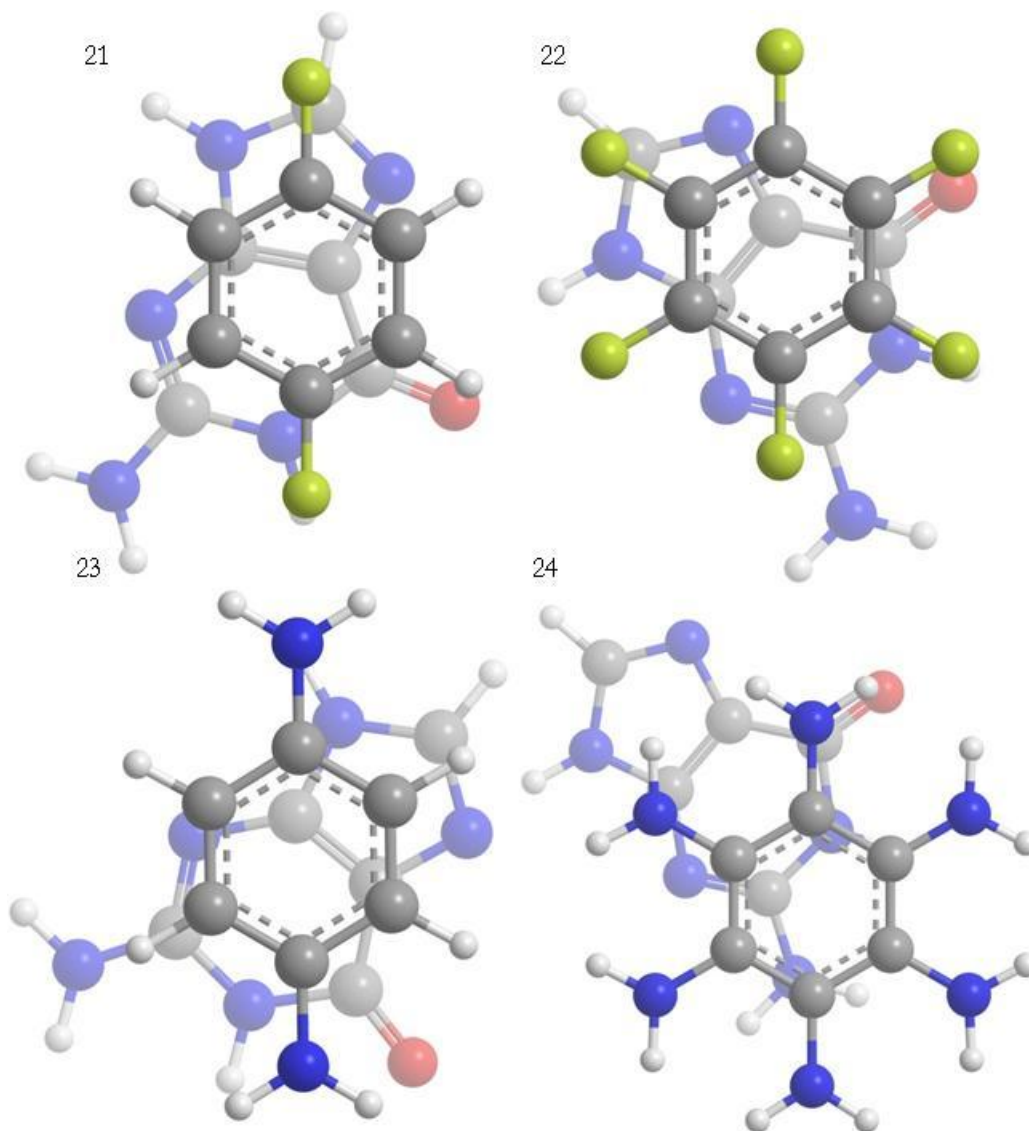


Figure 35: The pictures of the final structures for zero dipole diaminobenzene and hexaaminobenzene dimers are shown since they were found to be representative of the rest of the dimer structures. The electron deficient fluorobenzene rings stack over the part of the nucleobases with the most negative ESP. The electron rich aminobenzene rings stack over the part of the nucleobases with the most positive ESP. 1,5,9,13,17,21 are 1,4-difluorobenzene dimers with benzene, cytosine, thymine, uracil, adenine and guanine respectively. 2,6,10,14,18,22 are hexafluorobenzene dimers with benzene, cytosine, thymine, uracil, adenine and guanine respectively. 3,7,11,15,19,23 are 1,4-diaminobenzene dimers with benzene, cytosine, thymine, uracil, adenine and guanine respectively. 4,8,12,16,20,24 are hexaaminobenzene dimers with benzene, cytosine, thymine, uracil, adenine and guanine respectively.